The Nuclear Localization Signal of Hepatitis B Virus Core Protein:
Characterization by Expression as EGFP-Core Fusion Protein

Eingereicht von
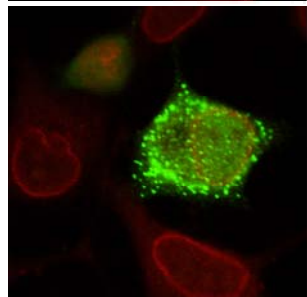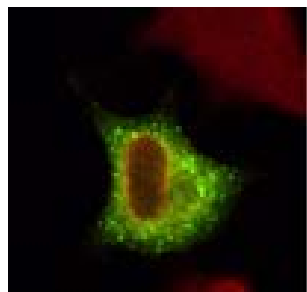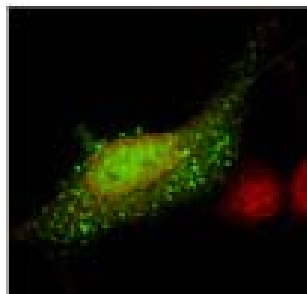**Aris Haryanto**

Giessen, 2006

The Nuclear Localization Signal of Hepatitis B Virus Core Protein: Characterization by Expression as EGFP-Core Fusion Proteins

INAUGURAL-DISSERTATION
zur Erlangung des Grades eines
Dr. med. vet.
beim Fachbereich Veterinärmedizin
der Justus-Liebig-Universität Giessen

Aris Haryanto

Aus dem Institut für Virologie
Fachbereich Veterinärmedizin
der Justus-Liebig-Universität Giessen
Betreuer: Prof. Dr. Heinz-Jürgen Thiel

und

dem Institut für Medizinische Virologie
Fachbereich Medizin
der Justus-Liebig-Universität Giessen
Betreuer: Prof. Dr. Michael Kann

The Nuclear Localization Signal of Hepatitis B Virus Core Protein: Characterization by Expression as EGFP-Core Fusion Proteins

INAUGURAL-DISSERTATION
zur Erlangung des Grades eines
Dr. med. vet.
beim Fachbereich Veterinärmedizin
der Justus-Liebig-Universität Giessen

Eingereicht von

Aris Haryanto
Tierarzt aus Jogjakarta, Indonesien

Giessen 2006

Erklärung

„Ich erkläre: Ich habe die vorgelegte Dissertation selbständig und ohne unerlaubte fremde Hilfe und nur mit den Hilfe angefertigt, die ich in der Dissertation angegeben habe. Alle Textstellen, die wörtlich oder sinngemäß aus veröffentlichten oder nicht veröffentlichten Schriften entnommen sind, und alle Angaben, die auf mündlichen Auskünften beruhen, sind als solche kenntlich gemacht. Bei den von mir durchgeführten und in der Dissertation erwähnten Untersuchungen habe ich die Gründsätze guter wissenschaftlicher Praxis, wie sie in der „Satzung der Justus-Liebig-Universität Giessen zur Sicherung guter wissenschaftlicher Praxis" niedergelegt sind, eingehalten."

Contents

Abbreviations

aa	amino acids
amp^r	ampicillin resistance
ATP	adenosine tri phosphate
bp	base pair
BSA	bovine serum albumin
ccc DNA	covalently closed circular DNA
CIP	calf intestinal alkaline phosphatase
CMV	cytomegalovirus
DHBV	duck hepatitis B virus
dNTP	deoxy nucleotide triphosphate
DMEM	Dulbecco's modified eagle's medium
DR	direct repeat
E. coli	Escherichia coli
E-cup	Eppendorf cup
ECL	enhanced chemiluminescence
EDTA	ethylendiamine tetra acetic acid
EGFP	enhanced green fluorescent protein
EGTA	ethylenglycol tetra acetic acid
ER	endoplasmic reticulum
FCS	fetal calf serum
FG repeat	phenylalanine glycine repeat
Fig	figure
HBe protein	hepatitis B e protein
HBc protein	hepatitis B core protein
HBs protein	hepatitis B surface protein
HBV	hepatitis B virus
HHBV	heron hepatitis B virus
hnRNP	heterogeneous nuclear ribonucleoprotein
kan^r/neo^r	kanamycin/neomycin resistance
kDa	kilo dalton
LB	Luria broth
LHBs	large hepatitis B surface protein
M	marker of DNA/protein
mab 414	monoclonal antibody 414
MHBs	middle hepatitis B surface protein
mRNA	messenger RNA
NE	nuclear envelope
NES	nuclear export signal
NLS	nuclear localisation signal
NPC	nuclear pore complex
nup	nucleoporin
ORF	open reading frame
PBS	phosphate buffered saline
PCR	polymerase chain reaction
pg RNA	pregenomic RNA
PKC	protein kinase C
Pol	polymerase
Pr	priming
PRE	post transcriptional regulatory element
Pro	promoter

rc DNA	relaxed circular DNA
RT	reverse transcriptase
SDS-PAGE	sodium dodecyl sulfate-polyacrylamide gel electrophoresis
SV40 Tag	simian virus 40 large T antigen
SHBs	small hepatitis B surface protein
TAE	tris acetate EDTA
TE	tris-EDTA
°C	degree celsius

1. Introduction

1.1. Nuclear Import of Viral Genomes

Many viruses make use of nuclear factors for their multiplication. For nuclear import of the viral genome two generally different strategies are described. First, the virus can rest in the cytoplasm until the cell undergoes mitosis. When the nuclear envelope temporarily dissembles, the viral genome can associate with nuclear factors and thus become enclosed in the newly assembling nucleus. Used by most retroviruses, this strategy restricts infection to dividing cells. Those viruses however that depend on nuclear factors for multiplication and that infect non-dividing cells must deliver their genome through the nuclear pore complexes (NPC). This is achieved by making use of the cellular transport machinery that facilitates the nuclear import of karyophilic proteins.

Nucleic acids are not karyophilic *per se* thus have to be associated in complex with karyophilic proteins. In all known cases, the karyophilic proteins are of viral origin and either part of the viral capsid (adeno-, herpes- and parvoviruses) or an element of a flexible protein-nucleic acid complex (Influenza- and HIV) (reviewed by Whittaker et al., 2000). Capsids frequently exceed the functional diameter of the nuclear pore that restricts karyophilic cargos to a diameter of 39 nm (Panté and Kann, 2002). Only small capsids as the one of parvoviruses and the hepatitis B virus (HBV) are small enough to pass the NPC. Larger capsids have to disintegrate prior to the import. As it was shown for herpesviruses and adenoviruses, this disintegration may occur at the nuclear pore or as shown for influenza virus and the human immunedeficiency virus. The flexible karyophilic structure comprising the genome may be already released in the cytoplasm.

1.2. Hepatitis B Virus

The Hepatitis B virus (HBV) is a small enveloped DNA virus that is composed of an outer envelope and an inner nucleocapsid. The nucleocapsid also termed core particle or capsid consists of a single protein species called core protein. The majority of capsids have a T=4 symmetry and a diameter of 36 nm, while the minority has a T=3 symmetry and a diameter of 32 nm (Crowther et al., 1994; Kenney et al., 1995). A functional difference is not known. Within the lumen of the capsid the 3.2 kb-long circular, partially double stranded viral DNA genome in enclosed. The HBV encodes for four partially overlapping open reading frames.

HBV is the prototype member of the hepadnavirus family that belongs to the pararetroviruses. They share a characteristic replication strategy, which includes a

multiplication of genomic information via an RNA intermediate. Within the capsid the RNA intermediate is converted into single stranded DNA of minus strand polarity. Concomitantly, the RNA in the resulting DNA-RNA hybrid is degraded by an RNase H acivity. The minus DNA strand is used as template for synthesis of the incomplete plus strand DNA. This genome maturation is mediated by the viral polymerase that comprises an RNase H-, RNA- and a DNA-dependent DNA polymerase activity. Due to the priming reaction of minus strand synthesis during which the tyrosine residue 67 of the polymerase serves as the acceptor for the first nucleotide, the polymerase becomes covalently linked to the minus strand DNA. In contrast to the orthoretroviruses, this genome maturation takes place within the capsids prior to secretion.

Upon infection of a new cell the resulting relaxed circular DNA form (rcDNA) of the virus becomes converted into a covalently closed circular DNA (cccDNA) within the nucleus. This process requires not only the repair of the single stranded region and ligation of the DNA ends but the removal of the polymerase and a short triple-stranded region. The cccDNA is used as an intranuclear template for RNA transcription including the RNA pregenome that encodes the viral polymerase and the core protein (reviewed by Jilbert and Mason, 2002).

1.3. Morphology and Structure of HBV

After negative staining and visualization by electron microscopy, HBV appears as double-shelled particle of 42 nm in diameter. The surface of the HBV virions consists of around 240 surface proteins of 3 different membrane-spanning polypeptides: The large (L), middle (M) and small (S) surface (HBs) protein. The HBs proteins are co-terminally with their carboxy end and differ in additional amino terminal domains. The LHBs consists of an S domain and a pre S1 plus pre S2 domain (Heermann et al., 1984). The preS1 domain of LHBs can be localized externally or internally (Bruss et al., 1994; Lambert and Prange, 2003). The MHBs contains only the preS2 and S domain, and the SHBs consists of only of the S domain. In infected hepatocytes, only a minority of the surface proteins is part of the virion but the majority is secreted as subviral particles (SVPs). Dependent upon the composition of the 3 surface proteins SVPs either form filaments or spheres of 20 nm. A schematic presentation of virus and SVPs is given in Figure 1.
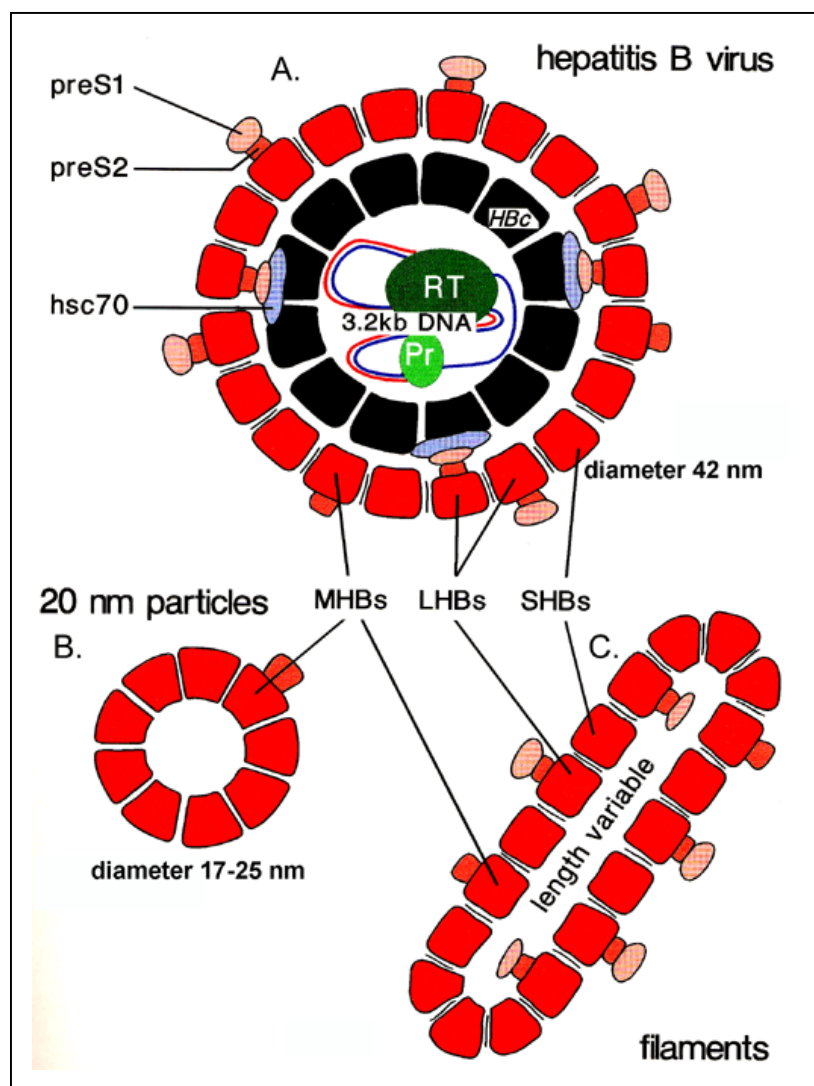
Figure 1. Schematic presentation of HBV and subviral particles. A: Virion. **B:** 20 nm particles. **C:** Filaments. The surface proteins are drawn in red. PreS1: Light red, preS2: Middle red, S: Dark red. The putative hsc70 bound to the preS1 is depicted in blue. The viral capsid forms the inner shell of the virion. Its core protein shown in black. Within the lumen the partially double stranded DNA is found (minus DNA strand: Blue line, plus DNA strand: Red line. The polymerase is drawn in green with a separated priming domain (Pr) in light green. The polymerase-bound heat shock proteins are not depicted. Figure from Kann and Gerlich (1997).

The surface proteins of the virus and SVP are assembled at the endoplasmic reticulum (ER) and bud into the lumen of post-ER intermediate compartment. Thus the lipids in the outer protein shell or the HBs particles are derived from an intracellular compartment and not from the plasma membrane.

Within virions the surface proteins enclose the capsid. The envelopment is mediated by an interaction of the core particle with the internally localized preS1 domain of LHBs (Bruss, 1997; Ponsel and Bruss, 2003). The envelopment requires DNA synthesis within the capsid (Gerelsaikhan et al., 1996) implying that the genome maturation induces a structural change of the capsid surface.

1.4. Classification

The molecular and biological similarity of HBV led to define the family of *Hepadnaviridae* (from Hepa = liver and DNA for the type of genome) (Howard, 1995). The mammalian viruses are called genus *Orthohepadnavirus* (e.g. HBV, WHV, GSHV). Because of significant structural differences the avian viruses form the separate genus *Avihepadnavirus* (e.g. DHBV, HHBV). For more details see Table 1.

Table 1. Members of family *Hepadnaviridae* and their hosts

Genus	Spesies and Strains	Host
Orthohepadnavirus	Hepatitis B Virus HBV, Dane et al., 1970	Human (*Homo sapiens sapiens)*
	Woodchuck Hepatitis Virus WHV, Summer et al., 1978	Woodchuck (*Marmota monax*)
	Ground Squirrel Hepatitis Virus GSHV, marion et al., 1980	Ground Squirrel (*Spermophylus beecheyi*)
	Woolly Monkey Hepatitis B Virus WMHBV, Lanford et al., 1998	Woolly Monkey (*Lagothrix lagotricha*)
	Arctic Ground Squirrel Hepatitis Virus ASHV, Testut et al., 1996 (tentative spesies)	Arctic Ground Squirrel (*Spermophylusparryi kennicotti*)
Avihepadnavirus	Duck Hepatitis B Virus DHBV, Mason et al., 1980	Peking Duck (*Anas domesticus*)
	Heron Hepatitis Virus HHBV, Feitelson et al., 1986	Heron (*Adrea cinerea*)
	Storck Hepatitis B Virus STHBV, Pult et al., 1998	White Storck (*Ciconia ciconia*)
	Snow Goose Hepatitis B Virus SGHBV, Chang et al, 1998	Snow Goose (*Anser caerulescens*)
	Grey Teal Hepatitis B Virus GTHBV, Li et al 1998	Grey Teal Duck (*Anasgibberfrons gracilis*)
	Maned Duck Hepatitis B Virus MDHBV, Li et al., 1998	Maned Duck (*Chenonetta jubata*)
	Ross Goose Hepatitis Virus RGHV, Testut et al., 1996 (unassigned virus in the family)	Ross Goose (*Anser rossi*)

Although containing a DNA genome thus differing from the RNA-containing *Retroviridae*, the common strategy of reverse transcription places them and the *Caulimoviridae* of plants into one related group of viruses called *pararetroviruses* (Toh et al., 1983).

1.5. Genome Organization of HBV

In the virion, the genome is circular and partially double stranded (Robinson et al., 1974). The genome is approximately 3200 nucleotides in length (Fauquet et al., 2005). The numbering of base pairs of the HBV genome is based on the cleavage site for the restriction enzyme Eco RI or at homologous sites, if the Eco RI site is absent. An alternative numbering, beginning with the first base of the precore start codon, is also used. There are at least seven subtypes of HBV, distinguished by sequence differences in the surface antigen gene.

Mammalian hepadnaviruses contain four overlapping open reading frames (ORFs). They encode seven different hepatitis B proteins (see Fig. 2) via transcription of five mRNAs. Every base pair in the HBV genome encodes at least one of the HBV proteins and eventually overlaps with regulatory elements for transcription, the site of polyadenylation, the encapsidation signal of the RNA pregenome (ε) and structural elements required for circularization of the minus strand DNA.

There two classes of mRNAs: Two of supergenomic and three of subgenomic length. All mRNA use a common polyadenylation signal and become exported into the cytoplasm without splicing. The longest mRNA comprises the start codon of the pre core/core ORF. Translation from this AUG generates a primary translation product that includes the precore sequence. The precore sequence leads to translocation into the ER where the signal peptide is cleaved partially. Then in the Golgi compartment the carboxy terminus is removed by proteases, which leads to secretion as a ~18 kDa protein called the HBeAg.

On the 34 bases shorter mRNA that serves as the RNA pregenome, the precore AUG is not present so that translation starts with 5' located start codon allowing synthesis of the core protein. The viral polymerase is encoded on a down stream located overlapping ORF. The initiation of polymerase translation - either by ribosomal frame shift or by internal initiation - is controversially discussed.

The longest subgenomic mRNA comprises the in-frame located ORFs of preS1, preS2 and S, encoding LHBs. Most abundant in infected cells is a shorter mRNA that encloses the start codons of the preS2 and the S ORF. However, in the majority of translation events not the first but the third AUG is used so that the S protein is overexpressed. The shortest mRNA encodes the HBx protein. The precise function of this translation product is unclear. It is transactivating numerous promoters and is essential for establishment of *in vivo* infection, as determined in the woodchuck using the WHV (Zoulim and Seeger, 1994). Furthermore, it is assumed that it is involved in the development of liver cell carcinoma (Tennant et al., 2004).
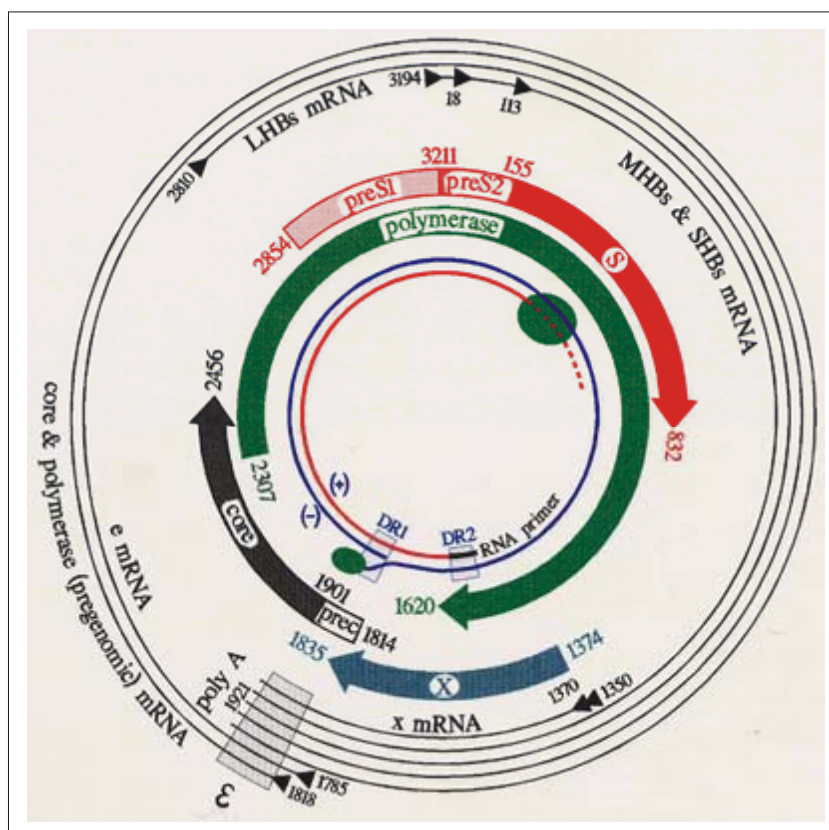
Figure 2. Genome organisation of HBV. The HBV genome as it is found in mature viruses is shown in the center with a negative DNA strand and incomplete positive strand. The positions of the direct repeats 1 (DR1) and 2 (DR2) are depicted at the beginning of the RNA primer for plus DNA strand synthesis. The primer domain of the viral polymerase is covalently linked to the 5' end of the minus DNA strand. The catalytic domains of the polymerase are drawn as a separated protein. The ORFs and their relative position on the genome with corresponding start and termination sites are shown outwards of the genome. The transcribed HBV RNAs are show in the outer region. The black triangles represent the different 5' ends of the RNAs. The common 3' end is located at position 1921, followed by a 300 nucleotides of poly (A) sequence. The encapsidaton signal ε is drawn as a dotted box. The numbering follows the isolate 991. Figure modified from Kann and Gerlich (2005).

1.6. Life and Replication Cycle of HBV

HBV must first attach to a cell capable of supporting its replication. The liver is the most effective cell type for replicating HBV, though the other extrahepatic sites have been found to be able to support the replication to some extent. Viral attachment often determines host and tissue specificity of a virus. However for HBV, the receptor(s) remain unclear. Consequently, the initial steps of HBV entry are poorly understood. Several differentiated and immortalized cell lines are capable of supporting viral replication if transfected with viral DNA (Sureau et al., 1986; Chang et al., 1987; Sells et al., 1987).

Viral uncoating does not require acidification in an endocytotic vesicle (Kock et al., 1996) and results in a released cytoplasmic nucleocapsid. The capsid is transported

through the nuclear membrane into the nuclear basket (Kann et al., 1999; Rabe et al., 2003). There the genome becomes released into the karyoplasm where the rc-form of the genome is repaired generating the cccDNA form of the viral genome. Unlike the *Retroviridae*, integration of HBV DNA into host cell DNA is not required for replication. In fact, integration of HBV DNA results in the disruption of one or more HBV ORFs and prevents transcription of functional pre genomic RNA (pgRNA). Once recircularized, enhancer and promoter allow transcription of the various HBV transcripts.

For the intracellular life cycle the pregenomic mRNA is most important. As the other mRNAs it becomes exported into the cytoplasm without being spliced. This unusual export is caused by the presence of the so-called post regulatory element (PRE) that is present on all HBV mRNAs (Zang and Yen, 1999). Its molecular mechanism is not fully understood. After synthesis of the polymerase, this enzyme binds to the ε-signal at the 5' end of this RNA being a prerequisite for specific encapsidation of this RNA into the capsid (Hirsch et al., 1990; Pollack et al., 1994), most likely by an interaction of the polymerase with the core proteins (Lanford et al., 1999).

DNA synthesis is initiated at a bulge region within ε during which the first deoxynucleotide becomes linked to Tyr63 of the polymerase (Tang and McLachlan, 2002). After synthesis of the first 3 nucleotides the complex of nucleotides and polymerase translocates to a DR1 (direct repeat 1) termed region closed to the 3' end of the pregenome. From there reverse transcription proceeds to the 5' end, being combined with the degradation of the RNA by an RNaseH activity of the polymerase. This activity leaves an oligonucleotide of ~18 bases undegraded, which translocates to a complementary region on the minus strand DNA (DR2). At this site the polymerase continues with plus strand DNA synthesis that spans the 3' and 5' end of the minus stranded DNA leading to circularization of the genome (reviewed by Kann and Gerlich, 2005).

Ongoing genome maturation only occurs after the polymerase is encapsidated. Consequently, the polymerase in the absence of the core proteins copies only a few nucleotides on its natural template (Gerelsaikhan et al., 1996). It must be thus concluded that a premature release of a replication intermediate leads to disruption of the viral life cycle. However, *in vivo* one to 10 HBV are sufficient to cause HBV infection in chimpanzees (Ulrich et al., 1989) making it most likely that the genome release is highly coordinated. Accordingly, only capsids containing a mature genome release it into the karyoplasm as determined in digitonin-permeabilized cells (Rabe et al., 2003).

The mature capsids have two possible fates: Early in infection the capsids direct the progeny viral DNA into the nucleus of the already infected cell. This leads to amplification

of the viral cccDNA to approx. 10-20 copies. Later in infection when sufficient amounts of surface proteins are synthesized, the mature capsids become enveloped by the surface proteins leading to secretion of progeny HBV.
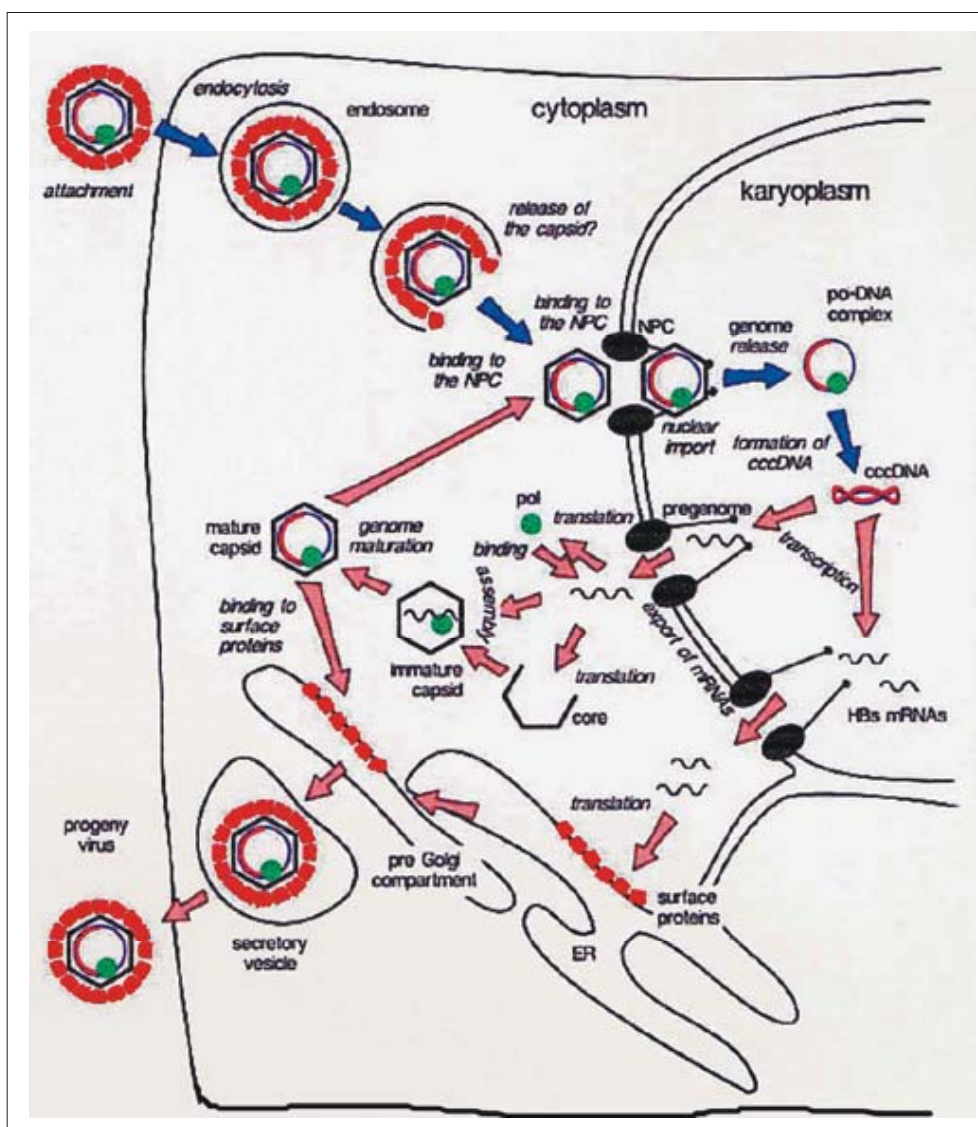
Figure 3.   Schematic drawing of the HBV life cycle. The attachment and entry of HBV into the cytoplasm is not unequivocally identified. According to most publications HBV enters the cell by endocytosis, followed by a pH-independent release of the capsid into the cytosol. The capsid binds to the nuclear pore (NPC) mediated by importin α and ß and is transported into the nuclear basket. There the DNA genome is released into the karyoplasm where repair and generation of the covalently closed circular DNA (cccDNA) occurs. This DNA serves as the template for transcription of the mRNAs. For genome replication, one mRNA spesies of supergenomic length is used and translated into core protein and - from an overlapping reading frame into the viral polymerase. Polymerase, cellular heat shock proteins (not shown) and RNA interact. This complex is specifically encapsidated by the core protein into particles (immature capsid). Within core particles the encapsidated RNA serve as the template for reverse transcription followed by second strand DNA synthesis (genome maturation). The core particle containing mature DNA genome can be either enveloped into the surface proteins (red blocks) and secreted as mature virus or can be transported to the nucleus following the import pathway during the initial infection. Figure modified from Kann and Gerlich (2005).

2. HBV Capsid

The core particles are involved in a number of important steps in the replication cycle of HBV, such as RNA packaging, DNA synthesis, recognition of viral envelope proteins and transport of the genome to and into the nucleus. Consequently, the 21.5 kDa capsid protein can be detected in the cytoplasm (Ou et al., 1986), nucleus (Mc Lachlan et al., 1987) or both (Chu and Liaw, 1987; Sureau et al., 1986) within infected hepatocytes . Its N terminal 144 amino acid residues form 5 α-helices and direct the assembly of the capsid particle (Gallina et al., 1989; Hatton et al., 1992). In contrast, the carboxyl terminus from residue 150 to 185 (HBV subtype adw) or 183 (ayw), is dispensable for particle assembly but mediates interactions between the capsid protein and the nucleic acid. This region contains four clusters of arginine residues (see Fig. 4) overlapping with up to seven serine residues (number depends upon the genotype) that are potential target sites for the protein kinase that is enclosed during capsid assembly. The first cluster of arginine residues is required for binding of viral DNA (Hatton et al., 1992; Nassal, 1992; Yu and Summers, 1991).
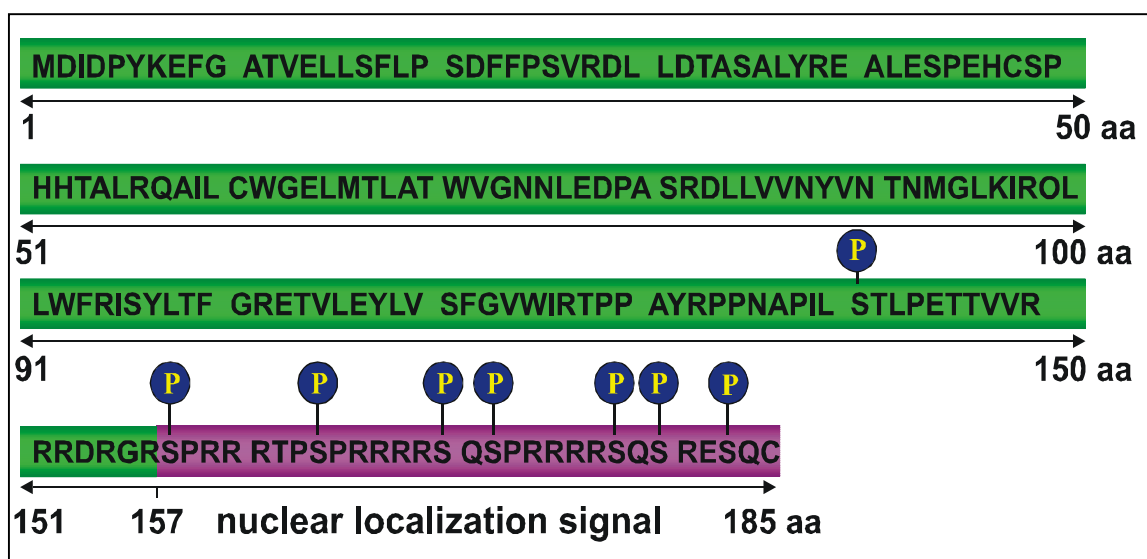
Figure 4. Primary amino acid sequence of HBV capsid protein. HBV capsid protein consists of 183 to 185 amino acids. The nuclear localization signal is located at the C terminus. It contains fours clusters of arginine residues and three overlapping SPRRR motifs. P indicates potential phosphorylation sites at serine residues.

After synthesis in the cytoplasm the core molecules form dimers (Zhou and Standring, 1992) that trimerize (Zlotnick et al., 1999). The resulting hexamers assemble to capsids. This assembly occurs spontaneously and is independent upon other viral proteins. *In vivo* a complex of pregenome, polymerase and the heat shock proteins Hsp40 and Hsc70 are encapsidated (Bartenschlager et al., 1990; Hirsch et al. 1990, Beck and Nassal 1998) while in the absence of the polymerase cellular RNA is encapsidated

unspecifically. Furthermore a cellular protein kinase becomes encapsidated that phosphorylates the serine residues between the arginine clusters to an unknown extent. After released from the reducing environment in the cytoplasm the core protein dimers become linked by disulphide bridges (Jeng et al., 1991). The capsids do not form a closed shell but contain 2 nm holes that allow diffusion of nucleotides and ATP into the lumen. They show spikes on their surface which have been successfully used as a carrier site for foreign epitopes in a highly immunogenic conformation (Pumpens and Grens, 2001). Although capsid formation does not require any other viral component, the presence of RNA strongly enhances the assembly (Seifer and Standring, 1995). This phenomenon is caused by stabilizing interaction of RNA and the arginine clusters. Consequently, truncated core proteins which are lacking NLS of the carboxy terminus show much slower assembly kinetics and are less stable than the wild type. The localization of carboxy terminus is however flexible. They are internally localized in RNA-containing core particles (Zlotnick et al., 1997) but genome maturation results in an exposure NLS on capsids surface (Rabe et al., 2003) presumably because of a weaker interaction to double-stranded DNA than to RNA. Whether this structural change is required for the interaction with the preS1 is not known.

3. Nuclear Import

The nucleus and cytoplasm are separated by the double membrane of the nuclear envelope. The outer membrane is continuously connected with the membrane of the endoplasmic reticulum. Transport between the cytoplasm and the nucleoplasm is highly regulated and occurs through protein-lined aqueous channels called nuclear pore complexes (NPC). This transport is facilitated by soluble transport receptors.

The best study receptors belong to the importin ß superfamily. While importin ß can directly bind to a karyophilic cargo if it exposes an importin ß binding domain (IBB) the indirect binding via the adapter protein importin α to a nuclear localization signal (NLS) seems to be the most abundant pathway. Both, IBB and NLS consist of multiple basic amino acids.

A second member of the importin ß superfamily is transportin that binds directly to the cargo via a leucine-rich M9 domain as it is found on protein A1 of the hnRNP complex. Further not as well characterized transport receptors comprise the proteins NTF2, Importin 5, RanBP6, Importin 7 and Transportin SR (reviewed by Fried and Kutay, 2003).
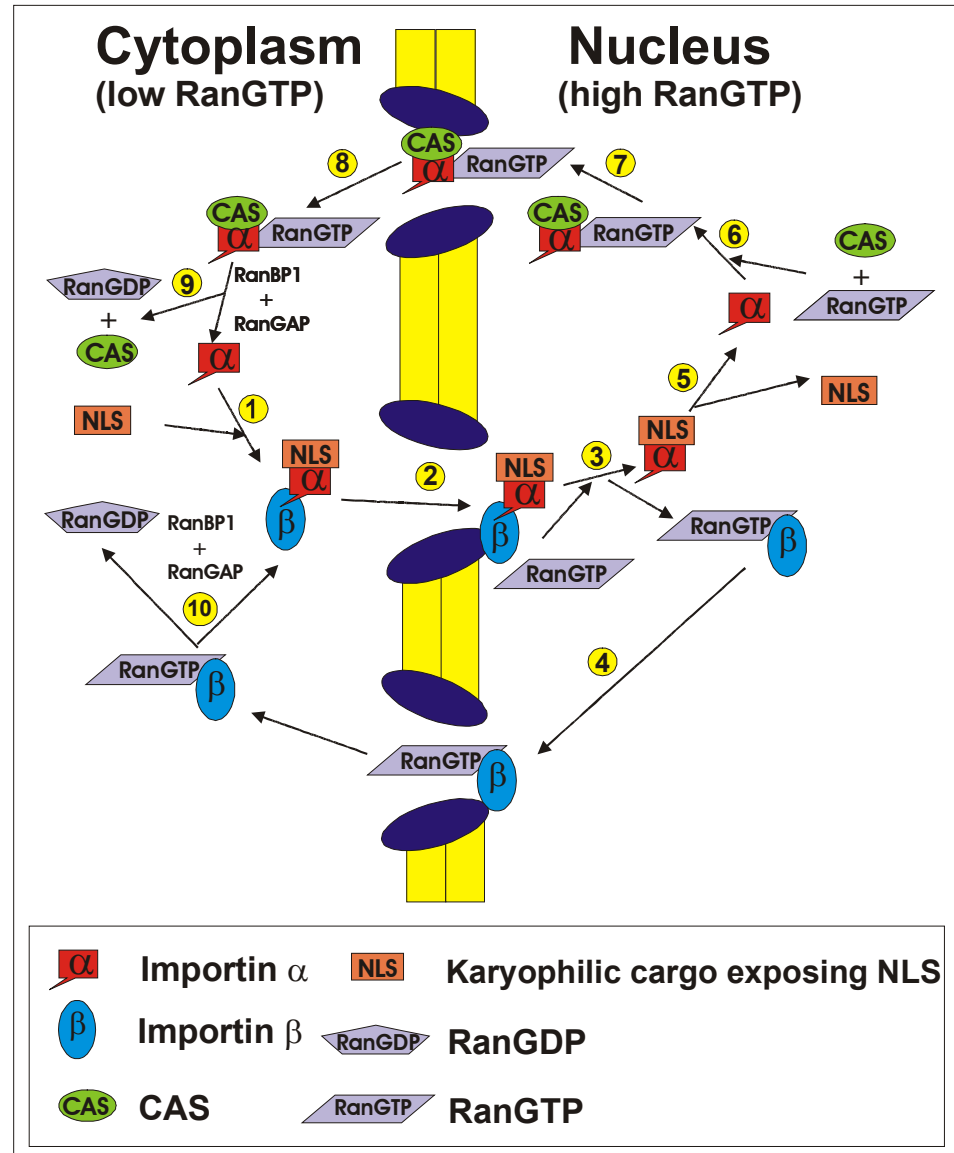
Figure 5. Pathway of the nuclear import cycle. 1) Importin α binds to the NLS of a karyophilic cargo followed by Importin ß binding to the complex. 2) Importin β mediates contact with NPC and the import of cargo/importinα/importin β complex from the cytoplasmic to the nuclear side of NPC. 3) Nuclear import is terminated by binding of RanGTP to importin β, which releases the complex from the NPC. 4) The importin β-RanGTP complex can directly exit from the nucleus. 5) Importin α releases karyophilic cargo. 6) Importin α binds to CAS and RanGTP for its re-export. 7) Importin α/CAS/RanGTP complex is exported to the cytoplasm through the NPC. 8) In the cytoplasm, Importin α/CAS/RanGTP complex is disassembled by hydrolysis of GTP to GDP. This reaction is catalysed by RanGAP and supported by RanBP1. 9) Importin α is released from Importin α/CAS/RanGTP complex. 10) Similarly, importin β is disassembled. Importin α and β can recombine for the next round of another cargo protein. Figure adapted from Görlich and Kutay (1999).

After formation of a cargo-import receptor complex, the transportin or importin β mediates binding to the cytosolic face of the NPC and subsequent transport through the nuclear pore into nuclear basket (Fig. 5). The molecular details of the passage through the nuclear pore, either active or by an "allowed diffusion" are still not fully known. Within the

basket, which is a cage-like structure formed by eight fibers derived from the karyoplasmic face of the NPC, the import complex becomes arrested. The import reaction is terminated by the interaction of transportin or importin with Ran in its GTP bound form (RanGTP). While the cargo diffuses deeper into the karyoplasm, the transport receptors become exported into the cytoplasm using NTF2 (Moore and Blobel, 1994; Paschal and Gerace, 1995). There, Ran-bound GTP is hydrolyzed to GDP. RanGDP shows however only a weak affinity to importins and transportin so that the receptors become released and can facilitate a new import reaction. The released RanGDP is imported into the karyoplasm by NTF2, followed by an exchange of GDP by GTP, catalyzed by the chromatin-bound protein RCC1. It is assumed the receptors participate in several hundred rounds of import.

3.1. Nuclear Pore Complex (NPC)

In vertebrates, the nuclear pore complex is an 8 fold-symmetric protein complex with a molecular mass of 125 MDa. It contains about 30 different proteins that are present in at least 8 fold redundancies. The NPC consists of a membrane-embedded framework (the spoke complex), which is formed by eight multidomain spokes with two rings on each face (Fig. 6). The ring facing the cytoplasm is decorated with eight 50 nm fibrils extending into the cytoplasm and the nuclear ring is capped with a basket-like assembly of eight thin, 50-100 nm filaments joined distally by a 30-40 nm diameter terminal ring. The center of the channel harbors a hydophobic framework through which the signal-mediated bi-directional transport of macromolecules occurs. The proteins that form the NPC are called nucleoporins (nups). Nups have been localized to discrete regions of the NPC and are often used as markers for this compartment. Approximately half of the nucleoporins contain a phenylalanine-glycine repeat motif (FG repeat) which play an important role in the nuclear transport of protein. Structure and function of the NPC is reviewed by Izaurralde et al. (1999).
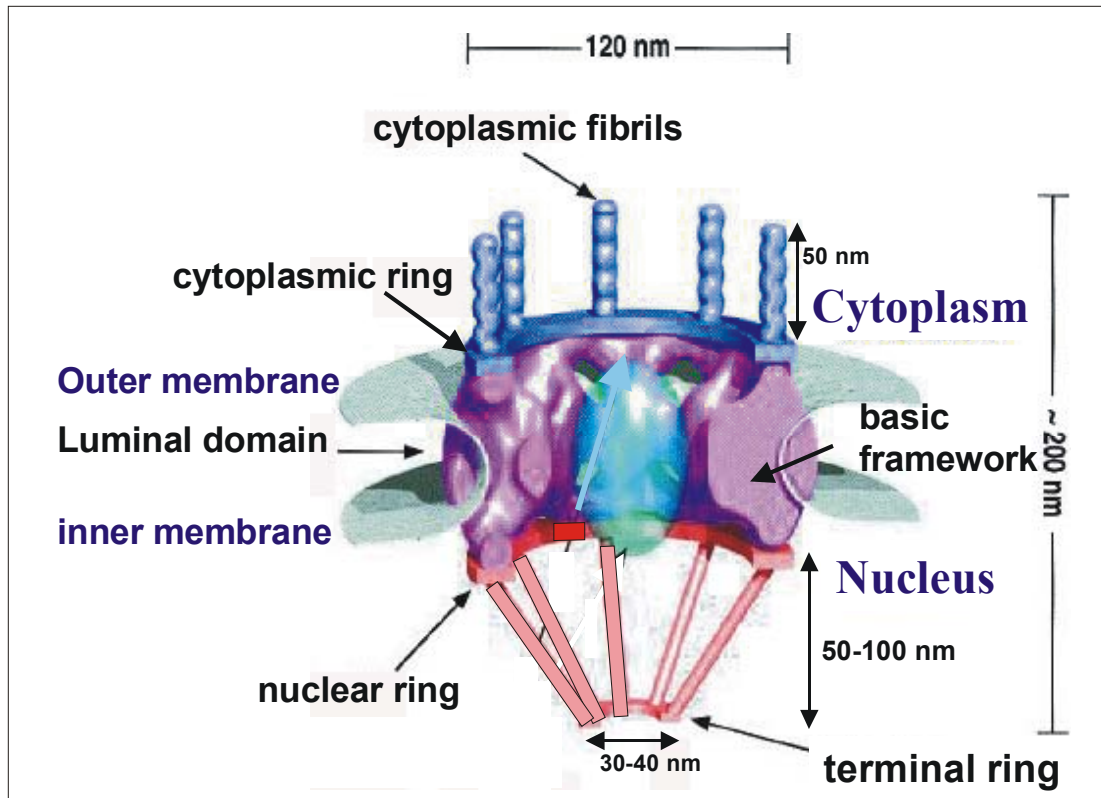
Figure 6. Model of nuclear pore complex. The major components include the basic framework, the gated channel, the cytoplasmic and nuclear rings, and the cytoplasmic fibrils and the nuclear basket. The structure in the lumen of the pore depicts an import complex in transit. Figure adapted from Izaurralde et al., (1999).

3.2. Nuclear Localization Signal (NLS)

Facilitated transport into and out of the nucleus is determined by specific sequence motifs that constitute localization signals. For import, these are called nuclear localization sequences (NLSs), and for export, nuclear export signal (NESs). They can confer nuclear transport competence to proteins restricted to the cytoplasm or the nucleus.

The first NLS to be identified was a short stretch of basic amino acids (PKKKRKV) in simian virus 40 (SV40) large T antigen (Kalderon et al., 1984). Similar sequences were subsequently found in numerous viral and cellular proteins with karyophilic properties. Other versions of this motif display a bipartite sequence, e.g. in nucleoplasmin (KRPAATKAAGQAKKK) (Robbins et al., 1991). As they were the first to be discovered, these import signals are called as classical NLSs. As determined by co-crystalization of importin α with NLS-peptides (Fontes, 2000), a lysine residue appears to be essential for the interaction.

4. Nuclear Localization of HBV Core Protein and Capsid

In histology of HBV infected human livers capsids mainly show a nuclear localization (Gudat et al. 1975, Furuta et al., 1975). This distribution is intrinsic for the HBV core protein since identical staining is found in HBV transgenic mice (Guidotti et al., 1994). In transfected cells nuclear localization is enhanced during G0/G phase but suppressed during the S phase (Yeh et al., 1993). Since hepatocytes in the liver are resting cells the latter observation is in accordance with the data obtained from histology.

The NLS of HBV core is located within the carboxy-terminus between amino acids 158 and 168 (158-PRRRTPSPRRR-168). Noteworthy, the capsid NLS does not comprise a lysine residue so that it must be speculated that the NLS shows only a weak interaction to importin α. Nonetheless, other NLS without lysine residues , as the Borna disease virus p10 protein, were identified in that additional the NLS flanking sequences were required (Wolff et al., 2002). However, at least in assembled capsids the redundancy of exposed NLS may compensate a poor binding affinity.

Phosphorylation of the core proteins within the context of the capsid was shown to be a prerequisite for the importin α/ß-mediated interaction of the particle with NPC (Kann et al., 1999). However, using protein conjugates with the HBV capsid NLS is was shown that the phosphorylation of the serine residue that is localized within NLS inhibits its functionality (Vlachou, PhD thesis 1999). These different observations may be interpreted that the phosphorylation occurs outside the NLS and is only responsible for the structural change that leads to the external exposure of the NLS. A similar phenomenon was observed for the SV40 Tag in which phosphorylation at a site directly adjacent to the NLS inhibits the NLS function (Jans and Jans, 1994), while further upstream phosphorylation enhances the NLS transport competence (Hübner et al., 1997).

5. Presentation of the Problem

Although being essential for the viral life cycle, the molecular details of the nuclear transport of the HBV core protein and capsid are only partially known. The understanding of the NLS - nuclear transport receptor interaction is mainly based on observations using biochemical assays as co-immune precipitations and *in vitro* transport assays. This work shall give corresponding *in vivo* evidence. By expressing fusion proteins of core and a marker protein, the strength of the capsid NLS shall be investigated.

2. Materials and Methods

2.1. Materials

2.1.1. Antibodies and Beads

Goat anti mouse antibody, Texas Red conjugated	DIANOVA, Hamburg
Goat anti rabbit antibody, FITC conjugated	DIANOVA, Hamburg
Mouse anti nuclear pores complex antibody (mAb 414)	BabCo, Freiburg
Rabbit anti EGFP antibody	CLONETECH, USA
Rabbit anti hepatitis B core antibody (Dako)	DakoCytomation, Hamburg
Dynabeads M-280, Sheep anti rabbit IgG	DYNAL, Hamburg
Dynabeads M-280, Sheep anti mouse IgG	DYNAL, Hamburg

2.1.2. Chemicals

Adenosintriphosphat	BOEHRINGER, Mannheim
Agarose (SEAKEM)	BOEHRINGER, Mannheim
Bayer 41-4109	BAYER, Leverkusen
ß-Mercaptoethanol	ROTH, Karlsruhe
Bromphenolblau	SIGMA, Deisenhofen
BSA (Bovine Serum Albumin)	ROTH, Karlsruhe
Coomasie brilliant blue R 250	MERCK, Darmstadt
Collagen	SIGMA, Deisenhofen
Creatinine phosphate	SIGMA, Deisenhofen
DABCO	SIGMA, Deisenhofen
Dithiothreitol (DTT)	SIGMA, Deisenhofen
dNTP	BOEHRINGER, Mannheim
EDTA	SIGMA, Deisenhofen
EGTA	SIGMA, Deisenhofen
Ethidium bromide	SERVA, Heidelberg
FITC-BSA	SIGMA, Deisenhofen
Fetal Calf Serum (FCS)	GIBCO-BRL, Karlsruhe
32γ ATP	AMERSH. PHARMA., Freiburg
Glyserin	MERCK, Damstadt
Goat serum	DIANOVA, Hamburg
Microsome	ROCHE, Mannheim
MOVIOL	HOECHST, Frankfurt
Nonindet P-40 (NP-40)	FLUKA, Buchs
Nupage Bis-Tris gel (4-12%)	INVITROGEN, Karlsruhe

Phenol	ROTH, Karlsruhe
Protease inhibitor	ROCHE, Mannheim
Staurosporine	SIGMA, Deisenhofen
Tfx-20 Transfection agents	PROMEGA, Mannheim
Tris-Base	ROTH, Karlsruhe
Triton x-100	SERVA, Heidelberg
Trypsine	GIBCO-BRL, Karlsruhe

2.1.3. DNA and Protein Markers

1 Kb plus DNA ladder	GIBCO-BRL, Karslruhe
^{14}C Methylated protein marker	AMERSH. PHARMA., Freiburg

2.1.4. Enzymes

CIP (Calf Intestinal Alkaline Phosphatase)	NEW ENG. BIOLAB, Frankfurt
Creatininphosphokinase (10 Unit/µl)	SIGMA, Deisenhofen
DNase I (10 Unit/µl)	ROCHE, Mannheim
Restriction endonucleases: Apa I, Ava I, Bgl II Bsp EI, Bsp MI, Hind III, Eco RI	NEW ENG. BIOLAB, Frankfurt
Proteinase K	BOEHRINGER, Mannheim
RNase A (1 Unit/µl)	ROCHE, Mannheim
SDS (Sodium Duodecyl Sulfat)	MERCK, Darmstadt
S_7 nuclease	ROCHE, Mannheim
T_4 DNA ligase	NEW ENG. BIOLAB, Frankfurt
T_4 polynucleotide kinase	NEW ENG. BIOLAB, Frankfurt
T_4 DNA polymerase	NEW ENG. BIOLAB, Frankfurt

2.1.5. Equipments

Binocular microscope	LEITZ, Wetzlar
Centrifuge BIOFUGE 15 R	HERAEUS, Hanau
Confocal laser scan microscope	LEICA Lasertech., Heidelberg
Desk Centrifuge 5415 C	EPPENDORF, Hamburg
Films for autoradiography	AMERSH. PHARMA., Freiburg
Nanosep 3K, 10K	PALL FILTRON, USA
Petri dishes	GREINER, USA
Rotors for ultracentrifuge	BECKMAN, München

Typhoon 9200	AMERSH. PHARMA., Freiburg
Ultracenfrifuge L5-50	BECKMANN, München
Ultrasonic sonicator UW-70	BENDELIN ELECTRO., Berlin
UV spectrophotometer Du-70	BECKMAN, München
24 and 96 well dishes	NUNC INC., USA

2.1.6. Kits

BSA Assay kit	UPTIMA, Frances
Gel extraction kit	QIAGEN, Hilden
Maxipreparation plasmid purification kit	QIAGEN, Hilden

2.1.7. Synthetic Oligonucleotides

Synthetic oligonucleotides were purchased from firma MWG-Biotech. The nucleotide sequences are:

2C sense (78 nucleotides):
5'-CTC GGG AAT CTC AAT GTC CTA GAA GAA GAA CTC CCT CGC CTC GCA GAC GAT CTC AAT CGC CGC CGC GTC GCT AGG GCC-3'

2C antisense (69 nucleotides):
5'-CTA GCG ACG CGG CGA TTG AGA TCT GCG TCT GCG AGG CGA GGG AGT TCT TCT TCT AGG ACA TTG AGA TTC-3'.

3C sense (129 nucleotides):
5'-CTC GGG AAT CTC AAC CTA GAA GAA GAA CTC CCT CGC CTC GCA GAC GCA GAT CTC AAT CGC CGC GTC GCC CTA GAA GAA GAA CTC CCT CGC CTC GCA GAC GCA GAT CTC AAT CGC CGC GTC GCT AGG GCC-3'

3C antisense (123 nucleotides):
5'-CTA GCG ACG CGG CGA TTG AGA TCT GCG TCT GCG AGGCGA GGG AGT TCT TCT TCT AGG GCG ACG CGG CGA TTG AGA TCT GCG TCT GCG AGG CGA GGG AGT TCT TCT TCT AGG ACA TTG AGA TTC-3'.

1 SV40 NLS sense (47 nucleotides):
5'-CCG GAA ACT ACT GTT GTT CCT AAG AAG AAG AGA AAG GTG TAG GGG CC-3'

1 SV40 NLS antisense (39 nucleotides):
5'-C CTA CAC CTT TCT CTT CTT CTT AGG AAC AAC AGT AGT TT-3'

2 SV40 NLS sense (68 nucleotides):
5'-CCG GAA ACT ACT GTT GTT CCT AAG AAG AAG AGA AAG GTG CCT AAG AAG AAG AGA AAG GTG TAG GGG CC-3'

2 SV40 NLS antisense (60 nucleotides):
5'- C CTA CAC CTT TCT CTT CTT CTT AGG CAC CTT TCT CTT CTT CTT AGG AAC AAC AGT AGT TT-3'

3 SV40 NLS sense (92 nucleotides):
5'-CCG GAA ACT ACT GTT GTT CCT AAG AAG AAG AGA AAG GTG CCT AAG AAG
AAG AGA AAG GTG CCT AAG AAG AAG AAG AGA AAG GTG TAG GGG CC-3'

3 SV40 NLS antisense (81 nucleotides)
5' C CTA CAC CTT TCT CTT CTT CTT AGG CAC CTT TCT CTT CTT CTT AGG CAC
CTT TCT CTT CTT CTT AGG AAC AAC AGT AGT TT-3'

2.1.8. Solutions and Buffers

Agarose running buffer (TAE pH 7.8)	40 mM	Tris-Acetat (ROTH, Karlsruhe)
	1 mM	EDTA (SIGMA, Deisenhofen)
Coomasie destaining solution	20 %	Methanol
	5 %	Essigsäure
Coomasie staining solution	0.1 % (w/v) Coomasie brilliant blue	
	7.5 %	Essigsäure
	50 %	Methanol
Moviol	2.4 g	Moviol (HOECHST, Frankfurt) in
	6.0 g	in Glycerin,
	12 ml	200 mM Tris-Buffer pH 8.5
		stored at - 20ºC.
PAGE running buffer 10 X 250 mM Tris-HCl (pH 8.3)		(ROTH, Karlsruhe)
	1920 mM	Glycin (ROTH, Karlsruhe)
	1 %	SDS (MERCK, Damstadt)
PBS (pH 7.4)	171 mM	NaCl (ROTH, Karlsruhe)
	3.4 mM	KCl
	10 mM	Na_2HPO_4
	1.9 mM	KH_2PO_4
TAE buffer (pH 7.8)	40 mM Tris-Acetat (pH 7.8)	(ROTH, Karlsruhe)
	1 mM EDTA (pH 8.0)	(SIGMA, Deisenhofen)
Tris-EDTA	10 mM Tris-HCl (pH 7.5)	(ROTH, Karlsruhe)
	1 mM EDTA (pH 8.0)	(SIGMA, Deisenhofen)

LB medium	10 g	Bacto Tryptone	(DIFCO Labor.,USA)
	10 g	Yeast Extract	(DIFCO Labor., USA)
	5 g	NaCl	(ROTH, Karlsruhe)
ad	1 L	dH$_2$O	
		autoclaved before used	

LB/Ampicilin agar dishes   LB- liquid medium was added to bacto agar at 15 g/L. After being autoclaved the medium was cooled to 50°C before Ampicillin was added to a final concentration of 100 µg/ml. 15 ml aliquots were given in 10 cm culture dishes for bacteria. The dishes were stored at 4°C.

LB/Kanamycin agar dishes   The dishes were prepared as described above but Kanamycin in a concentration was added to a concentration of 30 µg/ml instead of the Ampicillin.

DMEM high glucose   The desiccated powder was dissolved with H$_2$0 to a volume of 9 liter. 3.7 g/L NaHCO$_3$ were added and the pH was adjusted to 7.0 by CO$_2$ before the medium was sterilized by filtration and storage at 4°C. FCS in the required concentration was added to 500 mL of medium.

Medium for storage of cells	60 %	DMEM High Glucose
	20 %	FCS (PANSYSTEMS, Aidenbach)
	20 %	DMSO (MERCK, Darmstadt)

2.1.9. Cell Lines

HepG2	Human immortalized hepatoblastoma cell line
HepG2.2.15.	Human immortalized hepatoblastoma cell line, which is stable transfected with the HBV genome (Sells et al., 1987). The cells secrete infectious HBV.
HuH-7	Human Hepatoma cell line, established from a hepatocellular carcinoma of 57 year old Japanese.

2.1.10. Bacteria

E. coli strain XL-1 Blue   rec A-, lac-, end A1,gyr A96, thi, hsd R17, sup E44,

rel A1 (F', pro AB, lacIq, lacZ, M 15, Tn10 (Bullock

et al. 1987)

2.1.11. DNA Plasmid Vector
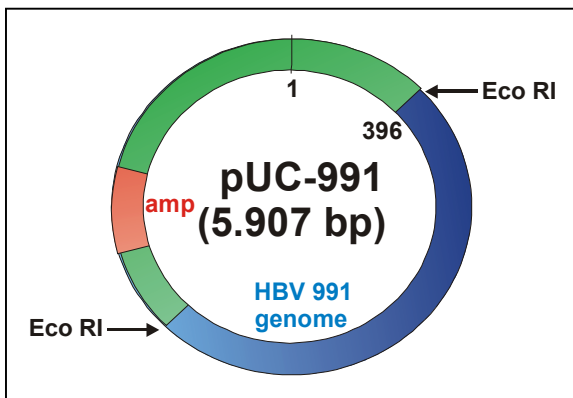
a. pUC-991

Figure 7. Schematic drawing of pUC-991 vector. pUC-991 derived from pUC19 (2686 bp). The entire HBV genome from isolate 991 (3221 bp) was subcloned into the multicloning site by Eco RI restriction site. The vector backbone contains ampicillin resistance gene (Amp^r).
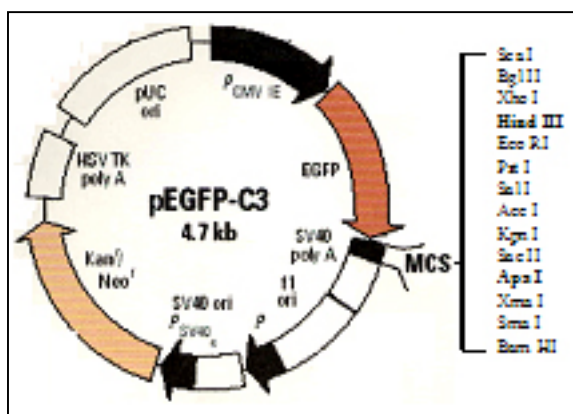
b. pEGFP-C3 (CLONETECH)

Figure 8. Schematic drawing of pEGFP-C3. pEGFP-C3 encodes a red-shifted variant of wild type GFP which has been optimized for brighter fluorescence and higher expression in mammalian cells. The multicloning site (MCS) localized between the EGFP coding sequences and the SV40 poly A. Gene cloned into the MCS will be expressed as fusion to the C terminus of EGFP if they are the same reading frame as EGFP and there are no intervening stop codons. The vector backbone contains an SV40 origin for replication in

mammalian cells expressing the SV40 T antigen. A neomycin resistance cassette (Neo[r]), consisting of the SV40 early promoter, the neomycin/kanamycin resistance gene of Tn5, and poly adenylattion signals from the Herpes simplex virus thymidin kinase (HSV TK), allows stable transfected eukaryotic cells to be selected using G418. A bacterial promoter upstream of this cassette expresses kanamycin resistance in E.coli. (Clonetech technical information).
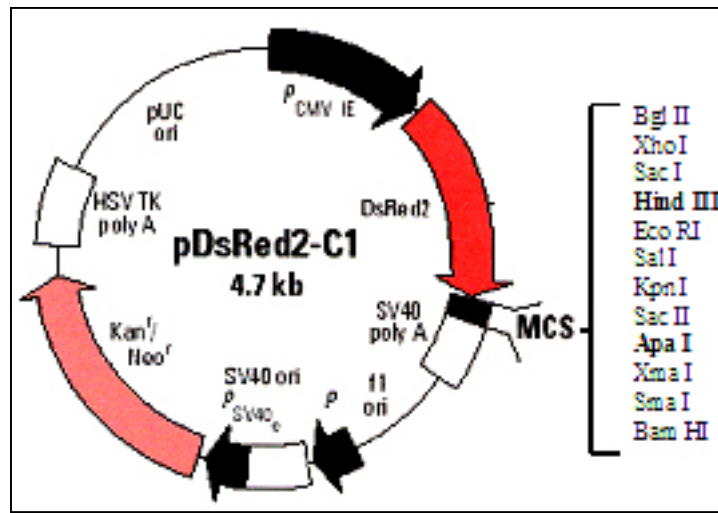
c. pDsRed2-C1 (CLONETECH)

Figure 9. Schematic drawing of pDsRed2-C1. pDsRed2-C1 encodes DsRed2, a DsRed variant that has been engineered for a faster maturation and lower non specific aggregation. The MCS is positioned between the DsRed2 coding sequence and the SV40 poly A. Gene cloned into the MCS will be expressed as fusion to the C terminus of DsRed2 if they are the same reading frame as EGFP and there are no intervening stop codons. The vector backbone contains an SV40 origin for replication in mammalian cells expressing the SV40 T antigen, a pUC origin of replication for propagation in E.coli and an f1 origin for single stranded DNA production. A neomycin resistance casette (Neo[r]), consisting of the SV40 early promoter, the neomycin/kanamycin resistance gene of Tn5, and polyadenylation signals from the Herpes simplex virus thymidin kinase (HSV TK) gene, allows stably transfected eukaryotic cells to be selected using G418. A bacterial promoter upstream of this cassette expresses kanamycin resistance in E.coli (Clonetech technical information).
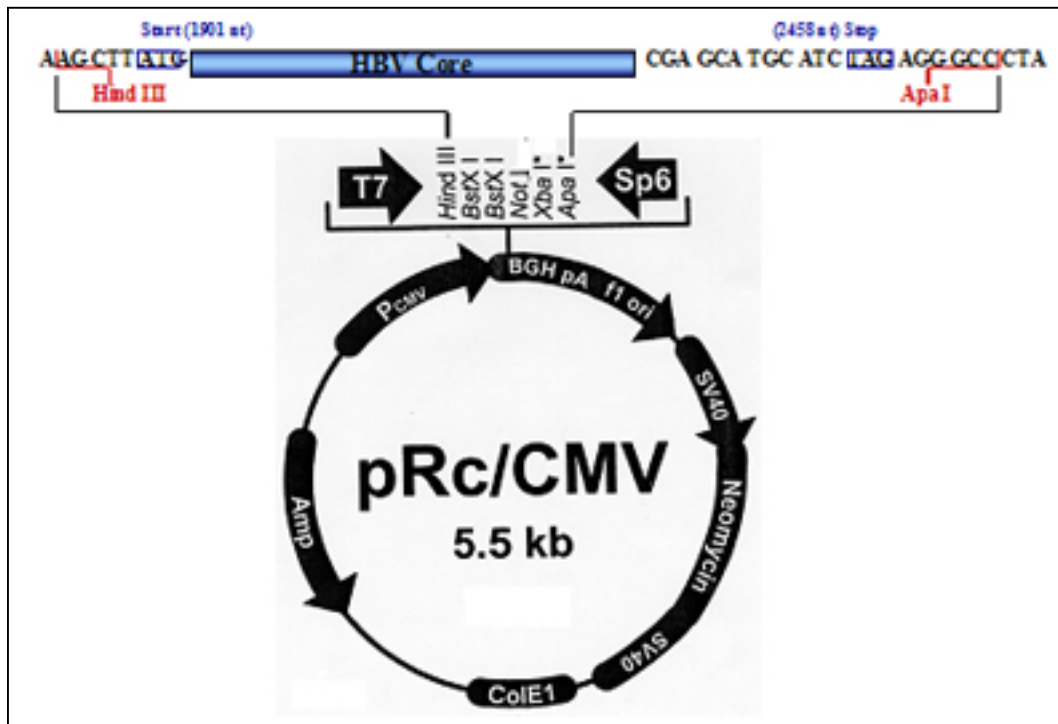
d. pRcCMV-Core

Figure 10. Schematic drawing of pRcCMV-Core. pRcCMV-Core expression vector derived from expression vector pRcCMV (5.5 kb). The HBV core (557 bp) was subcloned into the multicloning site between Hind III and Apa I restriction sites. The vector backbone contains an CMV promoter, neomycin and ampicillin resistance gene (Neo[r] and Amp[r]).

2.2. Methods

2.2.1. Nuclear Localization of Entire HBV Genome in HuH-7 Cell

To study the nuclear localization of entire HBV genome in hepatoma cell line HuH-7, DNA which encodes entire HBV genome from isolate 991 was isolated, purified and transfected into HuH-7 cell lines. The nuclear localization of the entire HBV genome was determined by immunofluorescent staining under confocal laser microscope and then quantified manually (see below).

a. Preparation of Entire HBV Genome

To prepare the entire HBV genome, plasmid vector pUC-991 which derived from pUC-19 and the entire HBV genome from isolate 991, was digested by Eco RI. 1 µl DNA pUC-991 (1 µg/µl) was digested with 1 µl Eco RI enzyme (2 U/µl) in total volume 10 µl in the buffer recommended by the vendor. After over night incubated at 37°C, the digestion products were separated by 1% gel agarose electrophoresis. The gel was stained by ethidium bromide (SERVA) and visualized using UV light. The expected bands appear at a size of 2686 bp (vector pUC-19) and 3199 bp (entire HBV genome). The 3199 bp band was extracted from the agarose gel (SEAKEM) and purified using a gel extraction purification kit (QIAGEN) according to the manufacturers recommendations. After that the DNA was transfected into HuH-7 cells.

b. Preparation of HuH-7

HuH-7 cells were seeded on the culture dish (FALCON) and incubated over night in the incubator CO_2 (HERAEUS) at 37°C. The growing cells were harvested and washed with PBS. The PBS was replaced by 1x trypsin in PBS (GIBCO-BRL), which has been preincubated at 37°C. While the dish with the cells was incubated at 37°C for 2-5 minutes, 0.5 ml 10% FCS containing medium (GIBCO-BRL) were added to the each well of 24 well dish containing collagen-treated cover slips (NUNC INC). The trypsin in PBS was removed and washed the cells with PBS. The PBS was changed with fresh 10% FCS containing medium. Each cover slip (MAGV) were filled with 2-5 drops cell suspension. Then the cells were allowed to grow over night at 37°C in humidified incubator at 5% CO_2.

2.2.2. DNA Plasmid Construction
a. pEGFP-Core 1C

Isolation of the HBV core open reading frame (ORF) was performed by digestion of 1 µl plasmid pRcCMV-Core (1 µg/µl) by the restriction enzyme Apa I (NEB) 5 U/µl

overnight at 25°C. The next day, the linear DNA fragment derived from this digest was digested with 2 U/µl Hind III (NEB) over night at 37°C. After separation of the DNA fragments by 1% agarose gel electrophoresis, the DNA was stained by ethidium bromide. Using UV light for visualization, the DNA fragment representing the HBV core ORF (557 bp) was isolated and purified using a Qiaquick gel extraction kit (QIAGEN).

To prepare the EGFP expression vector, 1 µl pEGFP-C3 (1 µg/µl) was digested with Apa I and Hind III as described above. After gel agarose electrophoresis a linear DNA fragment of 4702 bp was isolated and purified using Qiaquick gel extraction kit as described above. Enzymatic ligation between vector and insert by 3 U/µl T_4 DNA ligase over night at 20 °C generate pEGFP-Core 1C (5259 bp).

b. pEGFP-Core 2 C

Five µl DNA of pEGFP-Core 1C (1 µg/µl) were digested by Ava I (NEB) 1 U/µl at 37° over night in the recommended buffer. The next day, a further restriction digest by Apa I (5 U/µl) were performed, and incubated at 25°C over night. The fragments of DNA were run on 1% agarose gel electrophoresis, then stained with ethidium bromide. Under UV light two linear DNA fragments are seen in size 25 bp and 5234 bp. The DNA fragment 5234 bp was purified using standard protocol of Qiaquick gel extraction kit (QIAGEN). The pure DNA fragment 5234 kb was used as a vector.

As insert a synthetic oligonucleotide was used. The DNA insert for pEGFP-Core 2 C consist of 78 nucleotides (sense) and 69 nucleotides (antisense). The double stranded oligonucleotide contains the restriction sites for Ava I at the 5' and for Apa I at the 3' end. The hybridization was performed by mixing 10 µl DNA sense and 10 µl DNA antisense oligonucleotides that were adjusted to 1 µg/µl. After mixed gently the sample was incubated at 95°C for 2 minutes and then cooled down slowly at room temperature and was finally placed over night at 4°C. Before ligation, the double stranded oligonucleotide was treated with T_4 polynucleotide kinase to add a phosphate group to the 5' ends. The phosphorylation reaction consists of 10 µl DNA, 3 µl 1 mM ATP (BOEHRINGER), 1 µl (10 U/µl) T_4 polynucleotide kinase (NEB), 5 µl BSA (ROTH) at 50 ng/ml and H_2O to a final volume of 35.5 µl. The phosphorylation reaction was performed at 37°C for 1 hour. The T_4 polynucleotide kinase was inactivated at 65 °C for 20 minutes. Enzymatic ligation between this linear vector and synthetic oligonucleotide as described before to generate pEGFP-Core 2C (5312 bp).

c. pEGFP-Core 3 C

The experimental procedures to prepare the DNA vector and the insert of the synthetic oligonucleotide were performed as described for pEGFP-Core 2C (above). The DNA inserts of 3 Core NLS consists of 129 nucleotides (sense) and 123 nucleotides (antisense) respectively. Ligation between this linear vector and synthetic oligonucleotide generates pEGFP-Core 2C (5363 bp).

d. pEGFP-Core Δ NLS

One µl pEGFP-Core 1C (1 µg/µl) was digested by the restriction enzymes Bsp EI (NEB) 1 U/µl and Apa I (NEB) 5 U/µl. The single stranded ends from these digest were filled using T_4 DNA polymerase (NEB) 40 U/µl in the presence of 1 mM dNTP (BOEHRINGER). T_4 DNA polymerase can modify a sticky end strand to the blunt end strand, because of its activities not only as polymerase DNA 5' to 3' direction in a present of dNTP (BOEHRINGER) but also as exonuclease 3' to 5' direction. After enzymatic modification, the plasmid DNA was self ligated by T_4 DNA ligase 3 U/µl. The self ligation product generates pEGFP-Core ΔNLS (5130 bp), which lacks the C-terminus with its NLS.

e. pEGFP-Core 1 SV40 NLS

One µl pEGFP-Core 1C was cleaved in a double restriction digested using Bsp EI 1 U/µl and Apa I 5 U/µl enzymes in total volume 10 µl over night at 37°C. 1% agarose gel electrophoresis and subsequent stain by ethidium bromide showed two linear DNA fragments of 129 bp and 5130 bp. The large fragment was purified as described above and used as the vector. The insert of the synthetic oligonucleotide for 1 SV40 NLS consists of 47 nucleotides (sense) and 39 nucleotides (antisense), containing the restriction sites of Bsp EI at the 5' and of Apa I at the 3' end. Preparation of synthetic oligonucleotide and phoshorylation was performed as described above. The enzymatic ligation between vector and insert generated pEGFP-Core 1 SV40 NLS (5177 bp).

f. pEGFP-Core 2 SV40 NLS

The experimental procedures for preparation of the vector and the synthetic oligonucleotide are described above. The insert of the synthetic oligonucleotide for 2 SV40 NLS consists of 68 nucleotides (sense) and 60 nucleotides (antisense). The enzymatic ligation between vector and insert generated pEGFP-Core 2 SV40 NLS (5198 bp).

g. pEGFP-Core 3 SV40 NLS

Preparation was performed as for pEGFP-Core 1 SV40 NLS (above). The synthetic oligonucleotides for pEGFP core 3 SV40 NLS consists of 92 nucleotides (sense) and 81 nucleotides (antisense). The enzymatic ligation between vector and insert generated pEGFP-Core 3 SV40 NLS (5221 bp).

2.2.3. Ligation

For ligation 1 µl DNA vector and 5 µl DNA insert were ligated with T_4 DNA ligase (NEB) 3 U/µl in total volume 10 µl according to manufacture procedures. The enzymatic ligation was performed over night at room temperature (20-25°C).

2.2.4. Transformation

The ligation products were transformed into competent E. coli. 10 µl DNA were added into 50 µl competent E. coli XL-1 blue. After gentle mixing, the transformation reactions were cooled down on the ice for 10 minutes, then the transformation was accomplished by a heat shock at 42°C for 2 minutes. Then 1 ml LB medium was added and mixed gently. The E. coli were incubated at 37°C for 1 hour and platted onto an agar dish containing LB medium with 30 µg/ml Kanamycin. The dish was incubated at 37°C until the liquid has been absorbed. Then the dish was inverted and incubated over night at 37°C.

2.2.5. Minipreparation DNA Plasmid Isolation

After 16 hours, the bacterial colonies appeared. Using sterile yellow tips, the bacterial colonies were picked and grown in 2 ml Kanamycin (30 µg/ml) containing LB medium. The colonies were incubated in shaking incubator at 37°C overnight. The next day, 1.5 ml bacteria in LB medium was harvested and centrifuged at 6500 rpm for 5 minutes at room temperature. Supernatant was removed and the bacterial pellet was resuspended in 300 µl resuspension buffer (P1 buffer). Afterwards 300 µl lysis buffer (P2 buffer) was added before 300 µl neutralization buffer (P3 buffer) were added. The mix was centrifuged at 12.000 rpm for 10 minutes at room temperature. The clear supernatant was collected and the plasmid DNA was precipitated by adding 0.7 volumes of isopropanol. The solution was mixed gently and centrifuged immediately at 14000 rpm for 15 minutes at 4°C. The supernatant was decanted carefully and the DNA pellet were washed with 500 µl 70% ethanol and dried on air for 5-10 minutes. The DNA was dissolved in 20 µl H_2O. An aliquot (0.5 ml) the bacteria was stored at 4°C.

2.2.6. Restriction Analysis

To restriction analyse of pEGFP-Core 1C was used Bgl II. 1 µl DNA plasmid from each minipreparation sample was digested with 1 µl Bgl II (10 U/µl) in the 10 µl total volume. After over night incubation at 37°C, DNA fragments were run in 1% agarose gel, then stained by ethidium bromide. The same restriction analysis was performed using Apa I (50 U/µl) and Hind III (20 U/µl) enzymes. To restriction analysis of pEGFP-Core 2C and 3C were used also Apa I (50 U/µl) and Hind III (20 U/µl) enzymes. In contrast, Bsp MI (2 U/ µl) was used to restriction analyse of pEGFP-Core Δ NLS, pEGFP-Core 1 SV40 NLS, pEGFP-Core 2 SV40 NLS and pEGFP-Core 3 SV40 NLS. Digestion procedures were performed as described by Bgl II (above).

2.2.7. Maxipreparation DNA Plasmid Isolation.

After restriction analysis, the 0.5 ml of the positive clones were used to inoculate 250 ml LB kanamycin selective medium. The bacteria were grown at 37°C for 12-16 hours with shaking (300 rpm). The next day, 5 ml bacteria in LB medium were removed and 5 ml glycerine (MERCK) was added. This mixture was stored at -20°C. The remaining bacteria were sedimented and the plasmid DNA was isolated using a maxipreparation kit (QIAGEN). This preparation was performed according to the manufacture recommendations.

2.2.8. Preparation of Cell Culture

The cell cultures (HuH-7 and HepG2) were seeded on the culture dish and incubated in the incubator CO_2 at 37°C. After over night incubation, the growing cells were harvested and washed with PBS. The PBS was replaced by 1x trypsin in PBS, which has been preincubated in waterbath at 37°C for 10 minutes. While the dish with the cells was incubated at 37°C for 2-5 minutes, 0.5 ml 10% FCS containing medium were added to the each well of 24 well dish containing collagen-treated cover slips. The trypsin in PBS was removed and washed again the cells with PBS. The PBS was changed with fresh 10% FCS containing medium. Each cover slip were filled with 2-5 drops cell suspension. Then the cells were grown over night at 37°C in humidified incubator at 5% CO_2.

2.2.9. Transfection

Tfx-20 (PROMEGA) was used as transfection agent. For each well, 1 µl DNA (1 µg/µl) was mixed gently with 3 µl Tfx-20, which was than mixed with 300 µl FCS-free medium (GIBCO-BRL). The mixture was incubated at room temperature for 5-10 minutes. During the incubation, the medium in the 24 well dish were removed and replaced with

FCS free medium. The DNA/Tfx-20 reagent/FCS-free medium mixture were vortexed briefly, then added the mixture to the cells (300 µl per well) and incubated in the incubator at 5% CO_2 and 37 °C for 1 hour. During the incubation 10% FCS containing medium was warmed at 37°C in the waterbath. After 1 hour the FCS free medium was replaced with the 10% FCS containing medium and the dish was returned into the incubator for 24-48 hours.

2.2.10. Inhibitor Treatment

a. Staurosporine

Different concentrations of Staurosporine (10 nM, 40 nM and 100 nM) were added to cultured HuH-7 and HepG2 cells for different times (30 minutes, 1 hour, 2 hours, 4 hours and overnight) to determine the toxicity. After the incubation the cells were stained with Trypan blue. Dead cells appeared blue, whereas living cells remained transparent. Based on the result, HuH-7 cells tolerated Staurosporine (SIGMA) at 40 nM overnight, whereas HepG2 cell tolerated 100 nM overnight. For analyzing the effect of Staurosporine on the localization of the fusion proteins the plasmids were transfected and the inhibitor was added 1 hour post transfection before the transfected cell lines were incubated over night at 37°C.

b. Bayer 41-4109

One hour post transfection, the medium was changed and FCS free medium containing Bayer 41-4109 in final concentration 10 nM was added before further incubation at 37°C over night.

2.2.11. Indirect Immune Fluorescence

Cells were fixed on the cover slips with 3% paraformaldehyd (PFA) (SIGMA) in PBS at room temperature for 30 minutes. After fixation the cells were washed with 1x PBS three times before each well was filled with 500 µl 0.1% Triton X-100 (SERVA). The dish was incubated at room temperature for 10 minutes in order to permeabilize the cell membranes. After that, the wells were washed three times with 1x PBS three times. In the primary antibody mixture, mAb 414 was diluted in 1: 300 in antibody solution (1x PBS / 5% BSA/ 5% goat serum), whereas the anti capsid antibody was diluted 1: 200. For each cover slip 40 µl antibody mixture spotted on parafilm in a humidified box. The cover slips were placed with their cell side on the drop of antibody mixture. The humidified box was incubated at 37°C in the incubator. After 1 hour, the up side of cover slips were rinsed with 100 µl 1x PBS before replaced in the 24-well dish. The 24 well dish was washed three

times with 1x PBS. For secondary antibody reaction a goat Texas Red-labelled anti mouse antibody and an Alexa488 goat anti rabbit antibody were diluted 1: 100 in antibody solution. Forty of this antibody mixture was spotted on parafilm in the humidified box followed by transfer of the cover slips as described before. The box was incubated at 37°C for 45 minutes, the cover slips were rinsed, replaced and washed as described. Drops of Dabco-Moviol (SIGMA-HOECHST) were spotted on microscopical glass slides and the cover slips were placed on them. The glass slides were kept over night in the darkness at room temperature.

2.2.12. Immune Fluorescence Confocal Laser Microscopy

A drop of immersion oil was dripped on each of cover slips in the slide. The slide was put on the microscope. The cells were analyzed using a 63x apochromat objective by a LEICA DM IRBE. For the confocal analysis the cells were scanned by a laser power of 30%, a signal amplification of 85% and a pinhole size of 0.9 with a two-fold magnification. Eight pictures were merged. For the representation of Alexa 488, the FITC filter settings were used, for depicting Texas Red, the TRITC filter setting were used. The z position in all picture was adjusted to the equatorial level of the nuclei. The pictures were arranged using the ADOBE-PHOTOSHOP software program.

2.2.13. Quantification of the Intracellular Localization

The HBV capsid protein which found localized in the compartment of HuH-7 cells, was quantified manually using confocal laser microscope. The Amount of HBV capsid that found localized in the cytoplasm, nucleus or both of transfected were quantified in the absolute and relative values.

2.2.14. Quantification of the Cell Division

Two different cell lines (HuH-7 and HepG2) were seeded on a culture dish in the different concentration of FCS (2.5% and 10%). Then the cells were incubated over night in the incubator CO_2 at 37°C. After 24 hours, the growing cells were harvested and collected into 15 ml conical tube. The conical tube was centrifuged at 4500 rpm for 15 minutes, the supernatant was removed and pellet was resuspended by 1 ml medium. The cell suspension was mixed by vortexing. To calculate the start number of cell, 10 µl of cell suspension was pipetted into a haemocytometer counting chamber (NEUBAUER). The same number of cells were seeded and incubated at different serum concentration for 48 hours before the cell number was determined again.

2.2.15. Dimerisation Analysis of EGFP-Core 1C Fusion Protein.

Dimerization was analysed by immune precipitation using an anti-EGFP antibody. Therefore, pEGFP-core 1C vector was transfected into HepG2.2.15 cells that stably express the HBV genome.

a. Preparation of Cell Line and Transfection pEGFP-Core 1C into HepG2.2.15

HepG2.2.15 cells were grown on the collagenized culture dish. In the DMEM 10% FCS, the cells were incubated over night at 37°C. 30 µl DNA of pEGFP-Core 1C in concentration 1 µg/µl were transfected into HepG2.2.15 cells on a 6 cm culture dish. The cells were expended until 20 dishes (15 cm) could be harvested.

b. Isolation of Lysate from the Transfected Cells

Lysate was made from 20 dishes of growing cells. Cells were harvested using a rubber policeman in 1 ml PBS per dish. The cells were collected in a 50 ml conical tube and the cells were sedimented at 4500 rpm for 30 minutes at 4°C. The pellet was resuspended in 5 ml PBS and subjected to 3 freeze and thawing cycles in liquid nitrogen and at 37°C in a water bath. Then Triton X-100 was added to a final concentration of 0.1% and the solution was incubated at 37°C for 10 minutes followed by sonification using an ultrasonic sonicator (in 70% maximal capacity) for 60 seconds for three times. Insoluble components were removed by centrifugation at 15000 rpm for 20 minutes at 4°C. The lysate was treated with 20 ng/ml RNaseA, 20 U/ml S7 nuclease in 15 mM $MgCl_2$ for 1 hour at 37°C. The lysate was concentrated using a Nanosept 3K centrifugal concentrator at 4°C.

c. Concentration of EGFP-Core Fusion Protein

Nanosep 3K (PALL FILTRON) centrifugal concentrators were used to concentrate the lysate. In 2.5 ml of lysate 50 µl 1 mM DTT were added. 500 µl lysate was pipetted into sample reservoir of Nanosep 3K. Then the Nanosep 3K was centrifuged at 10000 rpm at 4°C until it was concentrated to 100 µl.

d. Phosphorylation using $^{32}\gamma$ATP

Before used, lysate of HepG2.2.15 (20 µg/µl) was phosphorylated using 10 µci $^{32}\gamma$ ATP (AMERSHAM PHARMACIA). By adding protease inhibitor, the phosphorylated lysates were incubated at 37°C for 3 hours.

e. Co-immune Precipitation

Thirty μCi [γ^{32}P]ATP and a protease inhibitor mixture (complete, EDTA-free tablet; Roche) was added to the lysate, which was adjusted to pH 7.0, 10 mM MgCl$_2$, 0.2 mM CaCl$_2$.and than incubated for 3 hours at 37°C. For immune precipitation 10 μL anti rabbit-coated biomagnetic beads (DYNAL) were incubated over night with 10 μl of anti capsid antibody (DAKO) in 100 μl PBS/0.1% BSA at 4°C. Unbound antibodies were removed using magnetic absorption to the wall of the tube. The pellet was dissolved in 150 μl PBS/0.1 % BSA and absorbed again. The washing was done 3 times. When precipitation was performed with the anti EGFP antibody, anti mouse coated biomagnetic beads and a monoclonal anti EGFP antibody were used instead. The beads were subjected to 300 μl of lysate over night at 4°C on a rotating wheel. The beads were washed 2 times with 1 ml PBS/0.1 % BSA and 1 x with PBS/0.1 % NP-40. The cups were changed for every washing step. Finally, the pellet was resuspended in 20 μl 1 x loading buffer, 5 min denaturated at 95°C and loaded onto a 4 - 12 % SDS PAGE (INVITROGENE). The gel was dried under vacuum at 80°C followed by exposure of a phosphoimager screen. After 3 days the screen was developed on a phosphoimager.

f. SDS PAGE

Each sample consists of 15 μl sample, 3.5 μl Nupage loading buffer (INVITROGENE) and 1.5 μl (1 mM) DTT (SIGMA). All samples were heated at 95°C for 10 minutes before loading. 20 μl were loaded. The electrophoresis apparatus (INVITROGENE) was attached to an electric power supply, a voltage was applied of 8V/cm to the gel. Then the voltage was increased to 15 V/cm and the Tris-Base 4-12% gel (INVITROGENE) was run until the bromophenol blue reaches the bottom of the resolving gel. The gel was dried under vacuum at 80°C followed by the exposure to a phosphoimager screen.

g. Phosphoimager Screening

A phosphoimager plat is a re-useable plat. Before used, the plat has to be cleaned from useless image by laser light for 20 minutes. The dried SDS gel was laminated and laid on the phosphoimager. To develop the image, the plat was exposed and stored in the casette (AMERSHAM PHARMACIA) and then incubated at room temperature in the dark room. After 3 days exposition, the phosphoimager plat was scanned by Typhoon 9200

(AMERSHAM PHARMACIA). Pictures were saved in IMAGE SQUAN program and worked in ADOBE PHOTOSHOP software program.

3. Results

3.1. Nuclear Localization of HBV Capsids After Transfection of the Entire HBV Genome into HuH-7 Cells

Immunohistochemical detection of the HBV core protein in human livers from HBV infected individuals shows that the HBV capsid stain occurs predominantly within the nucleus (Akiba et al., 1987; Serinoz et al., 2003). Nuclear localization was also observed in mice transgenic for HBV (Guidotti et al., 2002). Using this system it was shown that the nuclear membrane is impermeable for the entire capsid. Since liver cells divide only rarely, the nuclear capsids must be thus derived from capsid protein that either diffuses through the nuclear pore or from capsid protein that is actively transported through the pores. In both scenarios capsid formation occurs within the nucleus when the capsid protein concentration exceeds the minimal assembly concentration, as it was determined by others (Seifer and Standring, 1995).

To study the nuclear localization in more detail, I analysed the localization of the capsid and different core fusion proteins in human liver cell lines by transfection. First, the capsid was transiently expressed in the hepatoma cell line HuH-7 to validate whether transfection results in the same capsid localization than in human livers.
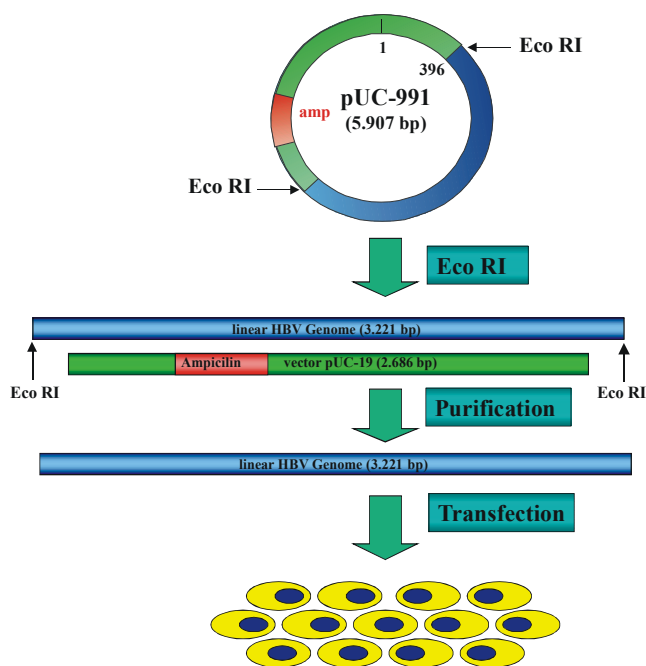
Figure 11. Preparation and transfection of the linear HBV genome into HuH-7 cells. Plasmid pUC-991 was digested with Eco RI. The digestion products were separated by 1% gel agarose electrophoresis. The 3221 bp band of the linearized HBV genome was purified and transfected into HuH-7 cells

In vivo the HBV transcripts are synthesized from a circular HBV DNA genome with overlapping promoters and open reading frames (ORF). Consequently, it cannot be excluded that a promoter is down-regulated by transcription of an overlapping ORF. In order to prevent artefacts by overexpression the capsid was thus expressed in the context of the HBV genome (experimental scheme in Fig. 11). Although the HBV genome has to be circular to express all viral gene products, a linear genome was used since circularization occurs after transfection, as it was determined by others (Sterneck et al., 1998).
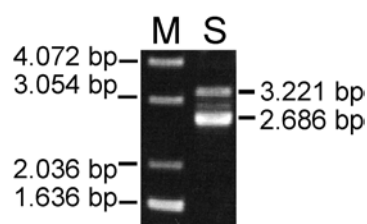
Plasmid pUC-991 that contains

Figure 12. Cleavage products of plasmid pUC-991 by Eco RI. Ethidium bromide stain after agarose gel electrophoresis. Plasmid pUC-991 contains a monomer of the HBV genome (isolate 991) cloned via the single Eco RI restriction site within the vector pUC-19. S shows the reaction products of an EcoRI digest. The vector backbone migrates as a linear DNA fragment of 2686 bp, the HBV genome migrated slower representing 3221 bp. M: DNA molecular weight marker (1 kb plus DNA ladder). Electrophoresis was done on a 1% agarose gel in TAE.
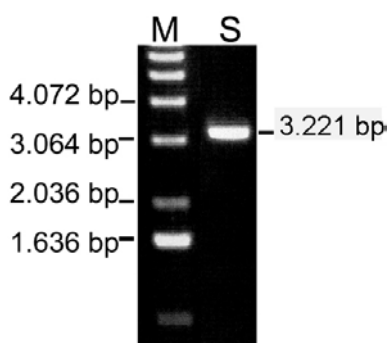
Figure 13. Electrophoresis of the linear purified HBV-991 genome. S shows the HBV-991 genome after purification. No contamination to the vector could be observed. M indicates the molecular weight marker. Electrophoresis and staining were done as in Figure 12.

a full-length linear HBV genome of genotype D (EMBL accession no. X51970) was digested by Eco RI allowing the separation of the HBV genome from the vector backbone. In this linearized HBV genome the ORFs of polymerase and surface protein are discontinuous but the overlapping X-transcription and core-transcription units are unaffected. After separation of the cleavage products on an agarose gel and subsequent ethidium bromide stain two cleavage products of 3221 bp (Fig. 12) representing the HBV genome and 2686 bp representing the pUC vector were detectable. The 3221 bp band was isolated, purified (Fig. 13) and transfected into HuH-7 cells. Twenty four hours after transfection, the transfected cells were fixed and an indirect immune stain against the capsid was performed (Fig. 14). To verify the location within the cell, an additional co-stain against the nuclear pore complexes (NPC) was done. The distribution of the capsid (depicted in green) and NPC (in red) was analysed by confocal laser scan microscopy. The observed localizations were classified in a number of cells as to be predominantly intranuclear, cytoplasmic or equally distributed

within these compartments. Representative fluorescence results are depicted in Fig. 14, the frequency of the distribution is shown in Tab. 1.
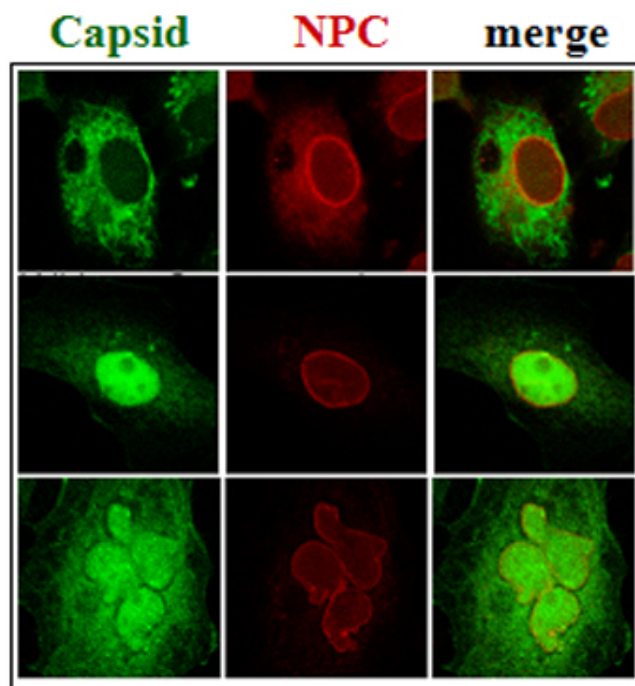

Figure 14. Indirect immune fluorescence of the HBV capsid in HuH-7 cells. Capsids were stained using an anti-capsid primary antibody and a FITC-labeled secondary antibody. The staining patterns are depicted in green (left column). The control stain of the NPCs was performed using a monoclonal antibody (mab) 414 as primary antibody and a Texas Red-labeled secondary antibody, which is shown in red (middle column). The overlay of both staining is shown in the right column. The panels show examples of cytoplasmic (upper row), nuclear (middle row) and an equal distribution (lower row).

Cytoplasm	Nucleus	Both	Total
26	71	3	100
26%	71%	3%	100%

Table 2. Distribution of HBV capsids after transient transfection of the HBV genome into HuH-7 cells. Absolute and relative numbers of cells showing an equal distribution or a predominantly nuclear or cytoplasmic localization of HBV capsids.

As in human HBV-infected livers, the HBV capsid staining was predominantly found within the nucleus (71%). Less frequently, the capsid localized within the cytoplasm (26%). Since the used anti capsid antibody recognizes capsid protein monomers and dimers at least 240 fold less than assembled capsids (Kann et at., 1999), it must be concluded that the stain reflects assembled capsids instead of unassembled capsid protein.

Only in a minority of cases, the capsids were found to show a more or less equal distribution between cytoplasm and nucleus (3%). This low frequency indicates that the capsids are not diffusing within the cells being in accordance to the *in vivo* situation in which the nuclear membrane is impermeable for the capsid. However the significant

number of cells that show different localizations indicates that the cells differ either in their nuclear transport capacity or in that they modify the core protein in a way that affects its nuclear import.

It was previously reported that the HBV capsid protein contains a nuclear localization signal (NLS) within amino acid 157-168 (PRRRTPSPRRR) (Kann et al., 1999) that interacts with the nuclear transport receptor importin α. This complex binds to importin ß that facilitates the nuclear transport of the capsid (Kann et al., 1999, Rabe et al., 2003).

The consensus motif for monopartite NLS is K-(K/R)-x-(K/R). Based on co-crystallisation of importin α with SV40 Tag and Lamin B2-NLS, it was proposed that NLS must contain a Lysine residue within the NLS that interacts with the binding pocket P2 of the importin α molecule (Fontes et al., 2000). The larger side chain of arginine should, according to this study, prevent efficient interaction between NLS and importin α.

The HBV capsid NLS should thus show only a weak interaction importin α but a similar NLS has been described for the HIV Vpr protein (Sherman et al., 2001). However, Vpr is part of the HIV preintegration complex that contains multiple NLS on different proteins (Vpr, MA, integrase) while nuclear transport of the HBV capsid protein is not supported by other karyophilic proteins. On the other hand, on capsids or assembly intermediates the HBV NLS is exposed in redundancy. Such a multiple exposure of an NLS increases the probability of interactions with importin α, assumed to enhance transport competence. Alternatively, additional interactions between the capsid protein and importin α outside the NLS-binding pocket may stabilize the importin α-NLS interaction, as it was shown previously for the BDV protein p10 (Wolff et al. 2000).

To analyze whether the redundancy of the HBV capsid NLS is a prerequisite for nuclear import, fusion proteins of the capsid protein and fluorescent marker proteins were expressed. It has been shown recently that N-terminal fusions of larger polypeptides to the amino-terminus of the core protein prevent capsid assembly (Koletzki et al., 1999).

3.2. Analysis of different Fluorescent Marker Proteins

First, I investigated the intrinsic localization of two commonly used marker proteins, DsRed (red fluorescencent) and EGFP (green fluorescent) by transient expression of the corresponding expression vectors pDsRed2-C1 and pEGFP-C3 in HuH-7 cells (Fig. 15a and b). Both proteins were expressed under the control of the P_{CMV} promoter. The transfection and cell culture conditions were identical to those used for the expression of the HBV capsid in the experiment before. As in this experiment, the staining of the NPCs was done using the same primary antibody. In pDsRed2 transfection an FITC-labelled
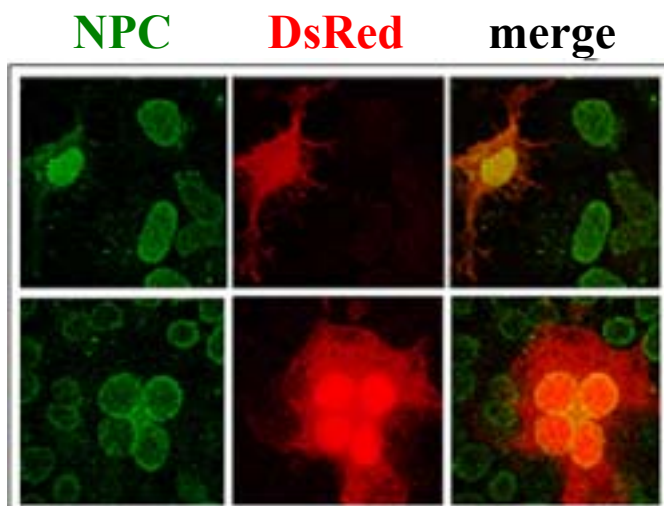
Figure 15a. Localization of DsRed in HuH-7 cells. DsRed (middle column) was found to be localized inside the cytoplasm (upper row) and within the nucleus (lower row) in a similar amount of cells. The nuclear pore complexes are shown in green; the overlays (merge) in the right column.
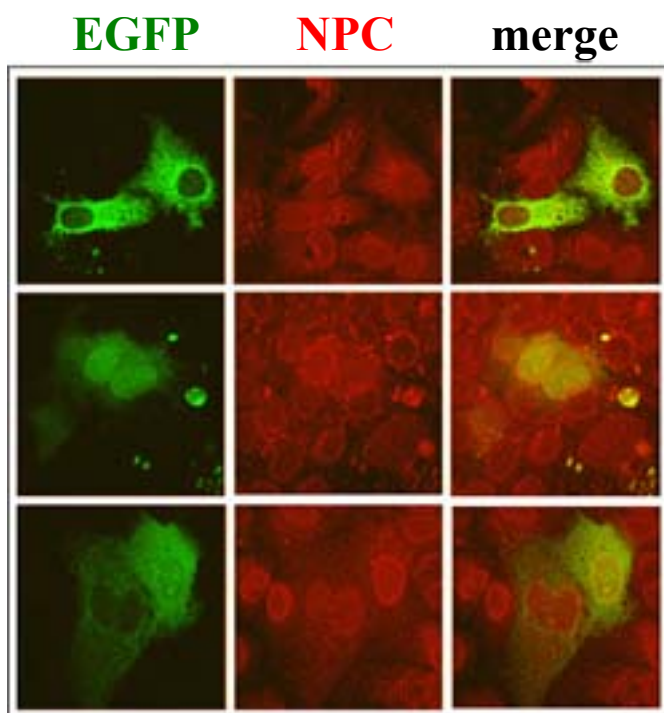

Figure 15b. Localization of EGFP in HuH-7 cells. In the majority of cells EGFP (green) localized predominantly in the cytoplasm (upper row). In a minority of cells EGFP was localized nucleus (midlle row) or throughout cytoplasm and nucleus (lower row, right cell). The nuclear pore complexes are shown in red; the overlays (merge) in the right column.

secondary antibody was used. For localisation of EGFP the secondary antibody was Texas Red labelled. Both transfections were done in parallel to exclude differences caused by the pre-cultivation of the cells prior to transfection. The number of cells showing a predominantly nuclear or cytoplasmic distribution was quantified (Tab. 2).

A proportion of both proteins localized inside the nucleus. In both cellular compartments both fusion proteins were distributed disperse, showing no association to cellular structures. They were only rarely found in both, cytoplasm and nucleus indicating that they are not freely diffusing. The significant number of cells showing a nuclear fluorescence however indicates that either both proteins are weakly karyophilic or that they are passively trapped upon reconstitution of the nuclear membrane following cell division. Since DsRed form tetramers with a resulting molecular weight of 89 kDa, a passive trapping upon cell division appears more likely assuming a diffusion limit of approximately 40-45 kDa through the nuclear pores (Dingwall and Laskey, 1992).

marker	cytoplasm	nucleus	both	total
DsRed2	7	10	0	17
	41%	59%	0	100%
EGFP	100	39	1	140
	71%	28%	1%	100%

Table 3. Distribution of DsRed and EGFP in HuH-7 cells after transient expression. Absolute and relative numbers of cells showing an equal distribution or a predominantly cytoplasmic or nuclear localization of the fusion proteins. Both transfections were done in parallel.

EGFP shows a much higher proportion of cytoplasmic localization, thus being more suitable for analysis of the HBV capsid NLS than DsRed. However, the significant proportion of nuclear EGFP showed that determination of the ratio of cells showing nuclear and/or cytoplasmic fusion protein is required.

3.3. Transport Competence of EGFP-Core Fusion Proteins

3.3.1. Cloning of pEGFP-Core Fusion Protein

To analyse the nuclear transport capacity of the capsid NLS a vector encoding EGFP that was fused in frame to the N-terminus of the capsid protein. For construction of this expression vector, plasmid pEGFP-C3 was cleaved by the restriction enzymes Apa I and Hind III that digest the vector within the multiple cloning site (MCS) downstream of the EGFP ORF. To obtain the capsid ORF, plasmid pRcCMV-Core was cleaved by the same restriction enzymes generating a 557 bp fragment that comprises the entire HBV core ORF (cloning strategy depicted in Fig. 16). The ethidium bromide staining of the purified DNA vector and insert after agarose gel electrophoresis is depicted in Fig. 17.

After ligation, the DNA was analyzed by analytical agarose gel electrophoresis showing different ligation products around 5-6000 bp (Fig. 18) that may reflect linear and circularized vector-insert ligation products. After transformation of *E. coli* XL-1 Blue, the plasmids in the obtained clones were subjected to two restriction analyses using Bgl II and Apa I/Hind III. An example is given in Fig. 19. Bgl II digests within the core ORF, generating fragments of 24 bp, 421 bp and 4814 bp, whereas a digest by Apa I and Hind III removes the entire insert thus generating a 557 bp and a 4702 bp fragment (see restriction map in Fig. 20).
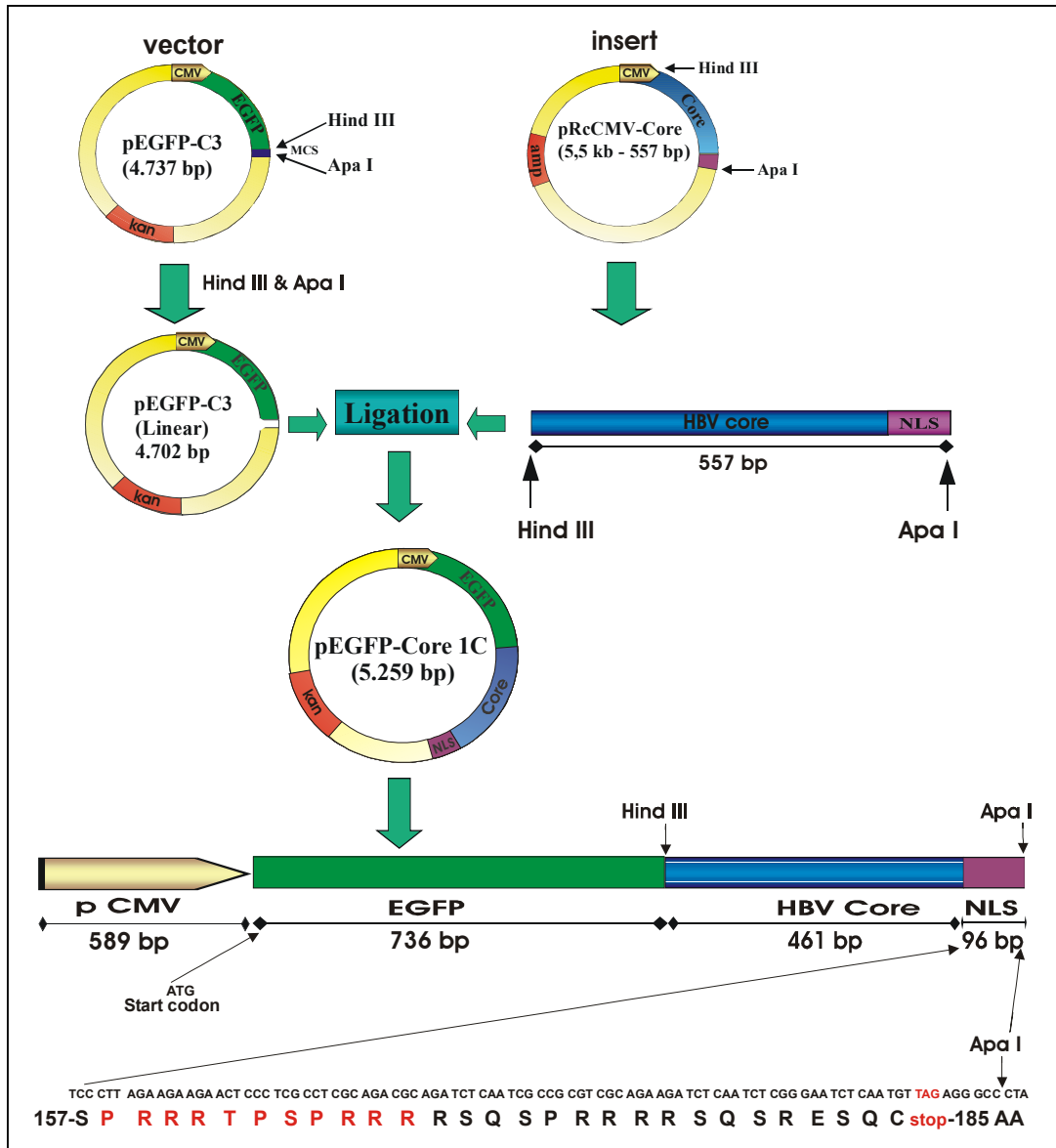
Figure 16. Cloning strategy of pEGFP-Core C1. Plasmids pEGFP-C3 and pRcCMV-Core were digested with Apa I and Hind III. After separation by agarose gel electrophoresis, the DNA fragments of 4702 bp (pEGFP-C3) and 557 bp (pRcCMV-Core) were purified and ligated with T4 DNA ligase.
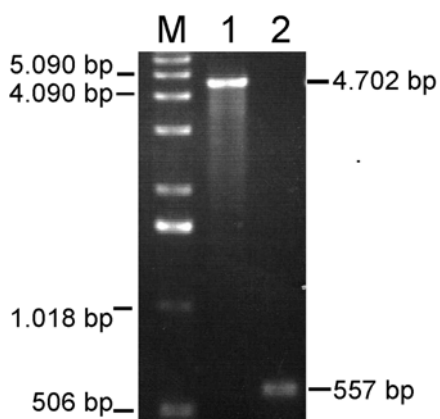

Figure 17. Purified vector and insert for cloning pEGFP-Core 1C. 1: 4702 bp vector-fragment derived from the Hind III and Apa I digest of plasmid pEGFP-C3. 2: 557 bp insert obtained from pRcCMV-Core, digested with Hind III and Apa I. M: DNA molecular weight marker 1 kb plus DNA ladder. The fragments were separated on a 1% agarose gel and stained with ethidium bromide.
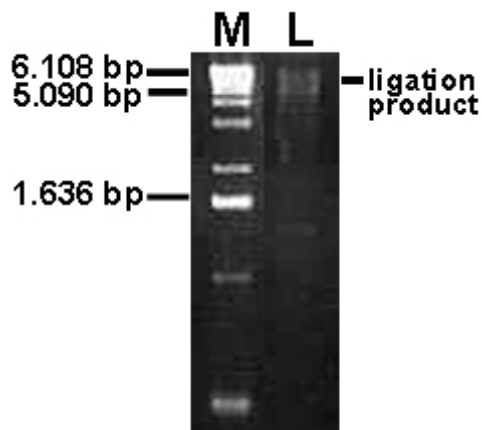
Figure 18. **Analysis of the pEGFP-Core C1 ligation products**. L: Ligation products for the generation of pEGFP-Core 1C. M: DNA molecular weight marker 1 kb plus DNA ladder. The ligation products were separated on a 1% agarose gel and stained with ethidium bromide.
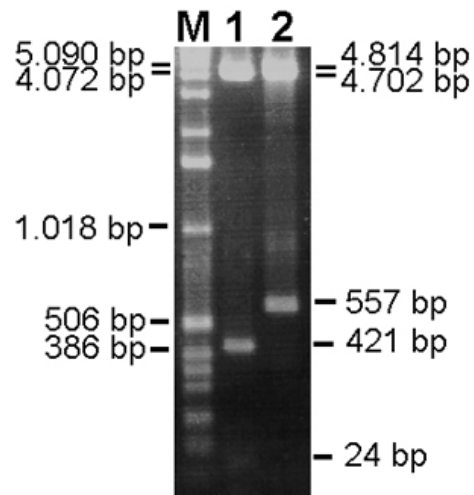
Figure 19. Restriction analysis of a positive pEGFP-Core C1 clone. Lane 1: pEGFP-Core 1C was digested with Bgl II enzyme showing bands of 421 bp and 4814 bp. The estimated position of the 24 bp fragment is indicated. Lane 2: pEGFP-Core 1C was digested with Hind III and Apa I showing a 4702 and a 557 bp band. M: DNA molecular weight marker 1 kb plus DNA ladder. The fragments were separated on a 1% agarose gel and stained with ethidium bromide.
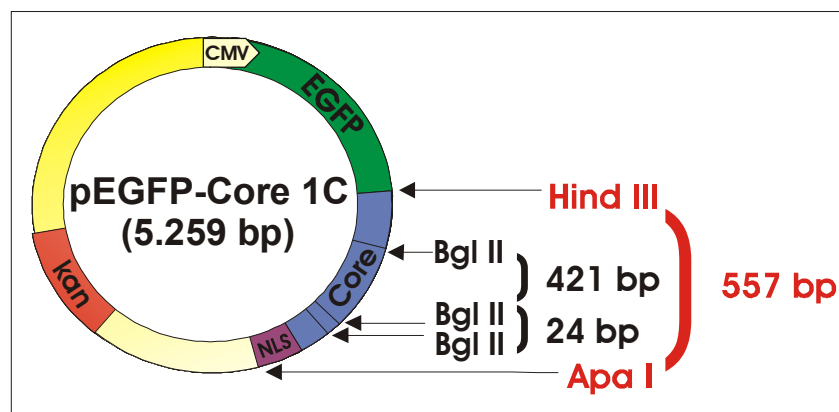
Figure 20. Restriction map of pEGFP-Core C1 for Bgl II, Hind III and Apa I.

.

3.3.2. Localization of EGFP-Core 1C

Having obtained the expression plasmid termed EGFP-core 1C (1C = one capsid NLS) it was transiently expresseded into HuH-7 cells. This transfection and staining was done in parallel to the transfection of pEGFP-C3 described above and is depicted in Fig. 21. The number of cells showing a predominantly nuclear or cytoplasmic localization of the fusion protein was quantified (Tab. 3).
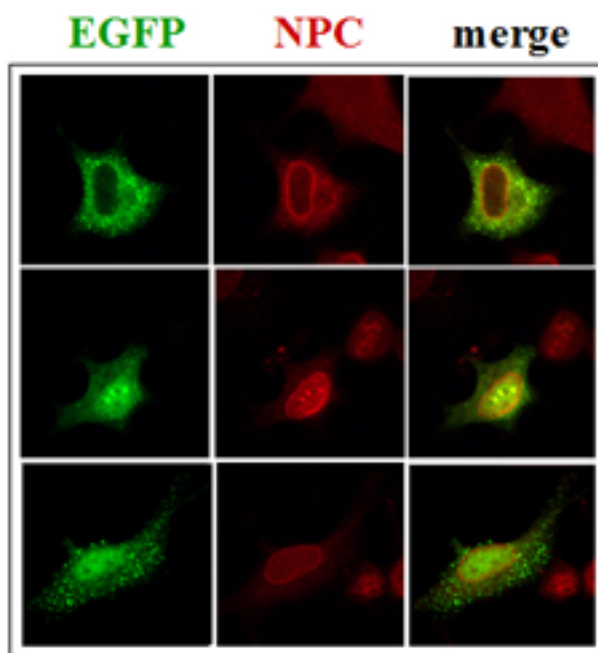

Figure 21. Localization of EGFP-Core 1C in HuH-7 cells. The fusion protein is shown in green (left column), the NPCs are stained by indirect immune fluorescence and are depicted in red (middle column). The overlay (merge) is shown in the right column. The shown cells are representative for 1 to 51 cells showing this EGFP-Core 1C protein distribution. Examples for the localization of EGFP without the capsid protein domain are given in Fig. 15b.

Figure 21 shows examples of the distribution of EGFP-Core 1C protein. Within both compartments the fusion protein enriches in distinct foci (middle row). The pattern differed from that of EGFP that shows a homogeneous distribution, from that of the capsid as shown after transfection of the entire HBV genome and from the nuclear capsid staining after subjection of virus-derived capsids to Digitonin-permeabilized cells (Rabe et al., 2003). The speckled nuclear staining is however in accordance with the previous observation of Vlachou who subjected a conjugate of FITC-BSA with the HBV capsid NLS to Digitonin-permeabilized cells (Vlachou, PhD thesis, 1999). It may be thus speculated that the exposed NLS leads

to another intranuclear distribution than it is found for the assembled capsids that do not expose the C-terminus on their surface. Most likely an interaction of this RNA-binding region causes an interaction with single stranded nucleic acids as it was described by others (Melegari et al., 1991).

Quantifying the ratio of cells with a predominantly cytoplasmic and nuclear distribution (Tab. 3) shows a difference to the EGFP protein in that the number of cells with a nuclear staining was nearly doubled from 28% (EGFP) to 54% (EGFP-Core 1C). As

in all experiments before only a minority showed localization in both cytoplasm and nucleus arguing against passive diffusion.

expressed protein	cytoplasm	nucleus	both	total
EGFP-Core 1C	43	51	1	95
	45%	54%	1%	100%
EGFP	100	39	1	140
	71%	28%	1%	100%

Table 4. Distribution of EGFP and EGFP-Core 1C in HuH-7 cells after transient expression. The distribution of EGFP-Core 1C protein was analysed in 95 cells. The fusion protein predominantly localized within the nucleus while EGFP localizes mainly in the cytoplasm. Both transfections were done in parallel.

It must be thus concluded that the capsid protein has some transport capacity although being unable to translocate all fusion proteins through the nuclear pore into the karyoplasm. However, since the difference was not striking, transient expression of the EGFP-core 1C protein was repeated three times in order to analyse the reproducibility of the assay and to validate the results (Tab. 4).

no.	expressed protein	cytoplasm	nucleus	both	total
1.	EGFP-Core 1C	43	51	1	95
		45%	54%	1%	100%
2.	EGFP-Core 1C	14	25	1	40
		35%	64%	1%	100%
3.	EGFP-Core 1C	40	64	1	105
		38%	61%	1%	100%
4.	EGFP-Core 1C	33	36	0	69
		48%	52%	0%	100%

Table 5. **Localization of EGFP-Core 1C fusion protein in HuH-7 in different transfections done at different time points.** The transfections were done at different times using the same plasmid stock for transfection. The nuclear localization was found in 52% - 64% of the cells. Corresponding, cytoplasmic localization ranged between 35% - 48%.

Although differences up to 13 % were observed between the different experiments, the fraction of cells showing nuclear fusion protein localization was always higher than the cells expressing EGFP without the capsid domain. Overall however the nuclear import capacity of the capsid protein appears to be not strong.

3.4. Localization of EGFP-Core Fusion Proteins with Redundant NLS in HuH-7 Cells.

3.4.1. Cloning of EGFP-Core 2C, 3C and ΔC Fusion Protein

3.4.1.1. EGFP-Core 2C

To analyse the strength of the core NLS, EGFP-Core 1 C was compared with other EGFP-Core fusion proteins, which comprised the capsid NLS either in a duplet or a triplet. The generation of the respective pEGFP-Core vectors was done by digesting pEGFP-Core 1C by Ava I and Apa I, followed by ligation with a double stranded synthetic oligonucleotide that encodes the amino acid sequence SPRRRTPSPRRRRSQSPRRRR in frame with the core ORF. The oligonucleotide harboured the restriction ends of Ava I and Apa I and was phosphorylated at their 5' ends. The cloning strategy is depicted in Fig 22.
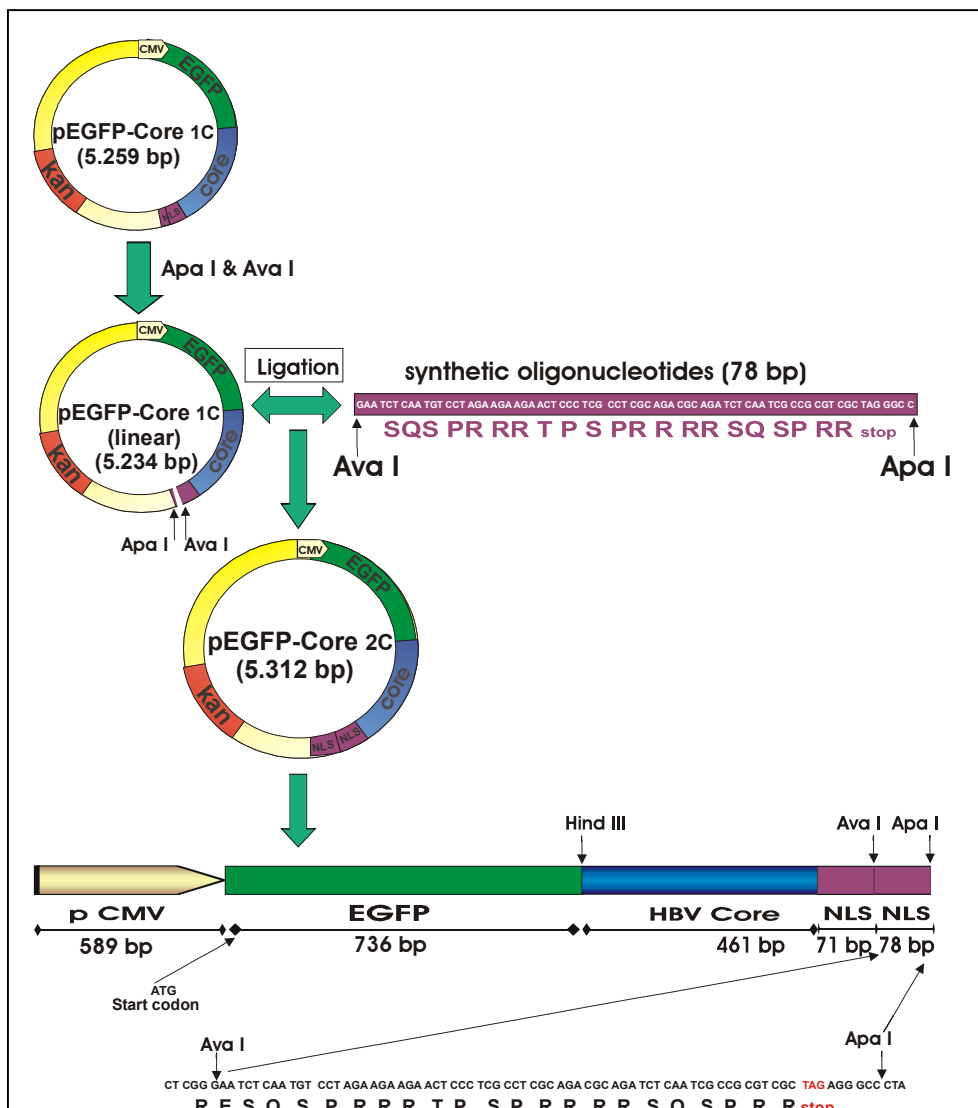
Figure 22. Cloning strategy of pEGFP-Core 2C. Plasmid pEGFP-Core 1C was digested with Ava I and ApaI. The large linear DNA fragment was ligated with a double stranded oligonucleotide encoding the capsid NLS.

After transformation of E. coli XL-1 blue, the plasmids in the obtained clones were purified and analyzed by restriction digests using Hind III and Apa I. Positive clones (lanes 1 and 6) showed two bands DNA of 610 bp and 4702 bp (Fig. 23).
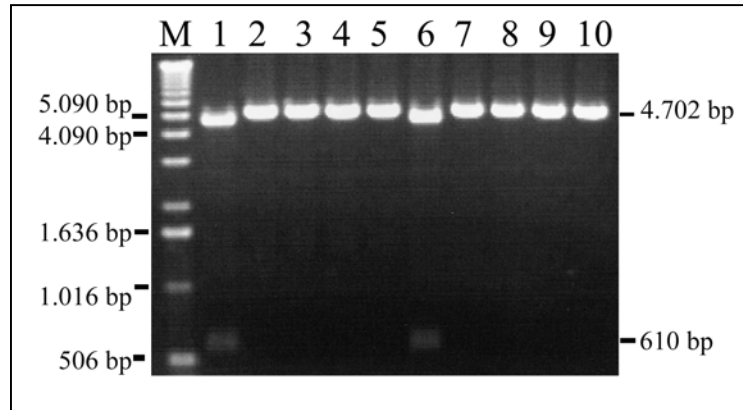

Figure 23. Restriction analysis of EGFP-Core 2C clones. Plasmid preparations of DNA from 10 clones were digested with Hind III and Apa I. The fragments were separated by 1% agarose gel electrophoresis followed by ethidium bromide staining. Lanes 1 and 6 show correct digestion products in which 2 bands of 610 bp and 4702 bp appear. M: DNA molecular weight marker 1 kb plus DNA ladder.

3.4.1.2. EGFP-Core 3C

To express an EGFP-Core fusion protein with a triple HBV core NLS the same cloning strategy as for generation of the pEGFP-Core 2C vector was used. The large pEGFP-Core Ava I and Apa I cleavage fragment was used as the backbone but a synthetic oligonucleotide encoding the amino acid sequence SPRRRTPSPRRRRSQSPR RRRSPRRR TPSPRRRRSQSPRRRR was inserted (see Fig. 24).

After transformation of E. coli XL-1 Blue, the plasmids in the obtained 10 clones were purified and analyzed by restriction digests using Hind III and Apa I. Positive clones (lane 1, 8 and 10) showed the expected two bands DNA of 661 bp and 4702 (Fig. 25).
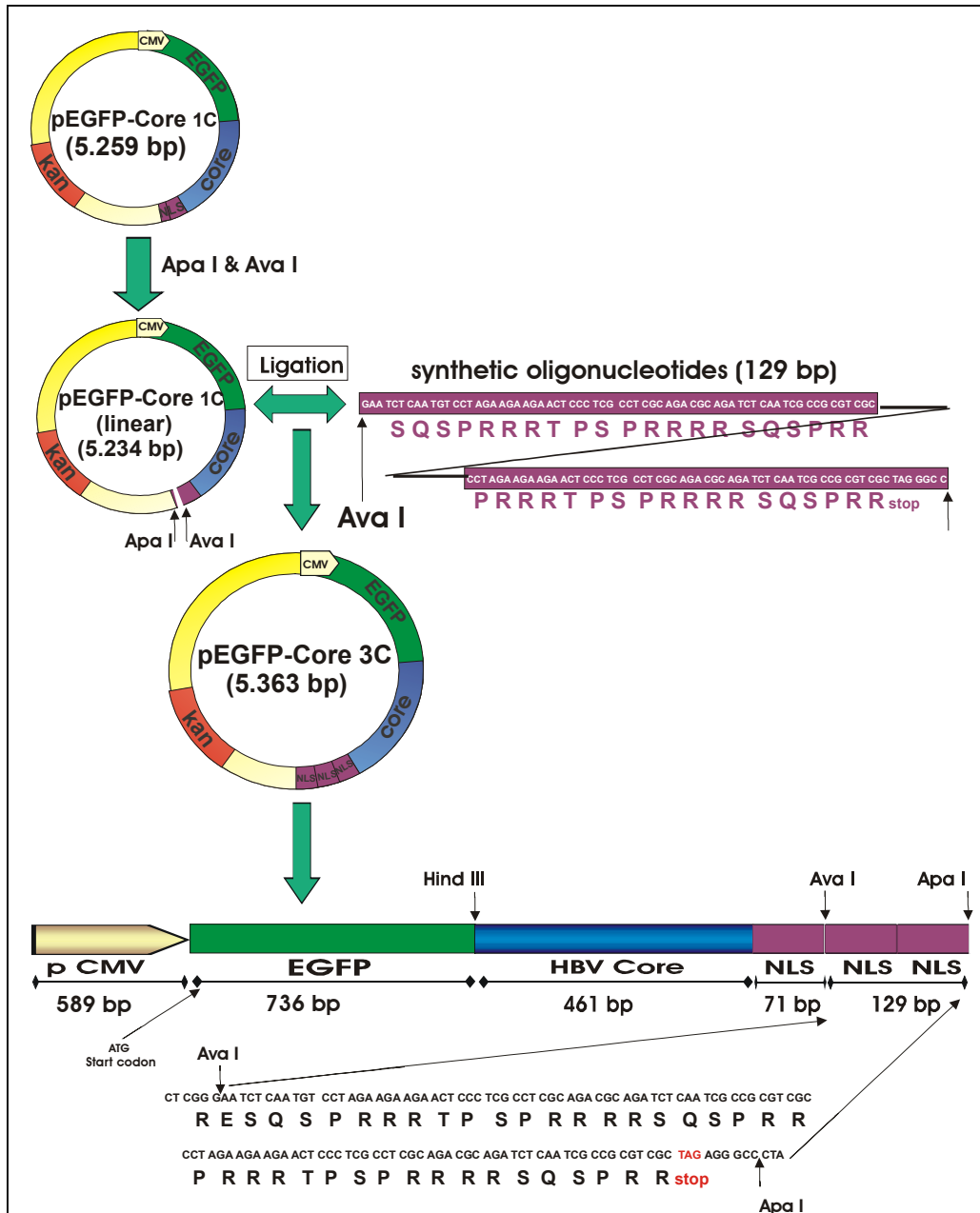
Figure 24. Cloning strategy of pEGFP-Core 3C. The cloning strategy of pEGFP-Core 3C was performed as described before for pEGFP-Core 2C. The synthetic oligonucleotides consist of double HBV core NLS between restriction site Ava I and Apa I.
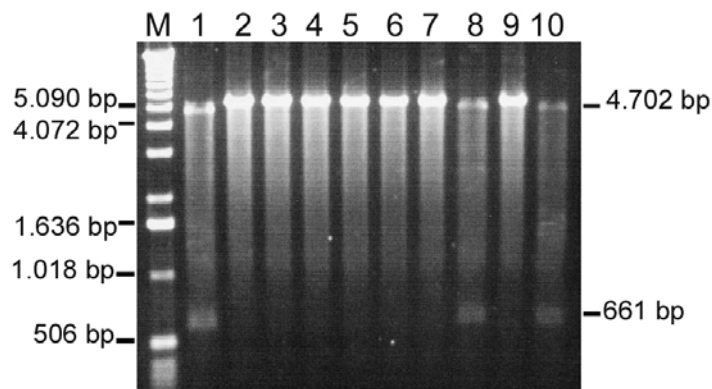

Figure 25. Restriction analysis of EGFP-Core 3C clones. 10 clones were analyzed by Hind III and Apa I. Fragments were separated by 1% agarose gel electrophoresis followed ethidium bromide staining. Lanes 1, 8 and 10 show correct digestion products in which 2 bands of 661 bp and 4702 bp appear. M: DNA molecular weight marker 1 kb plus DNA ladder.

3.4.1.3. EGFP-Core ΔC

Although not containing NLS, the experiments have shown that marker proteins as the EGFP and DsRed are not inert with regard to their nuclear localization. To exclude that the core protein backbone without the NLS-comprising C-terminus already affects the localization of the fusion proteins, a further expression vector serving as a negative control was generated. The expression plasmid, pEGFP-Core ΔC, encodes the EGFP-Core fusion protein being C-terminally truncated at amino acid 143 of the core protein. The cloning strategy was accomplished by restriction digest of pEGFP-Core 1C with Bsp EI and Apa I followed by filling the single stranded part of the resulting sticky ends into blunt ends using T_4 DNA polymerase and dNTP (see Fig.26). The isolated large fragment was purified and ligated.
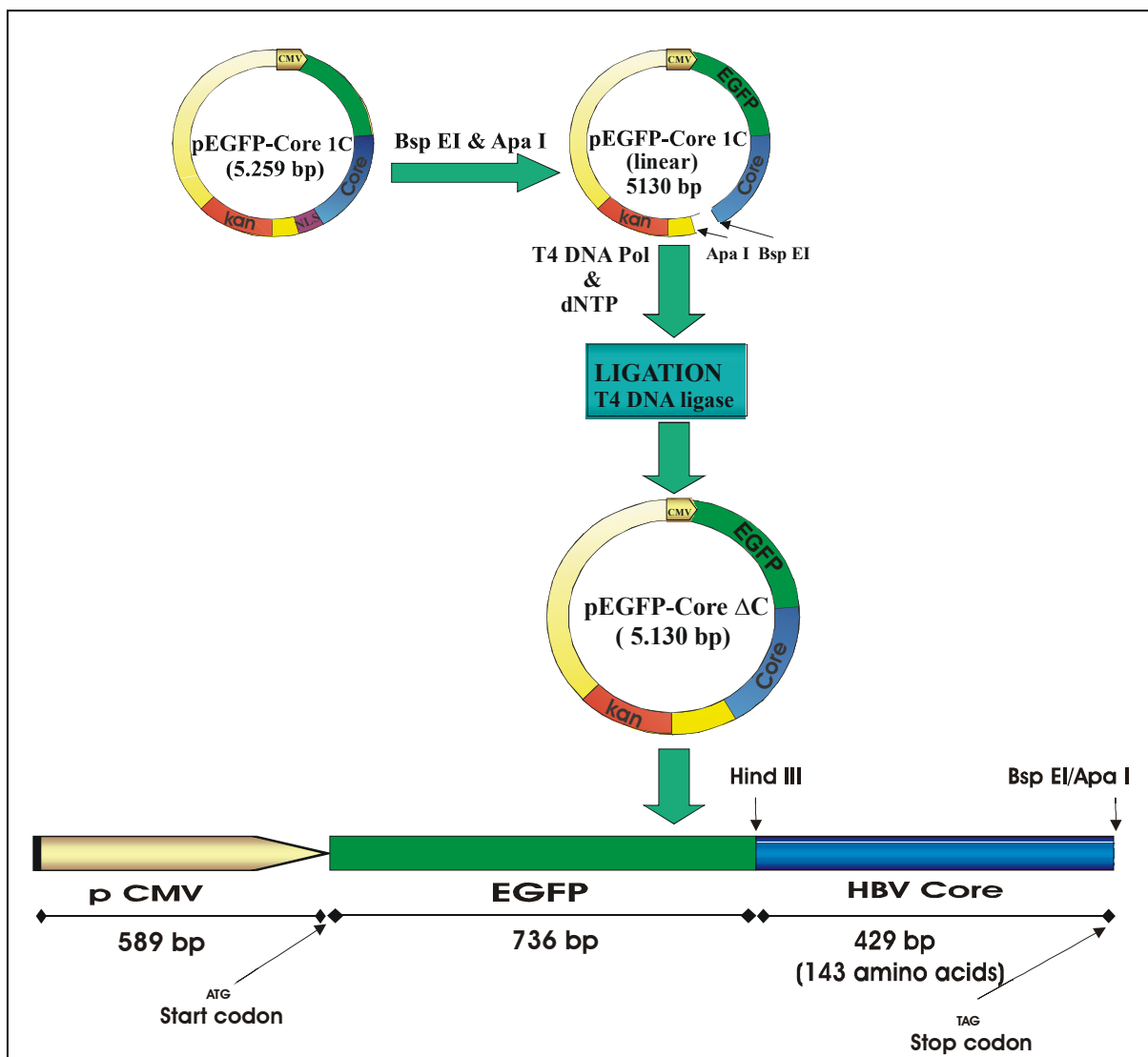
Figure 26. Cloning strategy of pEGFP-Core ΔNLS. Plasmid pEGFP-Core 1C was digested with Bsp EI and ApaI. The single stranded overlapping ends were converted into double stranded ends using T_4 DNA polymerase and dNTP. The purified large fragment was self ligated using T_4 DNA ligase.
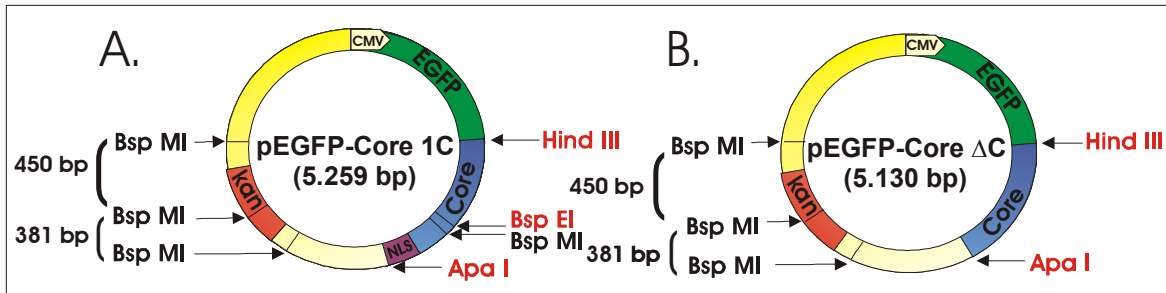
Figure 27. Restriction Map of pEGFP-Core C1 and pEGFP-Core ΔC. A. pEGFP-Core 1C digested with Bsp MI generates 4 bands of 381 bp, 450 bp, 1358 bp and 3070 bp. B. pEGFP-Core ΔC digested with Bsp MI only generates 3 bands of 381 bp, 450 bp and 4299 bp, because the Bsp MI site within the C terminus of core is removed.

Restriction analysis of the plasmids by Bsp MI showed that 8 out of 13 clones (2, 3, 4,5,6,7,9 and 11) encode the EGFP-Core ΔC protein, as determined from their cleavage products of 381 bp, 450 bp and 4229 bp (see Fig. 27, 28). Clone 1 most likely shows an incomplete digest of pEGFP-Core 1C that apparently was still present in the vector preparation.
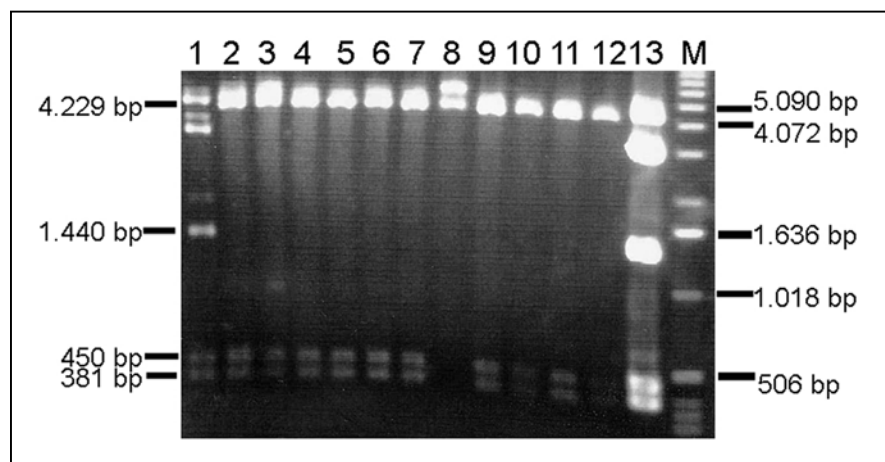
Figure 28. Restriction analysis of pEGFP-Core ΔC clones. Restriction analysis of 13 clones of pEGFP-Core ΔC by Bsp MI. Fragments were separated by 1% agarose gel electrophoresis and subsequently stained with ethidium bromide. Lanes 2, 3, 4, 5, 6, 7, 9 and 11 show correct digestion products in which 3 bands of 381 bp, 450 bp and 4229 bp appear. M: DNA molecular weight marker 1 kb plus DNA ladder.

3.4.2. Cloning of EGFP-Core 1, 2, 3 SV40 NLS

To compare the strength of the capsid NLS with a well-characterized NLS, the C-terminus of the capsid protein domain within the fusion protein was removed and replaced by that of the Simian Virus 40 (SV40) large T antigen. To obtain indirect data on the affinities of these NLS they were cloned in redundancy in close proximity following the idea that if a NLS shows a high affinity it should bind to importin α without diffusing from it. In this scenario the close proximity of the other adjacent NLS prevents binding of a second importin α molecule so that the NLS redundancy should not have an impact on nuclear transport. If the affinity between NLS and importin α is low, importin α can dissociate from the NLS but in case of a redundant NLS the probability of an interaction is increased.

3.4.2.1. EGFP-Core 1 SV40 NLS

The same cloning strategy as for pEGFP-Core 2C was used to generate the expression plasmid pEGFP-Core 1 NLS in which the physiological C-terminus of the core protein was replaced by the NLS of the SV40 Tag. Plasmid pEGFP-Core 1 C was digested with Bsp EI and Apa I. The large DNA fragment of 5123 bp lacking the DNA sequence that encodes the C-terminus was isolated. This vector backbone was ligated to the double-stranded, 5' phosphorylated oligonucleotide encoding the amino acid sequence PKKKRKV (see Fig. 29). This oligonucleotide exposes sticky ends compatible with the overhanging ends of the vector.
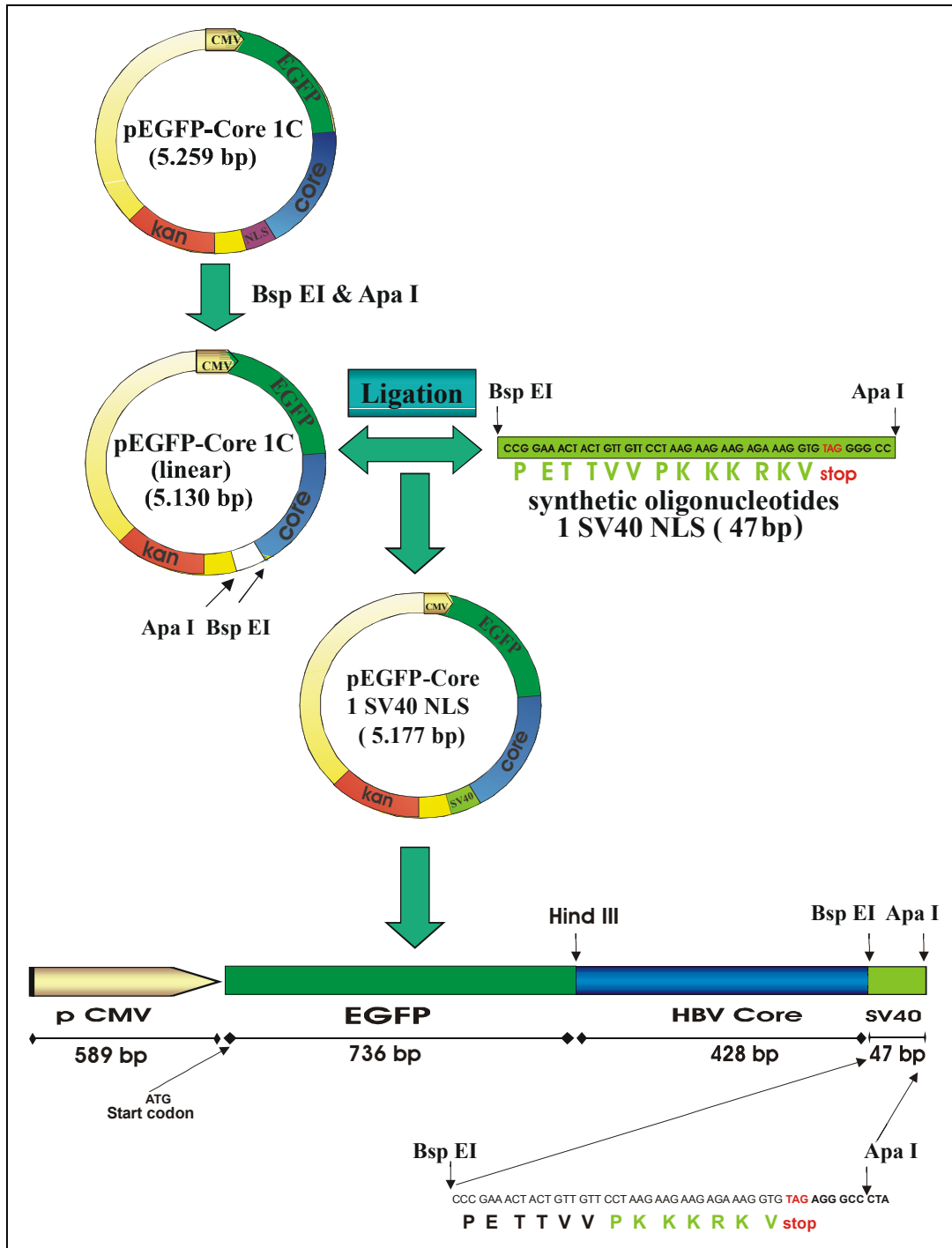
Figure 29. Cloning strategy of pEGFP-Core 1 SV40 NLS. Plasmid pEGFP-Core was linearized using Bsp EI and Apa I. The large linear pEGFP-Core 1C fragment was ligated with a synthetic double-stranded oligonucleotide showing Bsp E I and Apa I compatible ends and that encodes the NLS of the SV40 Tag.

The restriction analysis to identify positive clones was done according to the analysis of pEGFP-Core ΔC by using Bsp MI that should not be present in the final plasmids. Restriction analysis of the plasmids obtained from 6 clones by Bsp MI showed that all transformed clones contained plasmids with the correct restriction pattern of DNA

fragments (381 bp, 450 bp and 4346 bp; see Fig. 30). Clone 6 was expanded and the plasmid DNA termed pEGFP-Core 1 SV40 NLS was isolated.
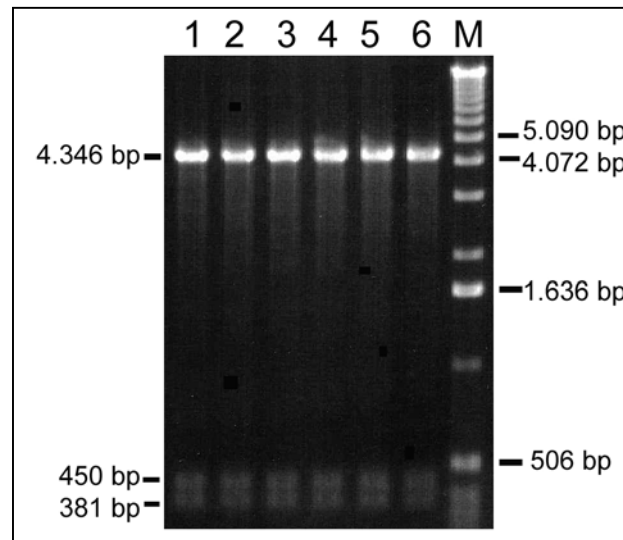

Figure 30. Restriction analysis of pEGFP-Core 1 SV40 NLS. Restriction analysis of 6 clones of pEGFP-Core 1 SV40 NLS by Bsp MI. Fragments were separated by 1% agarose gel electrophoresis and stained by ethidium bromide. All clones show correct digestion products in which 3 bands of 381 bp, 450 bp and 4346 bp appear. M: DNA molecular weight marker 1 kb plus DNA ladder.

3.4.2.2. EGFP-Core 2 SV40 NLS

The same cloning procedure was performed to obtain pEGFP-Core 2 SV40 NLS, which has a duplicated SV40 NLS at the C terminus. After digested by Bsp EI and Apa I, the linear large fragment of pEGFP-Core 1C was ligated with a synthetic, double stranded and phosphorylated oligonucleotide which encodes amino acid sequence PKKKRKV PKKKRKV (see Fig. 31).
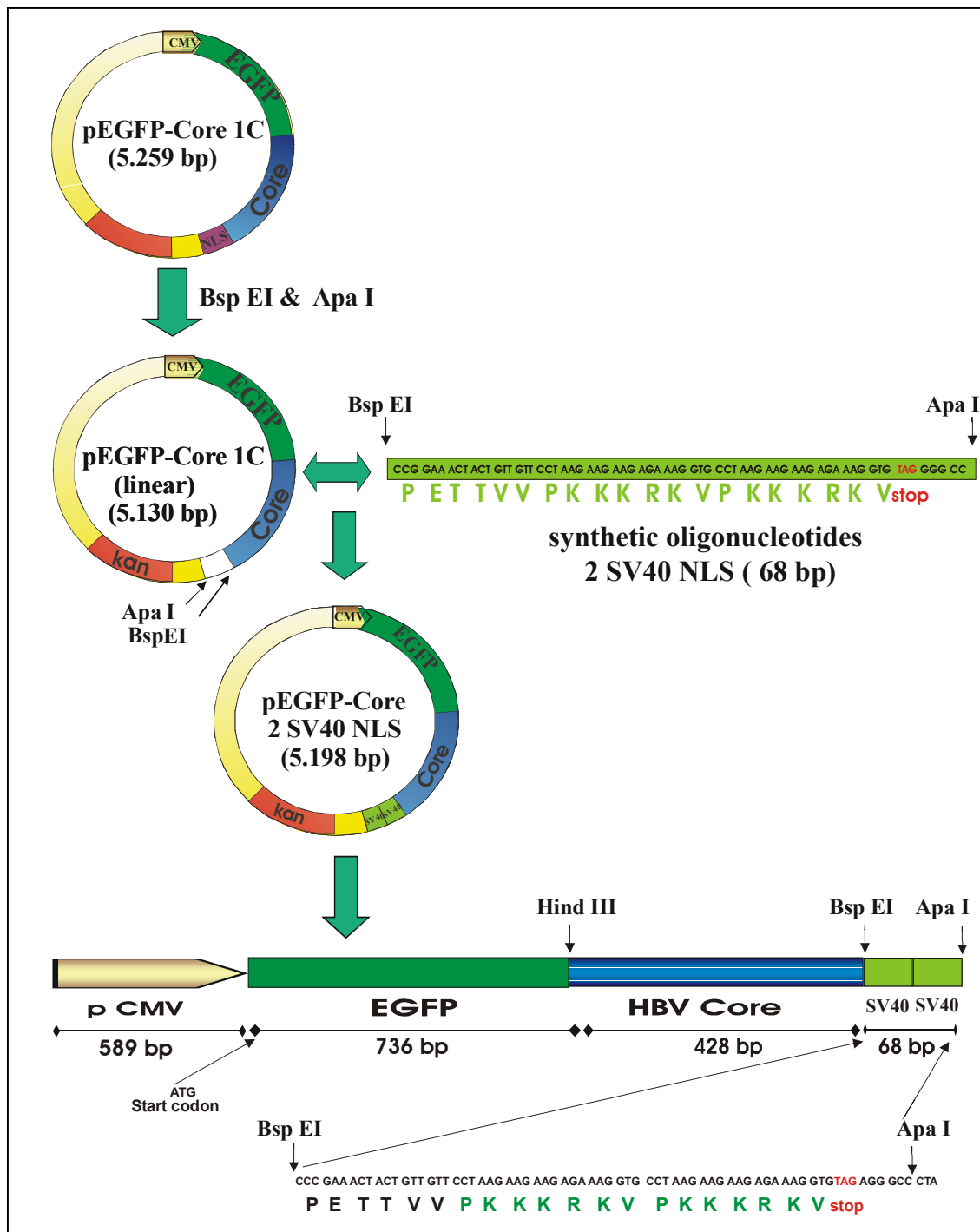
Figure 31. Cloning strategy of pEGFP-Core 2 SV40 NLS. The same procedure was performed with clone pEGFP-Core 2 SV40 NLS as described before. The synthetic oligonucleotide encodes 2 SV40 NLS and has artificial restriction site of Bsp EI and Apa I. The ligation product is pEGFP-Core with 2 SV40 NLS at C terminus.

Restriction analysis of 6 clones showed that all samples are positive clones, which generated bands of 381 bp, 450 bp and 4367 bp (see Fig. 32). Clone 6 was expanded and used for preparation of plasmid pEGFP-Core 2 SV40 NLS.
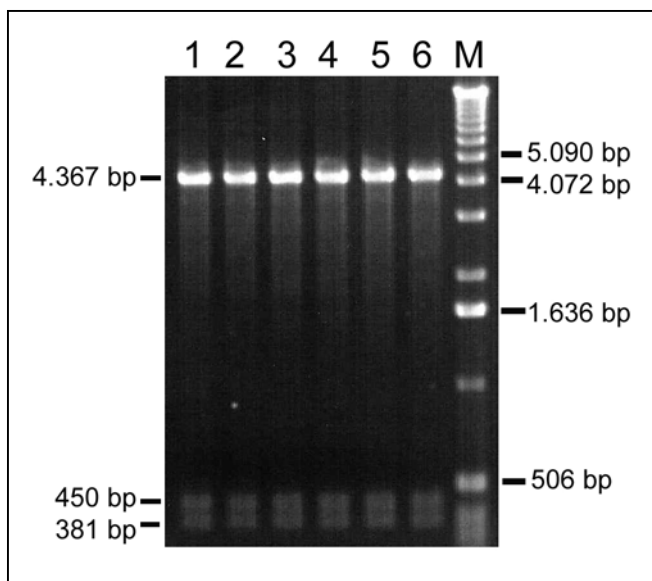
51

Figure 32. Restriction analysis of clones of EGFP-Core 2 SV40 NLS. After plasmid preparation, the DNAs were digested with enzyme Bsp MI. The fragments were separated on a 1% agarose gel and stained by ethidium bromide. All lanes showed bands of 381 bp, 450 bp and 4367 bp. M indicated the molecular weight markers 1 kb plus DNA ladder.

3.4.2.3. EGFP-Core 3 SV40 NLS

The same cloning procedure was performed to clone the EGFP-Core 3 SV40 NLS, which has a triple SV40 NLS at core C terminus. After digested with Bsp EI and Apa I, the linear pEGFP-Core was ligated with synthetic oligonucleotide which encodes amino acid sequence PKKKRKV PKKKRKV PKKKRKV (see Fig. 33 for cloning strategy).

Restriction analysis of the plasmids from the obtained clones by Bsp MI showed that with the exception of clone no 2, all plasmids showed the correct restriction pattern, generating fragments of 381 bp, 450 bp and 4390 bp (see Fig. 34). Clone no. 6 was expanded and used for large scale preparation of plasmid pEGFP-Core 3C.
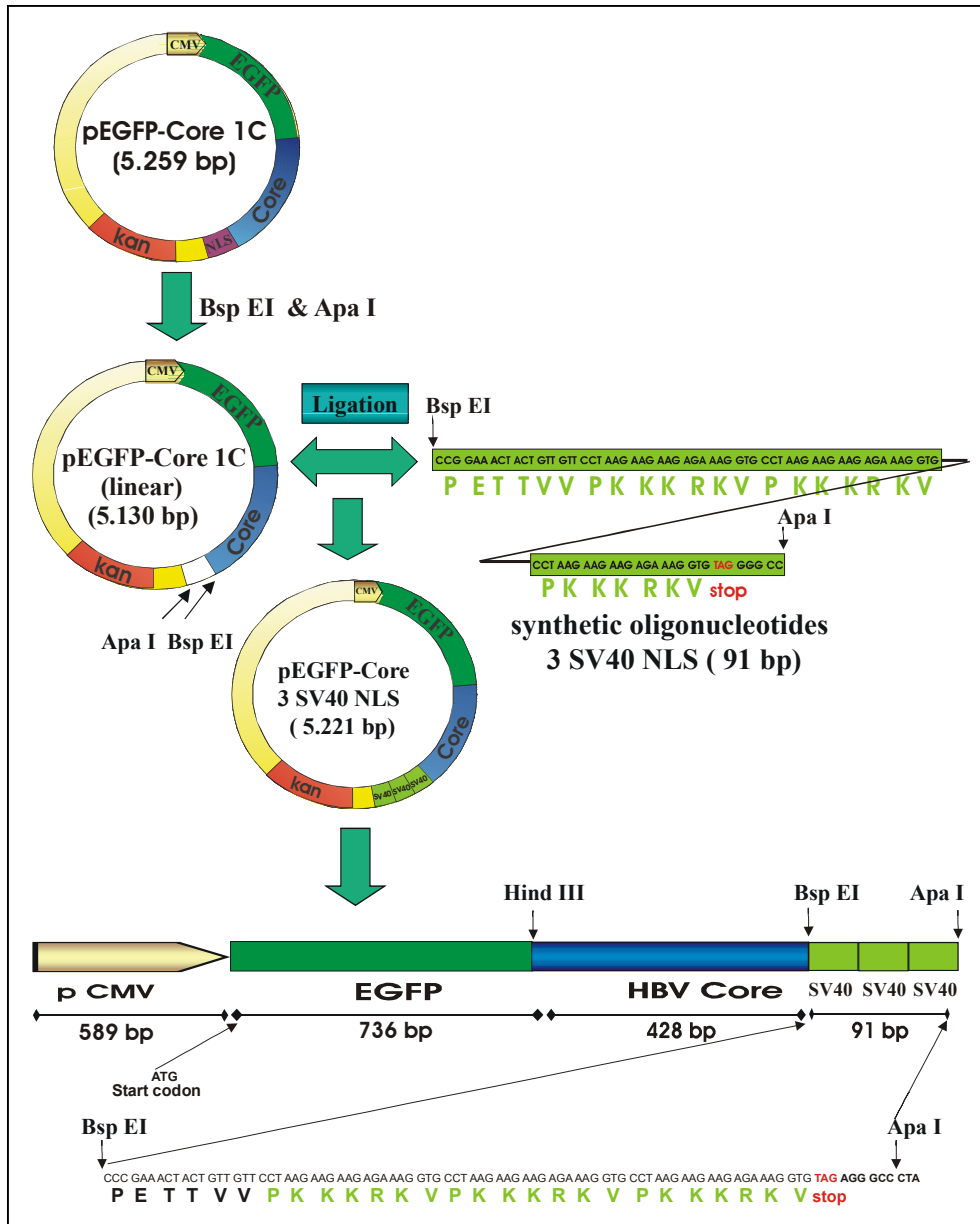
Figure 33. Scheme of cloning strategy of pEGFP-Core 3 SV40 NLS. The same procedure was performed with clone pEGFP-Core 3 SV40 NLS as described above. The synthetic oligonucleotide encodes 3 SV40 NLS and has artificial restriction site of Bsp EI and Apa I. The ligation product is pEGFP-Core with 3 SV40 NLS at C terminus.
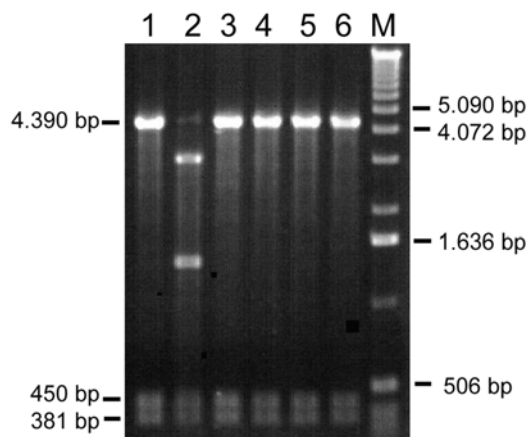

Figure 34. Restriction analysis of DNA EGFP-Core 3 SV40 NLS. After plasmid preparation, the DNAs were digested with enzyme Bsp MI. The fragments were separated on a 1% agarose gel and stained by ethidium bromide. Lanes 1, 3, 4, 5 and 6 showed bands of 381 bp, 450 bp and 4390 bp. M indicated the molecular weight markers 1 kb plus DNA ladder.

3.4.3. Intracellular Localization of pEGFP-Core Fusion Protein and its Redundants

To determine the localization of the pEGFP-Core fusion proteins with redundant capsid and SV40 NLS, all 7 plasmids were transfected into HuH-7 Cells. After fixation, the transfected cells were immunostained and, using confocal laser microscopy, the localisations of the EGFP fusion proteins were determined. Examples are given in figure 35. The number of cells with a predominantly nuclear, cytosolic localization or with a more or less equal distribution of EGFP fluorescence was quantified (Tab. 5).
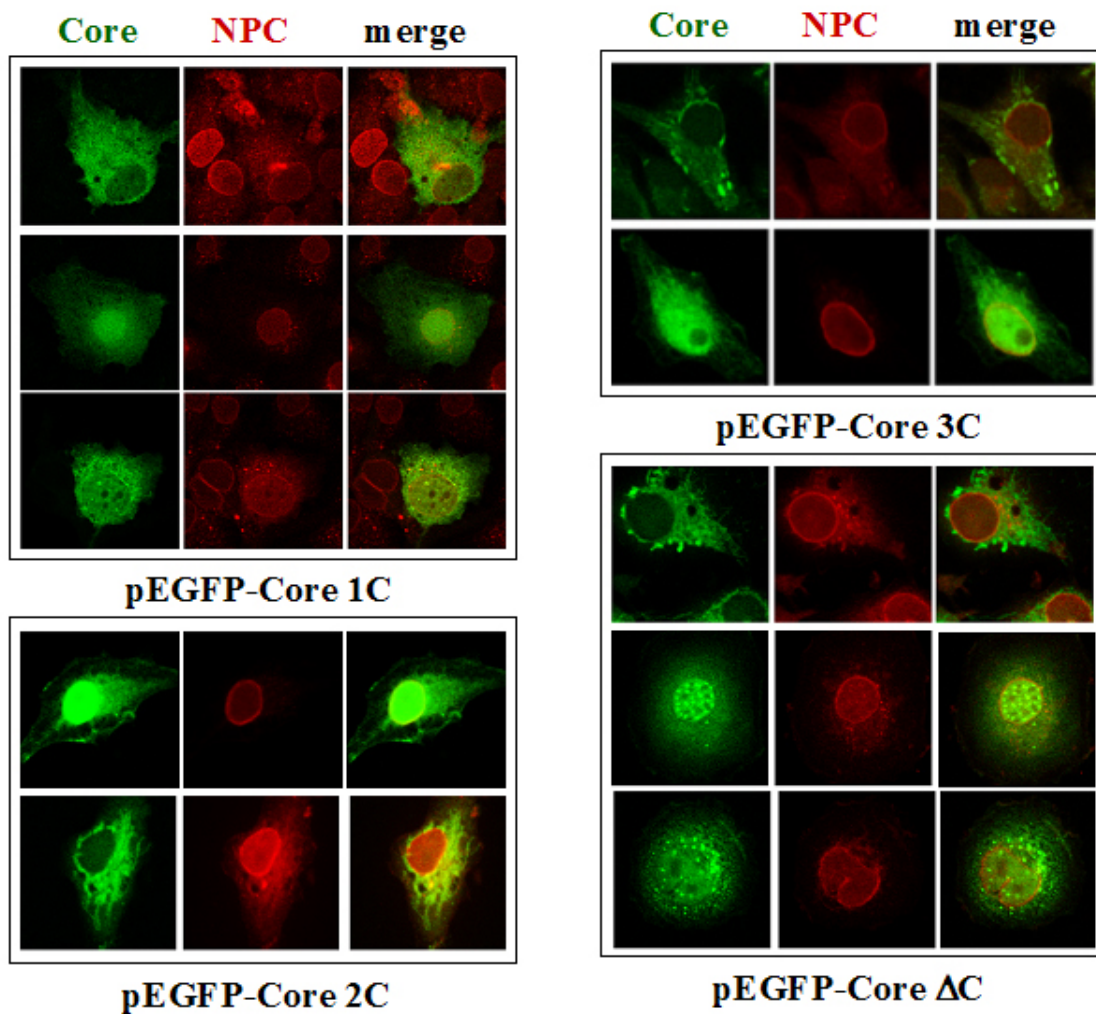

Figure 35 (part one). For legend see next page.

EGFP   NPC   merge

pEGFP-Core 1 SV40 NLS

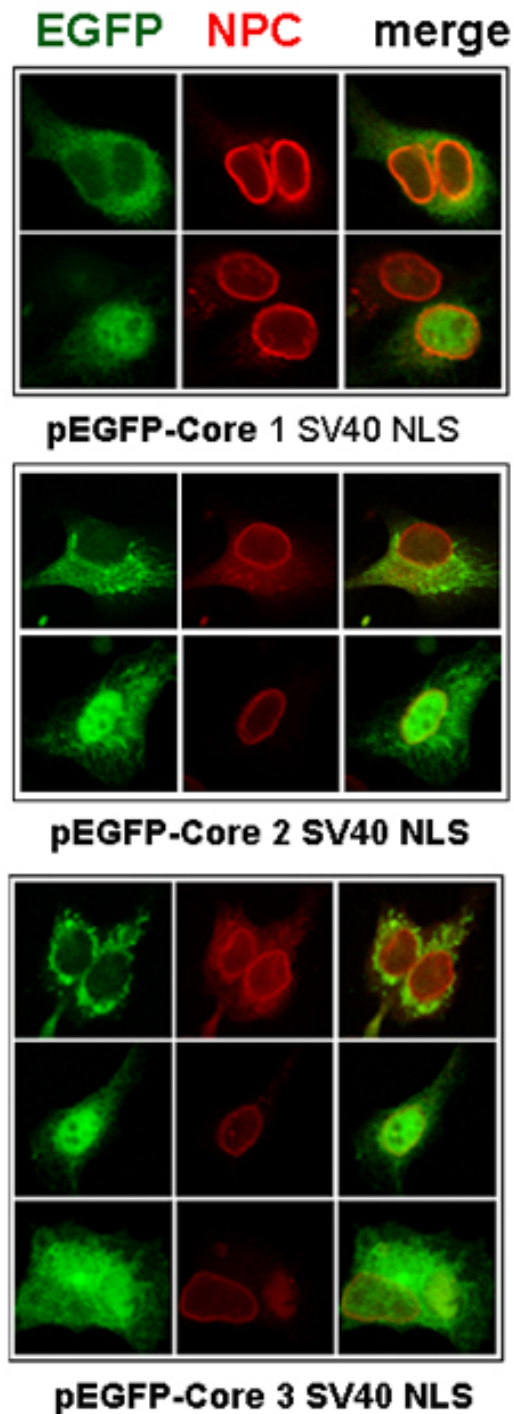pEGFP-Core 2 SV40 NLS

pEGFP-Core 3 SV40 NLS

Figure 35. Localisation of EGFP-Core ΔC, 1C, 2C, 3C and EGFP-Core 1, 2, 3 SV40 NLS in HuH-7 cells. All fusion proteins were either found predominantly in the cytoplasm (upper row) or in the nucleus (middle row) or in rare cases in both cytoplasm and nucleus (lower row) but with a different frequency (see Tab. 5). EGFP-Core fusion proteins are indicated by the green fluorescence, nuclear pore complexes are depicted as red rings. All transfections were done in parallel.

The quantification as depicted in table 5 showed that all fusion proteins exposing an NLS showed a higher ratio of nuclear EGFP than the control lacking the C-terminus. Redundancy of the HBV capsid NLS increased the transport competence from 75% nuclear capsids (1C) to 94% (3C). According to the divergence of the assays determined before, this difference seems to be significant. The import competence of the fusion protein EGFP-Core 2C is in between EGFP-Core 1C and EGFP-Core 3C. Redundancy of EGFP-Core fusion proteins harbouring the SV40 Tag NLSs showed an increasing transport competence correlated with redundancy of the NLS. However, this increase is not as high as observed for the capsid NLS and thus are possibly not significant.

The observation that redundancies of the NLS increase the rate of nuclear fusion protein to some extent indicates that both NLS allow the dissociation from importin α. Thus not only the probability of an importin α-NLS contact determines the nuclear import rate but the affinity between these binding partners. The dissociation from importin α is in accordance with the hypothesis of Schwöbel and Moore (2000) who speculated that an NLS must not be too strong in order to allow dissociation of cargo and import receptors within the nuclear basket. Comparing the import mediated by HBV capsid NLS and the

SV40 Tag NLS both NLS have the same transport capacity indicating that the affinity between importin α and the NLS is similar.

expressed protein	cytoplasm	Nucleus	both	total
EGFP-Core ΔC	29 55%	23 43%	1 2%	53 100%
EGFP-Core 1C	5 25%	15 75%	0 0%	20 100%
EGFP-Core 2C	2 18%	9 82%	0 0%	11 100%
EGFP-Core 3C	2 6%	33 94%	0 0%	35 100%
EGFP-Core 1 SV40 NLS	40 23%	135 77%	0 0%	175 100%
EGFP-Core 2 SV40 NLS	19 20%	75 80%	0 0%	94 100%
EGFP-Core 3 SV40 NLS	9 11%	74 88%	1 1%	84 100%

Table 6. Distribution of EGFP-Core ΔC, 1C, 2C, 3C and of EGFP-Core 1, 2, 3 SV40 NLS fusion proteins in HuH-7 cells. The different EGFP-Core fusion proteins were transfected in parallel. EGFP-Core ΔC serves as a negative control. The other fusion proteins either contain the natural HBV capsid NLS alone or in redundancy (EGFP-Core 1C, 2C, 3C) or the C-terminus downstream amino acid 143 was replaced by the NLS of the SV40 Tag as single, double or triple (EGFP-Core 1, 2, 3 SV40 NLS).

3.5. Effect of Staurosporine on the Localization of EGFP-Core 3 C and 3 SV40 NLS

The HBV capsid protein of the used isolate contains seven phosphorylation sites within the C-terminus comprising amino acids 140-183. One additional phosphorylation site is found upstream of the C-terminus in the flexible linker region at amino acid 139. The degree of phosphorylation, the responsible protein kinase, the used phosphorylation sites and the time point of phosphorylation are not fully understood yet. Phosphorylation at Serine residue 157 is required for pregenome packaging and the residues 164 and 170 are essential for polymerase activity (Gazina et al., 2000; Melegari et al., 2005). Moreover, serine 170 and/or 172 is phosphorylated in capsids from virions (Machida et al., 1991). Some phosphorylation at a non-specified site is essential for nuclear import of the capsids (Kann et al., 1999). However, for entire HBV capsids it is unclear whether the phosphate(s) within the C-terminus is/are required to allow NLS-importin α-interaction or whether phosphorylation induces a structural change that leads to the exposure of the NLS on the capsid surface. Unpublished studies using FITC-BSA-HBV capsid NLS conjugates revealed that phosphorylation within the NLS inhibits the transport capacity of the conjugate (A. Vlachou and M. Kann, pers. communication). However, for the SV40 Tag it was shown that a phosphate directly adjacent to the NLS has a negative effect on

nuclear import while phosphorylation at sites further upstream enhances NLS function (Jans, 1995; Hübner et al., 1997; Jans and Jans, 1994).

In order to analyse the effect of phosphorylation on nuclear transport of the EGFP-Core fusion proteins, cells were treated with a broad-range protein kinase inhibitor after transfection. EGFP-core 3C was used since this protein shows the strongest nuclear localisation thus allowing the best differentiation in case that inhibition of phosphorylation prevents nuclear import. As a control EGFP-Core 3 SV40 NLS was used lacking the C-terminus and the phosphorylation sites downstream of amino acid 143.
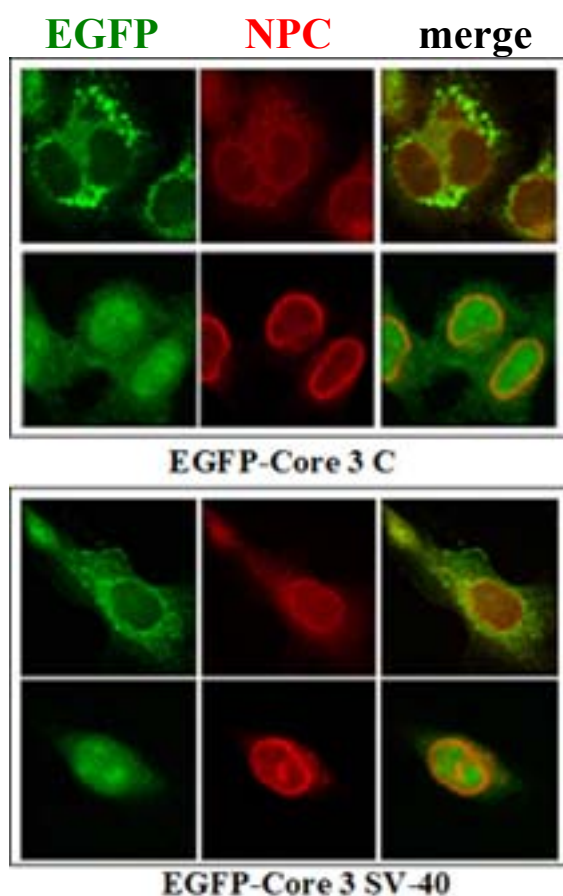

EGFP **NPC** **merge**

EGFP-Core 3 C

EGFP-Core 3 SV-40

Figure 36. Localization of EGFP-Core 1C in HuH-7 cells treated with Staurosporine. EGFP-Core 3C and 3 SV40 NLS fusion proteins localized in the cytoplasm (uuper row) or in nucleus (lower row). Their presence is indicated by the green fluorescence. The nuclear pore complexes are shown as red rim-like stains.

Transient expression revealed that the cytoplasmic and the nuclear appearance of both fusion proteins looked identical (Fig. 36) to their expression in untreated cells (Fig. 35). In all compartments the fluorescences looked condensed in some areas being more pronounced in the cytoplasm. Despite of low transfection efficiency, quantification of nuclear and cytoplasmic localisation in different cells however showed a dramatically changed localization (Tab. 6) in that the vast majority of fusion proteins were found within the cytoplasm. This changed distribution is in striking difference to EGFP that shows an unchanged localization pattern.

The only core protein phosphorylation site present in both fusion proteins is located at amino acid 141. In the SV40 Tag NLS no phosphorylation site is present. Assuming that the dramatic changes in the distribution pattern is caused by an inhibited phosphorylation of the core protein, one must conclude that this site has an essential function in the viral life cycle in that its phosphorylation is important for allowing the NLS

function. However, Staurosporine may have had additional effects. It prevents cell division so that passive trapping of proteins is inhibited.

protein	staurosporine	cytoplasm	nucleus	both	total
EGFP-Core 3 C	no	2	33	0	35
		6%	94%	0%	100%
	yes	13	0	0	13
		100%	0%	0%	100%
EGFP-Core 3 SV40	no	1	18	0	19
		6%	94%	0%	100%
	yes	32	0	0	32
		100%	0%	0%	100%
EGFP	no	18	5	0	23
		78%	28%	0%	100%
	yes	19	6	0	25
		76%	24%	0%	100%

Table 7. Distribution of EGFP, EGFP-Core 3C and pEGFP-Core 3 SV40 NLS in Staurosporine treated HuH-7 cells. Without Staurosporine EGFP-Core 3C and 3 SV40 NLS predominantly localized within the nucleus. Staurosporine treatment changed the distribution pattern in that the cells exclusively show a cytoplasmic localization of the fusion proteins. In contrast, localization of EGFP was not affected.

3.6. Effect of FCS on Intracellular Localization of EGFP-Core Fusion Proteins

3.6.1. Effect of FCS on Cell Division

To differentiate whether cell division (or related phenomena) or fusion protein phosphorylation effects nuclear localization, HuH-7 cells were grown in the presence of 2.5 and 10% FCS. In parallel to transfections with pEGFP-Core 3 SV40 NLS the cells were harvested and counted after seeding and at the time of fixation. The numbers of cells are given in Table 7.

FCS concentration	Start Cell Number	End Cell Number
2,5%	$7,12 \times 10^5$	$1,37 \times 10^7$
10%	$7,12 \times 10^5$	$1,65 \times 10^7$

Table 8. Cell division of HuH-7 cells at different FCS concentrations.

After 48 hours the number of cells differed only marginally. This observation is in accordance with the established phenomenon that HuH-7 cells cannot be arrested even in the absence of FCS.

3.6.2. Effect of Serum on the Localization of EGFP-Core 3 SV40 NLS in HuH-7 Cells

Visualization of EGFP-Core 3 SV40 NLS showed a significant effect caused by serum (see Fig. 37 and Tab. 8). While at 10% FCS only half of the cells showed a nuclear localization, all cells being grown at low serum concentrations showed a nuclear localization of the fusion protein.
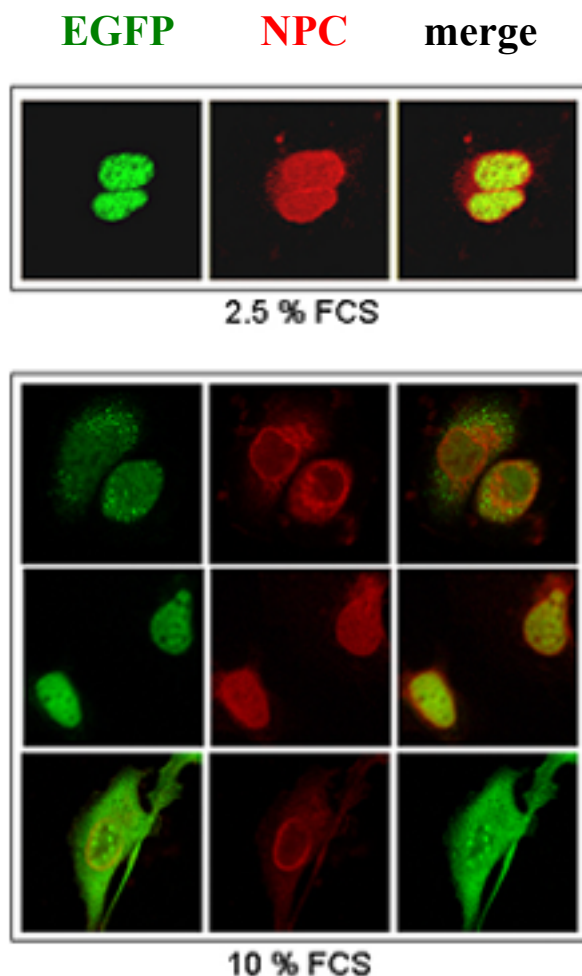

Figure 37. Fluorescence of EGFP-Core 3 SV40 NLS in HuH-7 cells at different FCS concentrations. EGFP-Core 3 SV40 NLS fusion protein at 2.5% FCS found only localized in the nucleus, whereas at 10% FCS, it localized in cytoplasm (upper row), nucleus (middle row) and both compartments (lower row). The presence of EGFP-Core fusion proteins is indicated by the green fluorescence. The nuclear pore complexes are shown as red rim-like stains.

FCS	cytoplasm	nucleus	both	total
2.5%	0	17	0	17
	0%	100%	0%	100%
10%	14	16	1	31
	45%	52%	3%	100%

Table 9. Quantification of intracellular localization of EGFP-Core 3 SV40 NLS in HuH-7 cells in the presence of different FCS concentrations. At the low concentration of FCS EGFP-Core 3 SV40 NLS localizes only in the nucleus. The higher concentration of FCS decreased a number of nuclear localization to 52%.

Apparently not cell division but serum concentration in the medium had an impact on nuclear import capacity of the fusion protein. It must be thus concluded that the inhibitory effect of Staurosporine may have been caused by its suppression of mitosis and not necessarily by its inhibition of core protein phosphorylation. Considering that growth factors generally induce protein kinases as e.g. the Ras-MEK-Erk cascade this result is nonetheless surprising because here - in contrast to the Staurosporine experiments - phosphorylation has a negative effect on nuclear transport. However, as for the SV40 Tag different phosphorylation sites with different effects may have been used.

3.7. Nuclear Localization of EGFP-Core Fusion Proteins in HepG2 Cells

If phosphorylation of the fusion proteins plays a crucial role for nuclear import of the fusion proteins one can expect that nuclear localization depends upon the cell line in which the proteins are expressed. Thus I analyzed the distribution of NLS-containing fusion proteins in another hepatoma cell line (HepG2 cells). HepG2 cells divide less rapidly than HuH-7 cells as shown in table 9. The transfection was done as described for HuH-7 cells in the presence of both 2.5% and 10% FCS. Localisation of the fusion proteins is shown in Fig. 38, and their distribution is depicted

FCS concentration	Start Cell Number	End Cell Number
2,5%	$2,19 \times 10^6$	$6,12 \times 10^6$
10%	$2,19 \times 10^6$	$8,64 \times 10^6$

Table 10. Cell division of HepG2 cells in different FCS concentration

in table 10. The nuclear fluorescence appeared to be different to that observed for HuH-7 cells. While HuH-7 cells showed a defined enrichment of the fusion proteins, HepG2 nuclei showed fluorescence within the entire karyoplasm with the exception of some spots looking similar to nucleoli.

Like for the HuH-7 cells there was an observable but relatively poor impact of the NLS redundancy. However, strikingly different the SV40 Tag mediated a much stronger nuclear localization than the capsid NLS that showed a poor transport capacity in comparison to its strength in HuH-7 cells. In addition both NLS were unaffected by the serum concentration in the medium.

expressed protein	cytoplasm	nucleus	both	total
EGFP-Core no NLS	28	4	0	32
(2,5% FCS)	87%	13%	0%	100%
EGFP-Core no NLS	15	2	0	17
(10% FCS)	88%	12%	0%	100%
EGFP-Core 1C NLS	18	2	0	20
(2,5% FCS)	90%	10%	0%	100%
EGFP-Core 1C NLS	23	4	0	27
(10% FCS)	85%	15%	0%	100%
EGFP-Core 2C NLS	26	6	0	32
(2,5% FCS)	81%	19%	0%	100%
EGFP-Core 2C NLS	14	3	0	17
(10% FCS)	82%	18%	0%	100%
EGFP-Core 3C NLS	25	6	0	31
(2,5% FCS)	80%	20%	0%	100%
EGFP-Core 3C NLS	14	4	0	18
(10% FCS)	78%	22%	0%	100%
EGFP-Core 1 SV40 NLS	22	26	0	48
(2,5% FCS)	46%	54%	0%	100%
EGFP-Core 1 SV40 NLS	9	9	0	18
(10% FCS)	50%	50%	0%	100%
EGFP-Core 2 SV40 NLS	15	28	0	43
(2,5% FCS)	35%	65%	0%	100%
EGFP-Core 2 SV40 NLS	16	18	0	34
(10% FCS)	47%	53%	0%	100%
EGFP-Core 3 SV40 NLS	16	31	0	47
(2,5% FCS)	34%	66%	0%	100%
EGFP-Core 3 SV40 NLS	12	20	0	32
(10% FCS)	38%	62%	0%	100%

Table 11. Frequency of the different fusion protein localizations in HepG2 cells. While the fusion protein without NLS localized like in the HuH-7 cells and independent upon serum concentration the distribution of the other EGFP-Core fusion proteins strongly differed from to that in HuH-7 cells.
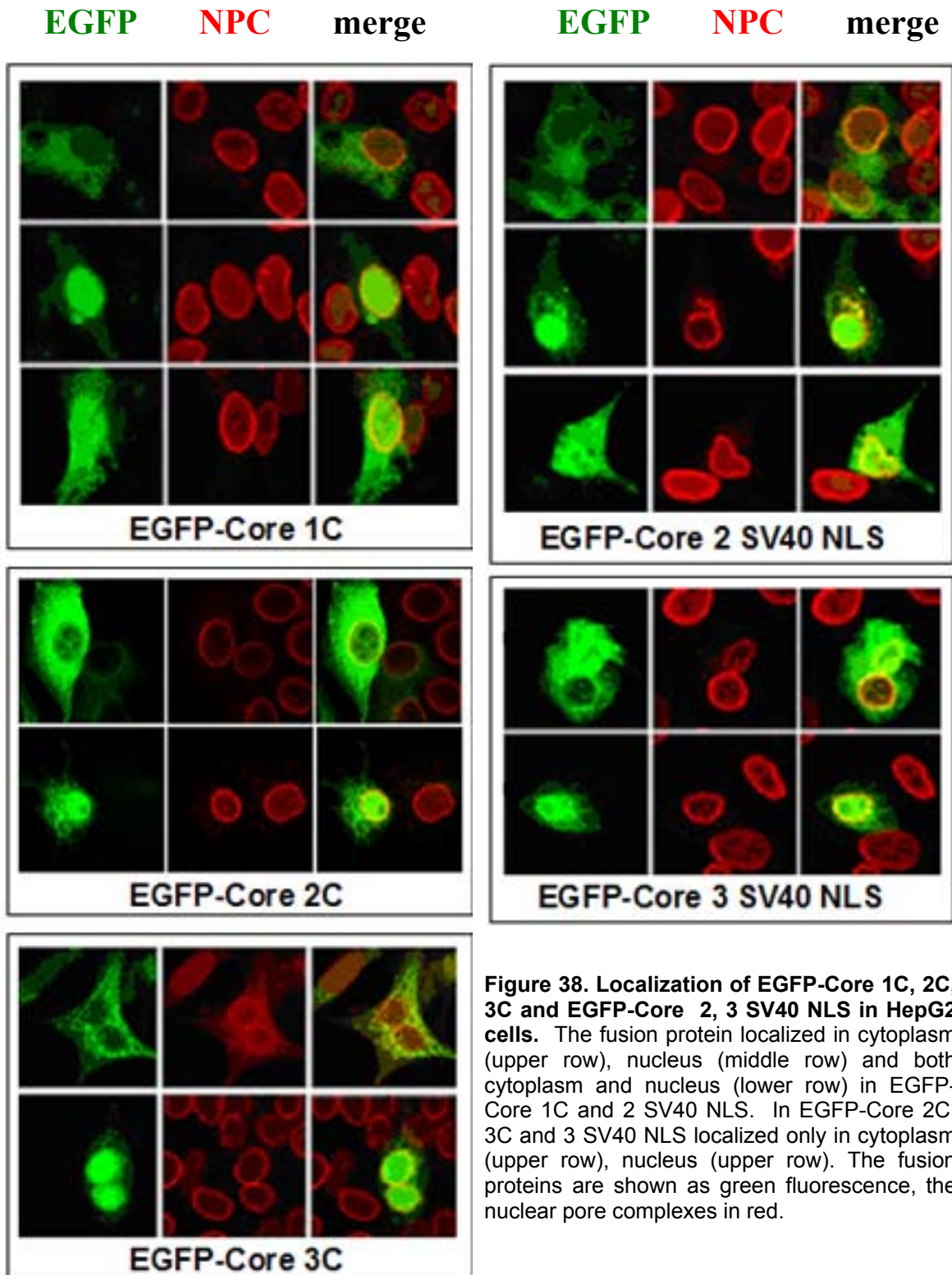
Figure 38. Localization of EGFP-Core 1C, 2C, 3C and EGFP-Core 2, 3 SV40 NLS in HepG2 cells. The fusion protein localized in cytoplasm (upper row), nucleus (middle row) and both cytoplasm and nucleus (lower row) in EGFP-Core 1C and 2 SV40 NLS. In EGFP-Core 2C, 3C and 3 SV40 NLS localized only in cytoplasm (upper row), nucleus (upper row). The fusion proteins are shown as green fluorescence, the nuclear pore complexes in red.

3.8. Dimerization of EGFP-Core 1C

As expected redundancy of NLS increased nuclear localization of the fusion proteins. However in all the experiments it remained unclear whether the fusion proteins were transported as mono- or dimers. For analysis of dimerization EGFP-Core 1C was transiently expressed in HepG2.2.15 cells that stably express HBV including the viral capsid. The successful transfections were determined by estimating the number of green fluorescing cells. The cells were lysed and the soluble proteins were subjected to a phosphorylation using $[\gamma^{32}P]ATP$. This kind of labelling was required since antibodies against the capsid protein monomer react only poorly, requiring large amount of protein. The radioactively labelled lysate was used for immune precipitations with biomagnetic beads. In a control precipitation the beads were coated with the same anti capsid antibody that was used for indirect immune fluorescence before. According to experiments of others (Kann, unpublished) this antibody recognizes conformational epitopes on two neighboring core protein dimers. For the second precipitation the beads were coated with an anti EGFP antibody. These antibody-coated beads were subjected to immune precipitation of the lysates.
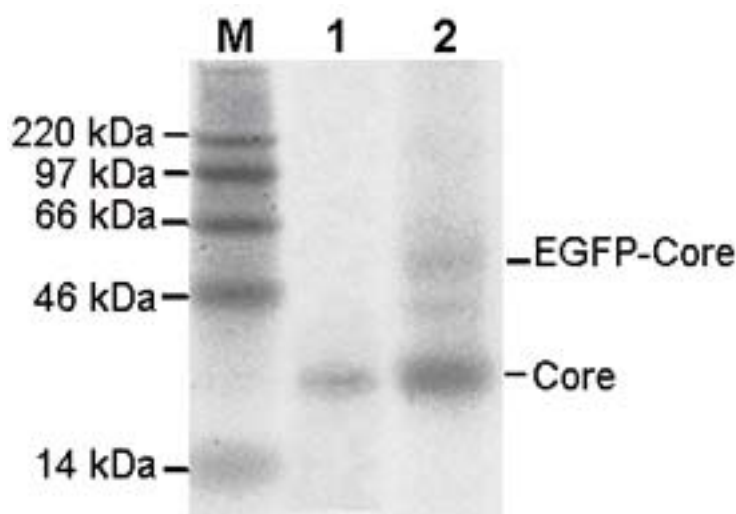
Figure 39. Immune precipitation of capsid proteins and fusion proteins with an anti-capsid antibody and an anti EGFP antibody. Proteins were phosphorylated with ^{32}P prior to precipitation. The figure shows the phosphoimager scan after separation by SDS PAGE. HBV capsid protein appears as a 21.5 kDa band, EGFP-Core 1C as a 48.5 kDa band. M: ^{14}C-labelled protein molecular weight marker; 1: Anti capsid antibody precipitated core protein from EGFP-Core 1C transfected HepG2.2.15 cells; 2: Anti EGFP antibody precipitated core and EGFP-core fusion protein from EGFP-Core 1C transfected HepG2.2.15 cells.

The precipitated proteins were separated by SDS PAGE and radioactive core proteins were visualized by phosphoimaging. Figure 39 shows that the anti capsid antibody precipitated the core protein from HepG2.2.15 cells. In this precipitation, no EGFP-Core fusion protein was precipitated, indicating that the fusion protein does not become incorporated into capsids. The anti EGFP antibody however precipitated not only the fusion protein but the wild-type capsid protein indicating that the fusion protein at least dimerizes.

3.9. Effect of the Assembly Inhibitor Bayer 41-4109 on the Localization of EGFP Core Fusion Proteins

Recently, an assembly inhibitor of HBV capsids was found (Deres et al., 2003). This inhibitor interacts with capsid formation. However, the site of interaction and the stage at which assembly is blocked - dimerization of the capsid protein monomers or the trimerization of the dimers - is yet unclear.

First the HBV genome was transfected into HuH-7 cells as described before. Twenty four hours after transfection, the inhibitor was added to one sample whereas a second one remained untreated. The successful inhibitor treatment was determined by real time PCR. Supernatant of cell culture was analyzed 48 hours post transfection. Unencapsidated viral DNA, as it may be have been derived from transfected genomes sticking to the dish or from lysed cells, was degraded prior to purification of viral DNA .

Real time PCR was done in triplets showing the addition of the inhibitor reduced the number of encapsidated viral genomes to 60%. This inhibition rate was significantly smaller than the one published for HepG2.2.15 cells in which virus secretion was reduced six fold (Deres et al., 2003). This difference may either mean that the cell type or may play a role, for instance that HuH-7 can export the inhibitor more efficiently than HeG2 cells. However, since the transfected HBV genome is genotype A and HepG2.2.15 cells express HBV of genotype D a genotype-specific binding of the inhibitor could not be excluded.

Next the effect of the inhibitor on localization of the fusion proteins was investigated. The experimental procedure was done as described before but the inhibitor was added after over night incubation following transfection. NPCs were stained after further 24 hours of incubation.

Figure 40 and 41 showed a changed distribution pattern within the nucleus. In contrast enrichment in defined areas the nuclear fluorescence filled the entire karyoplasm with the exception of some nucleoli-shaped areas.

When quantifying the number of cells with cytoplasmic or nuclear fluorescence (Tab. 11) a striking difference for the EGFP-core fusion proteins compared to capsid localization was observed. While EGFP-core 1C showed a nuclear localization in 52% of the untreated cells, Bayer 41-4109 treated cells showed a nuclear localization in only 11%. The same ratio or even more pronounced was observed for EGFP-Core 3C (57% versus 4%).
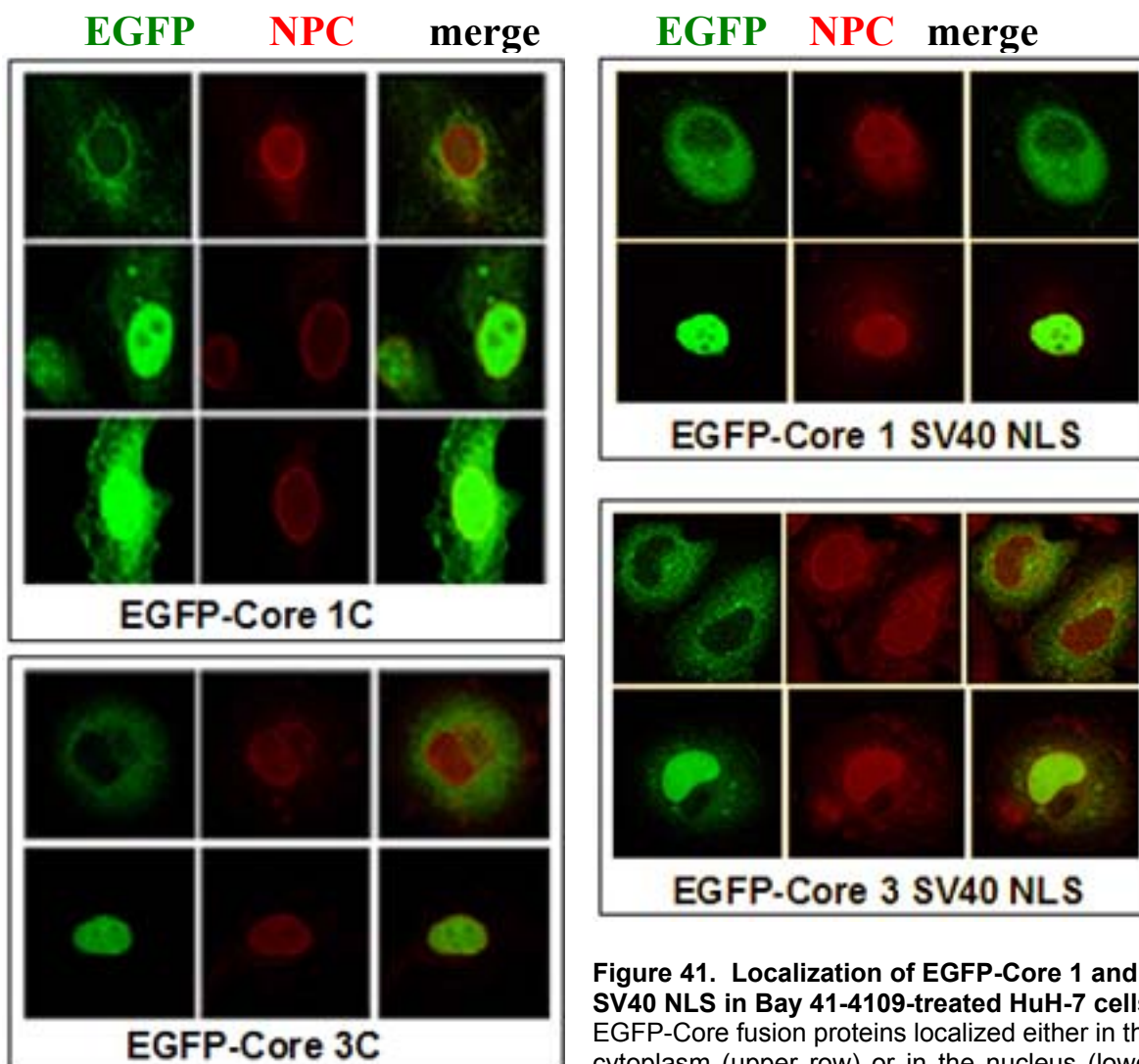
EGFP   NPC   merge

EGFP-Core 1C

EGFP-Core 3C

EGFP   NPC   merge

EGFP-Core 1 SV40 NLS

EGFP-Core 3 SV40 NLS

Figure 40. Localization of EGFP-Core 1C and 3C in Bayer 41-4109-treated HuH-7 cells. EGFP-Core 1C fusion proteins localized either in the cytoplasm (upper row), the nucleus (middle row) or in both compartments (lower row). EGFP-Core 3C fusion protein localized only in the cytoplasm (upper row) and nucleus (lower row). EGFP-Core fusion proteins are shown in green, the nuclear pore complexes in red.

Figure 41. Localization of EGFP-Core 1 and 3 SV40 NLS in Bay 41-4109-treated HuH-7 cells. EGFP-Core fusion proteins localized either in the cytoplasm (upper row) or in the nucleus (lower row). EGFP-Core fusion protein is shown in green, the nuclear pore complexes in red.

Apparently, dimerization increases the nuclear transport capacity of the fusion proteins. The effect of dimerization was much more pronounced when adding an additional NLS to the fusion protein. In contrast, the effect of the inhibitor on EGFP-Core SV40 NLS protein localization was not significant. Although the percentage of cells with cytoplasmic fluorescence increased in the inhibitor treated cells for both EGFP-Core 1 SV40 NLS and EGFP-Core 3 SV40 NLS, this difference was only marginal and with 10% not above the variation occurring between different transfections. The difference between

the EGFP-Core 1, 3C and EGFP-Core 1, 3 SV40 NLS may imply that the inhibitor interacts with the C-terminus of the capsid protein preventing binding of importin α to the NLS. This area overlaps with the nucleic acid binding domain (Hatton et al., 1992) of the capsid protein that stabilizes the capsid. As it was shown previously for DHBV capsids, mutations within this domain destabilize the viral capsid. It must be thus assumed that the described effect on capsid formation by Deres et al., (2003) is not necessarily a direct inhibition of assembly but may cause a reduced stability.

expressed protein	inhibitor	cytoplasm	nucleus	both	total
EGFP-Core 1C	No	33	36	0	69
		48%	52%	0%	100%
	Bayer 41-4109	82	10	1	93
		88%	11%	1%	100%
EGFP-Core 3C	No	33	44	1	78
		42%	57%	1%	100%
	Bayer 41-4109	86	4	0	90
		96%	4%	0%	100%
EGFP-Core 1 SV-40 NLS	No	19	75	0	94
		20%	80%	0%	100%
	Bayer 41-4109	23	57	0	80
		29%	71%	0%	100%
EGFP-Core 3 SV-40 NLS	No	9	74	1	84
		11%	88%	1%	100%
	Bayer 41-4109	21	79	0	100
		21%	79%	0%	100%

Table 12. Localization of EGFP-Core 1C, 3C and EGFP-Core 1, 3 SV40 NLS fusion protein in Bayer 41-4109-treated and untreated HuH-7 cells.

4. Discussion

4.1. Nuclear Localization of HBV Capsids After Transfection of the Entire HBV Genome into HuH-7 Cells

Upon infection with the human hepatitis B virus (HBV), the capsid or core particle predominantly localizes in the nuclei of the hepatocytes (Serinoz, 2003). Only in highly active infections, which result in high virus titers in the serum, capsids are found within the cytoplasm (Sansonno et al., 1988). Apparently, these phenomena are intrinsic to HBV since expression of the capsid in heterologous systems as in transgenic mice, results in the same distribution pattern (Guidotti et al., 1995). The nuclear localization is independent upon other viral gene products. Rabe et al. (2003) showed that in *in vitro* transport systems the capsids become imported into the nucleus. This import is associated with the release of the encapsidated viral genome into the karyoplasm, which is essential for the viral life cycle. In mice transgenic for the core protein, cytoplasmic capsid stain could only be observed in those cells that have recently undergone cell division. This observation was interpreted in that the nuclear membrane is impermeable for the entire capsid (Guidotti et al., 1994). Accordingly the diameter of the capsid being either 32 or 36 nm dependent upon the symmetry (Crowther et al., 1994) is close to the maximal functional diameter of the nuclear pore 30-40 nm (Newmeyer and Forbes, 1988; Akey, 1995) and far above the diffusion limit of FITC-dextran fluorescence labeled macromolecule lacks NLS of ~77 kDa (Kastrup et al., 2005). It must be thus assumed that the non-assembled proteins or assembly intermediates enter the karyoplasm and not the fully assembled capsids. Following this hypothesis the finding of assembled nuclear capsids as they can be visualized by electron microscopy (Furuta et al., 1975) can be explained by an intranuclear assembly of the subunits. Consistently, subunit expression leads to form capsids in the absence of other viral gene products after reaching a threshold concentration (Ceres and Zlotnick, 2002).

The single protein species out of which the capsids consists has a molecular weight of 21.5 kDa. This size would allow a passive entry into the nucleus by diffusion. However, even smaller karyophilic proteins as e.g. histones (Jäkel et al., 1999) with a MW of 14.3 to 39 kDa enter the karyoplasm by active transport.

The import of HBV capsid is mediated by the nuclear transport receptors importin α and ß. For binding to the importin α (Kann et al., 1999) a nuclear localization signal (NLS) must be exposed. The function of the NLS is influenced by phosphorylation of serine residues within the core protein (Vlachou Ph.D thesis, 1999). There are seven potential phosphorylation sites present in the core protein located at amino acids S-157, S-164, S-

170, S-172, S-178, S-180 and S-183 but there are only limited data on the extent of phosphorylation and on the sites that are used. Phosphorylation is required for NLS exposure and function (Kann et al., 1999) but the phosphate must not be added to the serine residue (aa 162) within the NLS (Vlachou Ph.D thesis, 1999). A phosphorylation site that is used localizes at serine residue aa 157 since its phosphorylation is required for packaging of the RNA pregenome -polymerase complex. The sites at amino acid 170 and/or 172 seem to become phosphorylated *in vivo*, as determined with phospho-site specific antibodies in virions (Machida et al., 1991) and S-164 and S-171 are required for polymerase activity (Melegari et al., 2005).

To allow these modifications it was required to analyze the nuclear import of the core protein in living cells instead of using *in vitro* transport assays. Consequently, the localization of the core protein was analyzed after expression in a human hepatoma cell line (HuH-7). This cell line expresses and secretes HBV at the level of a chronically HBV-infected individual after transfection with the viral genome. It was thus assumed that all modifications required for the viral life cycle occur. In fact, the evaluation of this system by expressing all viral gene products in the present work showed a predominantly nuclear localization of capsids similar to that observed *in vivo*. However, in 26% of the cells - more than normally found in chronic HBV carriers - the capsids remained in the cytosol. This phenomenon can be linked to cell division as nuclear core protein (or capsid-) localization does not occur in S phase (Yeh et al., 1993) and is linked to high viral load in patient sera (Naito et al., 1994).

4.2. Structure of the Fusion Proteins

Investigation of the core protein transport is complicated by its ability to assemble. To exclude these partially unpredictable structural changes the core protein was expressed as a fusion protein that was linked at its N terminus with the enhanced green fluorescent protein (EGFP). The fluorescent marker protein EGFP, which has a molecular weight of 27 kDa has been chosen because own experiments in HuH-7 cells revealed a weaker affinity to the nucleus than observed for an alternative marker protein DsRed. This was surprising because DsRed has a higher molecular weight (89 kDa) due to its tetramerization (Yarbrough et al., 2001) and should thus diffuse through the nuclear pores to a lower extent. However, since both proteins only showed a very low number of cells with an equal distribution in cytoplasm and nucleus (0 to 2%) it must be concluded that diffusion only plays a minor role in the distribution anyway and that the marker proteins become passively trapped inside the nuclei upon mitosis.
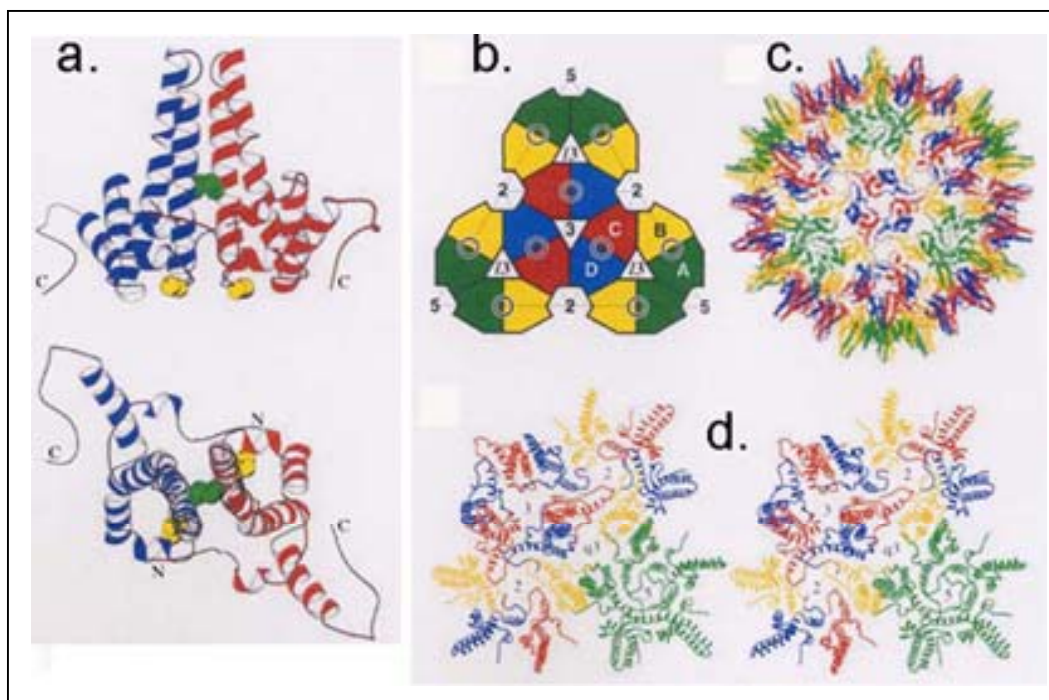
Figure. 42. Dimer of HBV capsid and its dimer packing in T=4 capsid.
a. Two orthogonal views of the HBV capsid dimer (subunit C and D) cys-61 which forms a disulfide bridge between the two monomers, is shown in green and cys-48 which does not form disulfides in yellow (Wynne et al., 1999). b. The arrangement of the four independent subunit in the T= 4 capsid showing one icosahedral face (Zlotnick et al., 1996). c. The HBV capsid viewed down an icosahedral three-fold axis. d. Packing of the dimers in the T=4 capsid in the region of a quasi three fold axis. Subunits A,B,C and D are shown in green, yellow, red and blue as in Böttcher et al. (1997).

N terminal fusions at the core protein are known to prevent capsid formation once exceeding a size limit of 40 amino acids as it was shown by Koletzki et al. (1999) who inserted parts of the Puumala hantavirus nucleocapsid protein. In fact these data could be confirmed in the present work in that the fusion proteins failed to become incorporated into capsid although – nonetheless – preserved their interaction with wild type core protein. This was not unexpected since the dimerization is mediated by the association of two α-helices in the center of the core proteins (see fig. 42) while the N-terminal arm of each monomer packs against the opposing subunit. Even a trimerization of the dimers, which is the next higher ordered structure in capsid assembly is likely since it involves contact of the dimers at aa 128 to 136 (Wynne et al., 1999).

As reported that redundancy of NLSs increases the nuclear transport competence of karyophilic proteins and complexes (Ludtke et al., 1999), the dimerization or subsequent trimerization of the dimers should have an impact on the nuclear translocation of the fusion proteins. This assumption was proven in the present work since the addition of Bayer 41-4109, an assembly inhibitor of the HBV capsid (Dienes et al., 1995), reduced the number of cells with nuclear fusion proteins with HBV NLSs drastically to one fourth.

4.3. Localization in HuH-7 Cells

4.3.1. Transport Competence of EGFP-Core Fusion Proteins

Different EGFP core fusion protein vectors were cloned and the encoding fusion proteins were expressed. To evaluate the strength of the HBV core NLS the C terminus exhibiting this signal (158-PRRTPSPRRR-168) was replaced by the NLS of the SV40 Tag (PKKKRKV) that shows a similar positive charge. The SV40 Tag NLS mediated a more or less similar proportion of nuclear fusion proteins in HuH-7 cells than the HBV core NLS, indicating a comparable affinity of importin α. This finding was surprising since the HBV capsid NLS does not show the consensus sequence (K(K/R)x-(K/R) namely in that the HBV NLS does not contain a K residue. Based on crystallography of importin α with NLS of Lamin B2 and SV40 Tag the longer side chain of the arginine residue, as in the HBV sequence, should not fit into the binding pocket P2 of the importin. However, as described in the result section there may be additional sites outside the NLS that interact with the importin α, stabilizing the binding as it was suggested for other proteins as the Borna virus p10 protein (Wolff et al., 2002) and SV40 Tag (Harreman, 2004).

In all transfections a significant proportion of fusion proteins stayed in the cytoplasm. As indicated by the low numbers of cells showing a distribution in both compartments of cytoplasm and nucleus, EGFP-Core fusion proteins are not diffusing throughout the cell. It must be thus concluded that cells with cytosolic fusion protein localization differ from those cells that allow nuclear import. One possibility might be a generally reduced nuclear import capacity of nuclei in dividing cells, as it was observed recently by others (Kann, unpublished) or that signal cascades that become changed upon cell division modify the fusion proteins e.g. by phosphorylation to reduce their import competence.

To get evidence for the effect of NLS redundancies, the HBV core NLS and the SV40 Tag NLS were fused to the EGFP core proteins in doublets or triplets. The second core NLS was separated from the first original one by 18 amino acids; the third NLS was separated from the second NLS by 8 amino acids. The sequences between the NLSs represent the natural primary amino acid sequence of the core protein C terminus. In contrast the second and third SV40 Tag NLS were directly fused with first or second SV40 Tag NLS, respectively. At least for the latter proteins it must be assumed that it is sterically impossible that more than one importin α/ß-complexes that has a molecular weight of 153 kDa can bind per fusion protein.

In all fusion proteins redundancy increased nuclear import to a comparable extent. Apparently, the spacers between the core protein NLSs did not allow binding of additional import receptors as it was assumed for the fusion proteins with the SV40 Tag NLS. The increase of transport competence thus indicates a higher probability that the transport

receptors interact with the NLS on a single fusion protein molecule. The hypothesis that multiple NLS increase the nuclear import reaction was supported by the observation that preventing dimerization by Bayer 41-4109 reduces the transport capacity of all fusion proteins.

4.3.2. Effect of Cell Cycle and Phosphorylation

As mentioned above the cell cycle may have had an impact on nuclear localization. The cell lines used in this work however did not allow synchronisation by serum starving. Nonetheless, the serum concentrations in the culture medium had a strong effect on localization in HuH-7 cells in that higher concentrations result in a more cytosolic localization. Since cell division was not significantly different is must be concluded that the signal cascades induced by growth factors in the serum mediated this effect. Although one may speculate that phosphorylation of the fusion proteins might have been the effector pathway, increasing serum concentrations may have other reasons as e.g. an effect on the nuclear transport capacity of the nuclear pore, as it was observed recently (Kann, unpublished).

The effect of phosphorylation was further investigated by treating transfected cells with Staurosporine. Staurosporine is an inhibitor predominantly of the protein kinase C (PKC) isoforms (Tamaoki et al., 1986). Targeting PKC was particularly interesting since other have shown that this kinase becomes encapsidated in capsids (Kann et al., 1993). Surprisingly, Staurosporine treatment had a dramatic effect on the localization of both types of fusion proteins - irrespectively whether they comprised the HBV core or the SV40 Tag NLS - in that inhibition of phosphorylation led to an exclusive cytoplasmic localization. As the transport receptors and the proteins of the nuclear pore are according to the current knowledge, not modified by phosphorylation the inhibition must have been affected the EGFP fusion proteins.

As the changed localization was observed as well with the fusion protein EGFP-Core 3 SV40 Tag NLS that exhibits only one of the potential core protein phosphate acceptor sites, it must be concluded that this serine residue at position 141 apparently plays a crucial role in nuclear transport of the HBV core protein. Although there is no experimental evidence on primary sequence analysis yet, Kann et al., 1993 revealed that this site represents a target site for PKC.

The observation that there are less cytoplasmic fusion proteins than in the EGFP-expressing untreated HuH-7 cells indicates that there was less passive trapping of the fusion proteins during mitosis. In fact, this assumption is supported by the observation that Staurosporine prevents cell division (Hofmann et al., 1988).

4.4. Localization in HepG2 Cells

The observation that cell culture conditions – maybe via phosphorylation – an effect the localization of the fusion proteins resulted in the investigation of another hepatoma cell line. HepG2 cells to not divide as rapidly as HuH-7 cells but like the HuH-7 cell line, they generate hepatitis B virions after transfection of the genome (Sells et al., 1988). Transfection of the fusion protein-encoding vectors led to a reduced number of successful transfections compared to HuH-7 cells. This was expected since the entry of the DNA plasmids into the nucleus depends upon mitosis. Due to the low number of fusion protein-positive cells the interpretations have to be taken with care. Nevertheless, as for the HuH-7 cells, redundancy of the NLS increased the proportion of cells with a predominantly nuclear localization. However, in HepG2 cells the SV40 Tag NLS showed a significantly higher nuclear import capacity than the HBV core protein NLS.

To evaluate the role of serum on the localization of the fusion proteins, EGFP-Core fusion proteins were expressed parallel in HepG2 cells that were incubated at the same serum concentrations as the HuH-7 cells. In HepG2 cells however, the serum had no effect on fusion protein localization. This observation strongly argues against that the inhibited nuclear import is caused by a generally reduced transport competence in the presence of higher amounts of growth factors. It supports that both cells have a different phosphorylation pattern. May be HepG2 cells allow less phosphorylation at serine residue 141 resulting in a reduced import of all fusion proteins. However, the responsible protein kinase is apparently uneffected by the serum level.

4.5. Molecular Implications for the Nuclear Import and the Viral Life Cycle

Taken together, the presented data show that the HBV capsid protein shows transport competence. To allow significant nuclear import however the NLS has to be exposed in redundancy. Only when exposed on different protein molecules high import rates occur being comparable to the prototype NLS of the SV40 Tag. Multimerizing the HBV NLS increases nuclear import but cannot fully compensate, implying that it is neither the affinity of importin α to the NLS nor the probability of a NLS-importin α interaction that restricts nuclear import reaction. More than one importin α/β complex should be bound per import complex. In conclusion it must be thus assumed that the capsid should be already partially assembled to be transported into the nucleus.

Regardless of these interpretations, phosphorylation of the core protein has an important effect on the nuclear import of the core protein. For the viral life cycle this observation is conclusive: Phosphorylation at S-157 is required for encapsidation of the pregenomic mRNA (Gazina et al., 2000), and phosphorylation at S-164 and S-170 are

essential for reverse transcription (Melegari et al., 2005). The function of the NLS is thus correlated with genome maturation and S-141 as shown in this work - appears to be essential as well. The observation however that S-164 should not be phosphorylated for the NLS function (Vlachou Ph.D thesis, 1999) implies that a dephosphorylation must occur after reverse transcription.

5. Summary

HBV core particles are involved in a number of important functions in the replication cycle of HBV. Nuclear import studies of cellular protein showed that HBV capsid binds to the nuclear pore complex, following the classical pathway of karyophilic proteins, which is mediated by the cellular proteins importin α and β. The transport of the capsid into the nucleus is facilitated by a nuclear localization signal that is located within the carboxyl terminal domain between amino acid 158 and 168 of the core protein. Unlike the NLS consensus sequence, HBV core NLS does not comprise a lysine residue, leading to the assumption that the NLS shows only weak interaction with importin α.

The understanding of the NLS and its nuclear transport receptor interaction is mainly based on observations using biochemical assays like co-immune precipitation and *in vitro* transport assays. This study was intended to provide corresponding *in vivo* evidence. By expressing fusion proteins of core and fluorescent marker protein, the strength of core NLS and the impact of phosphorylation was investigated.

To analyze the intracellular localization of HBV capsid in human liver cells, firstly the entire HBV genome was transfected into HuH-7 cells. The HBV capsid was found to be localized predominantly in the nucleus as it is *in vivo*. EGFP was chosen as a fluorescent marker protein to generate fusion protein with HBV core. The fusion protein was shown to form at least dimers but failed to assemble to capsids. This fusion protein was imported into the nucleus, redundancy of the HBV core NLS increased the translocation. Moreover the replacement of the theoretically weak HBV core NLS by the NLS of the SV40 Tag led to a similar transport competence.

The nuclear import was dependent upon phosphorylation as shown by Staurosporine treatment of transfected cells. The different fusion proteins used in these assays showed that serine 141 is the key amino acid that has to be phosphorylated. This phosphorylation however seems to differ in different cell lines and was apparently affected by the growth conditions of the cells. It must be thus concluded that there is a complex phosphorylation pattern of the core protein that affects different steps in the viral life cycle including nuclear transport. The coordination of these different phosphorylation steps remains to be elucidated.

6. Zusammenfassung

HBV Core-Partikel sind an einer Reihe wichtiger Funktionen im viralen Replikationszyklus beteiligt. Kernimportstudien mit zellulären Proteinen haben gezeigt, dass HBV-Kapside, dem klassischen Importweg karyophiler Proteine folgend, an den Kernporenkomplex binden. Dieser nukleäre Transport wird durch Importin α und β vermittelt. Der Kernimport der Kapside wird durch ein Kernlokalisationssignal, welches in der carboxyterminalen Domäne zwischen den Aminosäuren 158 und 168 des Core-Proteins lokalisiert ist, erleichtert. Das Kernimportsignal des HBV Core-Proteins enthält im Gegensatz zu der Konsensussequenz des NLS keinen Lysinrest, was zu der Annahme führte, dass nur eine schwache Interaktion zwischen dem NLS und Importin α eingegangen wird.

Das Verständnis über das Kernlokalisationssignal und die Interaktion mit dessen Transportrezeptor basiert hauptsächlich auf Ergebnissen von biochemischen Versuchen, wie Koimmunpräzipitationen und *in vitro* Transportstudien. In dieser Arbeit sollten entsprechende *in vivo*- Beweise gefunden werden. Durch die Expression von Fusionsproteinen, bestehend aus dem Core- und einem fluoreszierenden Markerprotein, sollten die Stärke des Core-NLS und der Einfluss der Phosphorylierung untersucht werden.

Zur Analyse der intrazellulären Lokalisation von HBV-Kapsiden in menschlichen Leberzellen wurden HuH-7 Zellen zunächst mit dem gesamten Genom des Hepatitis B Virus transfiziert. Wie auch im lebenden Organismus waren die HBV-Kapside überwiegend im Nukleus lokalisiert. Für die Generierung eines HBV-Core-Fusionsproteins wurde EGFP als Markerprotein verwendet. Es konnte gezeigt werden, dass dieses Fusionsprotein in der Lage ist, Dimere zu bilden, ein Assembly zu Kapsiden jedoch ausblieb. Das Fusionsprotein wurde in den Zellkern importiert, wobei die Redundanz der HBV-Core NLS die Translokation erhöhte. Darüber hinaus zeigte der Austausch des theoretisch schwachen Core-NLS gegen das Kernlokalisationssignal des SV40 Tag eine ähnliche Transportkompetenz.

Durch die Behandlung von transfizierten Zellen mit Staurosporine konnte gezeigt werden, dass der nukleäre Import von der Phosphorylierung abhängig ist. Untersuchungen mit unterschiedlichen Fusionsproteinen weisen darauf hin, dass es sich bei Serin 141 um eine besondere wichtige Aminosäure handelt, welche phosphoryliert werden muss. Diese Phosphorylierung scheint sich in verschiedenen Zelllinien zu unterscheiden und offenbar durch die Wachstumsbedingungen der Zellen beeinflusst zu werden. Die vorliegenden Ergebnisse lassen den Schluss zu, dass das Core-Protein ein

komplexes Phosphorylierungsmuster aufweist, welches im viralen Lebenszyklus unterschiedliche Schritte, inklusive nukleärer Transport, beeinflusst. Die Aufklärung der Koordination dieser unterschiedlichen Phosphorylierungen bleibt zukünftigen Studien vorbehalten.

7. References

Acs G, Sells MA, Purcell RH, Price P, Engle R, Shapiro M, and Popper H. Hepatitis B virus produced by transfected Hep G2 cells causes hepatitis in chimpanzees. *Proc Natl Acad Sci.* USA 84: 4641-4644, 1987.

Akey CW. Structural plasticity of the nuclear pore complex. *J Mol Biol 248*: 273-293, 1995.

Akiba T, Nakayama H, Miyazaki Y, Kanno A, Ishii M, and Ohori H. Relationship between the replication of hepatitis B virus and the localization of virus nucleocapsid antigen (HBcAg) in hepatocytes. *J Gen Virol* 68 (Pt 3): 871-877, 1987.

Bartenschlager R, Junker-Niepmann M, and Schaller H. The P gene product of hepatitis B virus is required as a structural component for genomic RNA encapsidation. *J Virol* 64: 5324-5332, 1990.

Beck J and Nassal M. Formation of a functional hepatitis B virus replication initiation complex involves a major structural alteration in the RNA template. *Mol Cell Biol* 18: 6265-6272, 1998.

Böttcher B, Wynne SA, and Crowther RA. Determination of the fold of the core protein of hepatitis B virus by electron cryomicroscopy. Nature 387: 88-91. 1997

Bruss V. A short linear sequence in the pre-S domain of the large hepatitis B virus envelope protein required for virion formation. *J Virol* 71: 9350-9357, 1997.

Bruss V, Lu X, Thomssen R, and Gerlich WH. Post-translational alterations in transmembrane topology of the hepatitis B virus large envelope protein. *EMBO J* 13: 2273-2279, 1994.

Bullock PA, Joo WS, Sreekumar and Mello C. Initiation of SV40 DNA replication in vitro: analysis of the role played by sequences flanking the core origin on initial synthesis events. *Virology 227*: 460-473, 1997.

Ceres P and Zlotnick A. Weak protein-protein interactions are sufficient to drive assembly of hepatitis B virus capsids. *Biochemistry* 41: 11525-11531, 2002.

Chang CM, Jeng KS, Hu CP, Lo SJ, Su TS, Ting LP, Chou CK, Han SH, Pfaff E, Salfeld J, and et al. Production of hepatitis B virus in vitro by transient expression of cloned HBV DNA in a hepatoma cell line. *EMBO J* 6: 675-680, 1987.

Chu CM and Liaw YF. Intrahepatic distribution of hepatitis B surface and core antigens in chronic hepatitis B virus infection. *Gastroenterology* 92: 220-225, 1987.

Crowther RA, Kiselev NA, Bottcher B, Berriman JA, Borisova GP, Ose V, and Pumpens P. Three-dimensional structure of hepatitis B virus core particles determined by electron cryomicroscopy. *Cell* 77: 943-950, 1994.

Deres K, Schroder CH, Paessens A, Goldmann S, Hacker HJ, Weber O, Kramer T, Niewohner U, Pleiss U, Stoltefuss J, Graef E, Koletzki D, Masantschek RN, Reimann A, Jaeger R, Gross R, Beckermann B, Schlemmer KH, Haebich D, and

Rubsamen-Waigmann H. Inhibition of hepatitis B virus replication by drug-induced depletion of nucleocapsids. *Science* 299: 893-896, 2003.

Dienes HP, Gerken G, Goergen B, Heermann K, Gerlich W, and Meyer zum Buschenfelde KH. Analysis of the precore DNA sequence and detection of precore antigen in liver specimens from patients with anti-hepatitis B e-positive chronic hepatitis. *Hepatology* 21: 1-7, 1995.

Dingwall C and Laskey R. The nuclear membrane. *Science* 258: 942-947, 1992.

Fauquet CM, Mayo MA, Maniloff J, Desselberger U and Ball LA. Virus Taxonomy: Classification and nomenclature of viruses. 8th Report of the internationale Committee on the taxonomy of viruses. Elsevier Acad. press. 381-383. 2005.

Fontes MR, Teh T, and Kobe B. Structural basis of recognition of monopartite and bipartite nuclear localization sequences by mammalian importin-alpha. *J Mol Biol* 297: 1183-1194, 2000.

Fried H and Kutay U. Nucleocytoplasmic transport: taking an inventory. *Cell Mol Life Sci* 60: 1659-1688, 2003.

Furuta S, Nagata A, Kiyosawa K, Takahashi T, and Akahane Y. HBs-Ag, HBc-Ag and virus-like particles in liver tissue. *Gastroenterol Jpn* 10: 208-214, 1975.

Gallina A, Bonelli F, Zentilin L, Rindi G, Muttini M, and Milanesi G. A recombinant hepatitis B core antigen polypeptide with the protamine-like domain deleted self-assembles into capsid particles but fails to bind nucleic acids. *J Virol* 63: 4645-4652, 1989.

Gazina EV, Fielding JE, Lin B and Anderson DA. Core protein phosphorylation modulates pregenomic RNA encapsidation to different extent in human and duck hepatitis B virus. *J. Virol 74*: 4721-4728. 2000.

Gerelsaikhan T, Tavis JE, and Bruss V. Hepatitis B virus nucleocapsid envelopment does not occur without genomic DNA synthesis. *J Virol* 70: 4269-4274, 1996.

Görlich D and Kutay U. Transport between the cell nucleus and the cytoplasm. *Annu Rev Cell Dev Biol* 15: 607-660, 1999.

Gudat F, Bianchi L, Sonnabend W, Thiel G, Aenishaenslin W, and Stalder GA. Pattern of core and surface expression in liver tissue reflects state of specific immune response in hepatitis B. *Lab Invest* 32: 1-9, 1975.

Guidotti LG, Martinez V, Loh YT, Rogler CE, and Chisari FV. Hepatitis B virus nucleocapsid particles do not cross the hepatocyte nuclear membrane in transgenic mice. *J Virol* 68: 5469-5475, 1994.

Guidotti LG, Matzke B, Schaller H, and Chisari FV. High-level hepatitis B virus replication in transgenic mice. *J Virol* 69: 6158-6169, 1995.

Guidotti LG, Morris A, Mendez H, Koch R, Silverman RH, Williams BR, and Chisari FV. Interferon-regulated pathways that control hepatitis B virus replication in transgenic mice. *J Virol* 76: 2617-2621, 2002.

Gupta D, Syed NA, Roesler WJ, and Khandewal RL. Effect pf overexpression and nuclear Translocation of constitutively active PKB-α on cellular survival and proliferation in HepG2 cells. *J. Cell. Biol*. 93: 513-525. 2004.

Harreman MT, Kline TM, Milford HG, Harben MB, Hodel AE and Corbett AH. Regulation of nuclear import by phosphorylation adjacent to nuclear localization signals. *J Biol Chem* 279: 20613-20621, 2004.

Hatton T, Zhou S, and Standring DN. RNA- and DNA-binding activities in hepatitis B virus capsid protein: a model for their roles in viral replication. *J Virol* 66: 5232-5241, 1992.

Heermann KH, Goldmann U, Schwartz W, Seyffarth T, Baumgarten H, and Gerlich WH. Large surface proteins of hepatitis B virus containing the pre-s sequence. *J Virol* 52: 396-402, 1984.

Hirsch RC, Lavine JE, Chang LJ, Varmus HE, and Ganem D. Polymerase gene products of hepatitis B viruses are required for genomic RNA packaging as wel as for reverse transcription. *Nature* 344: 552-555, 1990.

Hofmann J, Doppler W, Jakob A, Maly K, Posch L, Uberall F and Grunicke HH. Enhancement of the antiproliferative effect of cis-diamminedichloroplatinum (II) and nitrogen mustard by inhibitors of protein kinase C. *Int J Cancer* 42: 382-388. 1988.

Howard CR. The structure of hepatitis B envelope and molecular variants of hepatitis B virus. *J Viral Hepat* 2: 165-170, 1995.

Hübner S, Xiao CY and Jans DA. The protein kinase CK2 site (Ser[111/112]) enhances recognition of the Simian Virus 40 large T-antigen nuclear localizationsequence by importin. *J. Biol Chem 272*: 17191-17195, 1997.

Izaurralde E, Kann M, Pante N, Sodeik B, and Hohn T. Viruses, microorganisms and scientists meet the nuclear pore. The EMBO Journal. 18.(2). 289-296. 1999.

Jans DA. The regulation of protein transport to the nucleus by phosphorylation. *Biochem J* 311 (Pt 3): 705-716, 1995.

Jans DA and Jans P. Negative charge at the casein kinase II site flanking the nuclear localization signal of the SV40 large T-antigen is mechanistically important for enhanced nuclear import. *Oncogene* 9: 2961-2968, 1994.

Jäkel S, Albig W, Kutay U, Bischoff FR, Schwamborn K, Doenecke D and Görlich D. The importin β/importin 7 heterodimer is a functionalnuclear import receptor for Histone H1. *The EMBO journal.* 18 (9). 2411-2423. 1999.

Jilbert AR and Mason WS. Hepatitis B Virus. In Encyclopedia of Life Sciences. Macmillan Publishers Ltd., Nature Publishing Group. www.els.net. 2002.

Kalderon D and Smith AE. In vitro mutagenesis of a putative DNA binding domain of SV40 large-T. *Virology* 139: 109-137, 1984.

Kann M, Thomssen R, Koschel HG and Gerlich WH. Characterization of the endogenous proten kinase activity of the hepatitis B virus. *Arch. Virol. Suppl.* 8:53-62, 1993

Kann M, Kochel HG, Uy A, and Thomssen R. Diagnostic significance of antibodies to hepatitis B virus polymerase in acutely and chronically HBV-infected individuals. *J Med Virol* 40: 285-290, 1993.

Kann M, Bischof A, and Gerlich WH. In vitro model for the nuclear transport of the hepadnavirus genome. *J Virol* 71: 1310-1316, 1997.

Kann M, Sodeik B, Vlachou A, Gerlich WH, and Helenius A. Phosphorylation-dependent binding of hepatitis B virus core particles to the nuclear pore complex. *J Cell Biol* 145: 45-55, 1999.

Kann M and Gerlich WH. Structure and Molecular Virology. In *Viral Hepatitis*. Third ed. Zuckermann HC and Thomas AJ. Churchill Livingston. 149-180. 2005.

Kastrup L, Oberleithner H, Ludwig Y, Schäfer C and Shahim V. Nuclear envelope barrier leak induced by dexamethasone. *J Cell Physiol.* 2005.

Kenney JM, von Bonsdorff CH, Nassal M, and Fuller SD. Evolutionary conservation in the hepatitis B virus core structure: comparison of human and duck cores. *Structure* 3: 1009-1019, 1995.

Kock J, Borst EM, and Schlicht HJ. Uptake of duck hepatitis B virus into hepatocytes occurs by endocytosis but does not require passage of the virus through an acidic intracellular compartment. *J Virol* 70: 5827-5831, 1996.

Koletzki D, Biel SS, Meisel H, Nugel E, Gelderblom HR, Kruger DH, and Ulrich R. HBV core particles allow the insertion and surface exposure of the entire potentially protective region of Puumala hantavirus nucleocapsid protein. *Biol Chem* 380: 325-333, 1999.

Lambert C and Prange R. Chaperone action in the posttranslational topological reorientation of the hepatitis B virus large envelope protein: Implications for translocational regulation. *Proc Natl Acad Sci U S A* 100: 5199-5204, 2003.

Lanford RE, Kim YH, Lee H, Notvall L, and Beames B. Mapping of the hepatitis B virus reverse transcriptase TP and RT domains by transcomplementation for nucleotide priming and by protein-protein interaction. *J Virol* 73: 1885-1893, 1999.

Liao W and Ou JH. Phosphorylation and nuclear localization of the hepatitis B virus core protein: significance of serine in the three repeated SPRRR motifs. *J Virol* 69: 1025-1029, 1995.

Ludtke JJ, Zhang G, Sebestyen MG and Wolff JA. A nuclear localization signal can enhance both the nuclear transport and expression of 1 kb DNA. *J Cell Sci 112*: 2033-2041, 1999.

Machida A, Ohnuma H, Tsuda F, Yoshikawa A, Hoshi Y, Tanaka T, Kishimoto S, Akahane Y, Miyakawa Y, and Mayumi M. Phosphorylation in the carboxyl-terminal domain of the capsid protein of hepatitis B virus: evaluation with a monoclonal antibody. *J Virol* 65: 6024-6030, 1991.

McLachlan A, Milich DR, Raney AK, Riggs MG, Hughes JL, Sorge J and Chisari FV. Expression of hepatitis B virus surface and core antigens: influences of pre-S and precore sequences. *J. Virol*. 77: 12950-1260. 1987.

Melegari M, Jung MC, Schneider R, Santantonio T, Bagnulo S, Luchena N, Pastore G, Pape G, Scaglioni PP, Villa E, and et al. Conserved core protein sequences in hepatitis B virus infected patients without anti-HBc. *J Hepatol* 13: 187-191, 1991.

Melegari M, Wolf SK, and Schneider RJ. Hepatitis B virus DNA replication is coordinated by core protein serine phosphorylation and HBx expression. *J Virol* 79: 9810-9820, 2005.

Moore MS and Blobel G. Purification of a Ran-interacting protein that is required for protein import into the nucleus. *Proc Natl Acad Sci U S A* 91: 10212-10216, 1994.

Naito M, Matsuda H, Okuno H, Kim H, Azuma M, Kashiwagi T, Mitsutani N, koizumi T, Kawaguchi G and Kobayashi Y. Hepatitis B virus carrier with low titer of antibody to hepatitis B core antigen. *Hepatogastroenterology*. 3: 235-238. 1994.

Nassal M. The arginine-rich domain of the hepatitis B virus core protein is required for pregenome encapsidation and productive viral positive-strand DNA synthesis but not for virus assembly. *J Virol* 66: 4107-4116, 1992.

Newmeyer DD and Forbes DJ. Nuclear import can be separated into distint steps in vitro: nuclear pore binding and translocation. *Cell 52*: 641-653. 1988.

Ou JH, Laub O and Rutter WJ. Hepatitis B virus gene function: the precore region targets the core antigen to cellular membranes and causes the secretion of the e antigen. *Proc. Natl. Acad. Sci.* USA 83: 1578-1582, 1986.

Pante N and Kann M. Nuclear pore complex is able to transport macromolecules with diameters of about 39 nm. *Mol Biol Cell* 13: 425-434, 2002.

Paschal BM and Gerace L. Identification of NTF2, a cytosolic factor for nuclear import that interacts with nuclear pore complex protein p62. *J Cell Biol* 129: 925-937, 1995.

Pollack JR and Ganem D. Site-specific RNA binding by a hepatitis B virus reverse transcriptase initiates two distinct reactions: RNA packaging and DNA synthesis. *J Virol* 68: 5579-5587, 1994.

Pumpens P and Grens E. HBV core particles as a carrier for B cell/T cell epitopes. *Intervirology* 44: 98-114, 2001.

Rabe B, Vlachou A, Pante N, Helenius A, and Kann M. Nuclear import of hepatitis B virus capsids and release of the viral genome. *Proc Natl Acad Sci U S A* 100: 9849-9854, 2003.

Robbins J, Dilworth SM, Laskey RA, and Dingwall C. Two interdependent basic domains in nucleoplasmin nuclear targeting sequence: identification of a class of bipartite nuclear targeting sequence. *Cell* 64: 615-623, 1991.

Robinson WS, Clayton DA, and Greenman RL. DNA of a human hepatitis B virus candidate. *J Virol* 14: 384-391, 1974.

Sansonno DE, Fiore G, Bufano G, and Manghisi OG. Cytoplasmic localization of hepatitis B core antigen in hepatitis B virus infected livers. *J Immunol Methods* 109: 245-252, 1988.

Schwöbel ED and Moore MS. The control of gene expression by regulated nuclear transport. *Essays Biochem* 36: 105-113. 2000.

Seifer M and Standring DN. Ribonucleoprotein complex formation by the human hepatitis B virus polymerase. *Intervirology* 38: 295-303, 1995.

Sells MA, Chen ML, and Acs G. Production of hepatitis B virus particles in Hep G2 cells transfected with cloned hepatitis B virus DNA. *Proc Natl Acad Sci U S A* 84: 1005-1009, 1987.

Sells MA, Zelent AZ, Shvartsman M, and Acs G. Replicative intermediates of hepatitis B virus in HepG2 cells that produce infectious virions. *J Virol* 62: 2836-2844, 1988.

Serinoz E, Varli M, Erden E, Cinar K, Kansu A, Uzunalimoglu O, Yurdaydin C, and Bozkaya H. Nuclear localization of hepatitis B core antigen and its relations to liver injury, hepatocyte proliferation, and viral load. *J Clin Gastroenterol* 36: 269-272, 2003.

Sherman MP, de Noronha CM, Heusch MI, Greene S, and Greene WC. Nucleocytoplasmic shuttling by human immunodeficiency virus type 1 Vpr. *J Virol* 75: 1522-1532, 2001.

Sterneck M, Kalinina T, Gunther S, Fischer L, Santantonio T, Greten H, and Will H. Functional analysis of HBV genomes from patients with fulminant hepatitis. *Hepatology* 28: 1390-1397, 1998.

Sureau C, Romet-Lemonne JL, Mullins JI, and Essex M. Production of hepatitis B virus by a differentiated human hepatoma cell line after transfection with cloned circular HBV DNA. *Cell* 47: 37-47, 1986.

Tamaoki T, Nomoto H, Takahashi I, kato Y, Morimoto M and Tomita F. Staurosporine, a potent inhibitor of phospholipid/Ca^{++}dependent protein kinase. *Biochem Biophys Res Commun.* 135. 397-402. 1986.

Tang H and McLachlan A. A pregenomic RNA sequence adjacent to DR1 and complementary to epsilon influences hepatitis B virus replicatin efficiency. *J. Virol.* 303. 199-210. 2002.

Tennant BC, Toshkov IA, Peek SF, Jacob JR, Menne S, Hornbuckle WE, Schinazi RD, Korba BE, Cote PJ, and Gerin JL. Hepatocellular carcinoma in the woodchuck model of hepatitis B virus infection. *Gastroenterology* 127: S283-293, 2004.

Toh H, Hayashida H, and Miyata T. Sequence homology between retroviral reverse transcriptase and putative polymerases of hepatitis B virus and cauliflower mosaic virus. *Nature* 305: 827-829, 1983.

Ulrich PP, Bhat RA, Seto B, Mack D, Sninsky J, and Vyas GN. Enzymatic amplification of hepatitis B virus DNA in serum compared with infectivity testing in chimpanzees. *J Infect Dis* 160: 37-43, 1989.

Vlachou A. Untersuchung von Wechselwirkungen zwischen Hepatitis B Virus Nukleocapsiden und dem Zellkern. Dissertation im Fachbereich Biologie der JLU Giessen. 1999.

Whittaker GR, Kann M, and Helenius A. Viral entry into the nucleus. *Annu Rev Cell Dev Biol* 16: 627-651, 2000.

Wolff T, Pfleger R, Wehner T, Reinhardt J, and Richt JA. A short leucine-rich sequence in the Borna disease virus p10 protein mediates association with the viral phospho- and nucleoproteins. *J Gen Virol* 81: 939-947, 2000.

Wolff T, Unterstab G, Heins G, Richt JA, and Kann M. Characterization of an unusual importin alpha binding motif in the borna disease virus p10 protein that directs nuclear import. *J Biol Chem* 277: 12151-12157, 2002.

Wynne SA, Crowther RA, and Leslie AG. The crystal structure of the human hepatitis B virus capsid. *Mol Cell* 3: 771-780, 1999.

Yarbrough D, Wachter RM, Kallio K, Matz MV, and Remington SJ. Refined crystal structure of DsRed, a red fluorescent protein from coral, at 2.0-A resolution. *Proc Natl Acad Sci U S A* 98: 462-467, 2001.

Yeh CT, Wong SW, Fung YK, and Ou JH. Cell cycle regulation of nuclear localization of hepatitis B virus core protein. *Proc Natl Acad Sci U S A* 90: 6459-6463, 1993.

Yu M and Summers J. A domain of the hepadnavirus capsid protein is specifically required for DNA maturation and virus assembly. *J Virol* 65: 2511-2517, 1991.

Zang WQ and Yen TS. Distinct export pathway utilized by the hepatitis N virus posttrancriptional regulatory element. *Virology,* 259: 299-304. 1999.

Zhou S and Standring DN. Hepatitis B virus capsid particles are assembled from core-protein dimer precursors. *Proc Natl Acad Sci.* U S A 89: 10046-10050, 1992.

Zlotnick A, Cheng N, Conway JF, Booy FP, Steven AC, Stahl SJ, and Wingfield PT. Dimorphism of hepatitis B virus capsids is strongly influenced by the C-terminus of the capsid protein. *Biochemistry*. 1996. 35(23):7412-7421, 1996.

Zlotnick A, Cheng N, Stahl SJ, Conway JF, Steven AC and Wingfield PT. Localization of the C terminus of the assembly domain of hepatitis B virus capsid protein: implications for morphogenesis and organization of encapsidated RNA. *Proc Natl Acad Sci.* U S A 94: 9556-9561, 1997.

Zlotnick A, Johnson JM, Wingfield PW, Stahl SJ, and Endres D. A theoretical model successfully identifies features of hepatitis B virus capsid assembly. *Biochemistry* 38: 14644-14652, 1999.

Zoulim F and Seeger C. Reverse transcription in hepatitis B viruses is primed by a tyrosine residue of the polymerase. *J Virol* 68: 6-13, 1994.

8. Acknowledgements

Specially, I deeply thank to my dear wife Dr. Nastiti Wijayanti, S.Si., M.Si., who shared most of my time in meaningful insight and for her love and support in hard times of my life, for her understanding and patient assistance.

Last but not definitely least, I would like to acknowlegde to my family in Indonesia specially for my mother (in memoriam Sept 26th, 2004) and my father, who always gave me prayer and blessing for my study in Giessen. As well as to all of my family members who always support me during my study in Germany.

Finally, my most deeply gratitude to Allah SWT, my lord who has given me health, strength, opportunity, ability, ease and many other bounties which enable me to work and finish my study in Germany.

9. Appendixes

9.1. List of Figures

9.2. List of Tables

10. Curriculum Vitae

1. Personal Data

Name : Aris Haryanto
Date of Birth : January, 25th 1971
Place of birth : Jogjakarta, Indonesia
Nationality : Indonesian
Sex : Male
Marital Status : Married
Religion : Islam
Email : arisharyanto@yahoo.com
Resident Address : Blunyah Gede 79, Jogjakarta 55284, Indonesia

2. Education Background

a. School Education
1977 - 1983
SDN Baciro II, Elementary School, Jogjakarta

1983 - 1986
SMPN 8, Junior High School, Jogjakarta

1986 - 1989
SMAN 8, Senior High School, Jogjakarta

May 15th, 1989
Abitur

b. University Education
August 14th, 1989 – August 19th, 1993
Doctorandus of Medical Veteriner (Drs.Med.Vet), Faculty of Veterinary Medicine, Gadjah Mada University, Jogjakarta, Indonesia.
Thesis : ***Effect of Pb Asetat Solution Treatment to Routine Blood Description in Fruit Bats (Microptheropus sp.)***

August 28th, 1993 – December 19th, 1994
Doctor of Veterinary Medicine (DVM), Faculty of Veterinary Medicine, Gadjah Mada University, Jogjakarta, Indonesien.

September 2nd, 1996 – September 29th, 1999
Master of Science (M.Sc.), Study Program of Biotechnology, Post Graduated Program, Gadjah Mada University, Jogjakarta, Indonesia.
Thesis : ***Variance of Gene Sequence Encode for C-terminus Latent Membrane Protein 1 (lmp-1) of Epstein-Barr virus in Nasopharyngeal Carcinoma Patients.***

October 1st, 2001 – December 21st, 2005
Promotion in Institute of Medical Virology and Institute of Veterinary Virology Justus-Liebig-University Giessen, Germany.
Dissertation: ***The Nuclear Localization Signal of Hepatitis B Virus Core Protein: Characterization by Expression as EGFP-Core Fusion Protein***

c. German Course
  September 2nd, 2000 - Marc 8th, 2001
  Goethe Institute Jakarta, Indonesia
  April 4th, 2001- September 25th, 2001
  Goethe Institute Mannheim, Germany